NTNU
Norwegian University of
Science and Technology

Compressed air energy storage for clean offshore energy supply

Jacopo Degl'Innocenti

Master of Science in Engineering and ICT
Submission date: June 2018
Supervisor: Lars Olof Nord, EPT
Co-supervisor: Luca Riboldi, EPT

Norwegian University of Science and Technology
Department of Energy and Process Engineering

NTNU

Norwegian University
of Science and Technology

Department of Energy
and Process Engineering

EPT-M-2017-112

MASTER THESIS

for

Student Jacopo Degl'Innocenti

Spring 2018

English title:
Compressed air energy storage for clean offshore energy supply

Background and objective

The attempt to reduce the environmental impact of oil and gas installations has been the driver for researching energy efficient solutions to supply energy offshore. This process led to novel concepts involving complex offshore power plants integrating different forms of energy, including renewable and conventional sources. Within this context, the possibility to store energy may become of primary importance, although challenging for offshore applications. Compressed energy storage is a promising option. The compressed air could be stored subsea or underground, therefore limiting the footprint of the energy storage on the offshore installation. The thesis will investigate the technical feasibility and the performance of offshore energy supply concepts based on renewable energy and compressed energy storage.

The objectives of the thesis are to:
- Evaluate feasible process configurations based on compressed energy storage system (CAES) for continuous supply of energy to an offshore installation.
- Dimension the system in accordance with energy requirements and constraints of the offshore installation selected as case study.
- Investigate the performance of the process configurations selected.

The work is in collaboration with Università degli Studi di Pisa, Italy.

The following tasks are to be considered:

1. Literature review on CAES and offshore energy supply.
2. Define models in Matlab of the various components of the system to study.
3. Evaluate possible process configurations and pinpoint the most promising ones for the selected case study.
4. Design the offshore systems.
5. Perform process simulations of the concepts defined and critically analyse the performance.

When the thesis is evaluated, emphasis is put on processing of the results, and that they are presented in tabular and/or graphic form in a clear manner, and that they are analyzed carefully.

The thesis should be formulated as a research report with summary, conclusion, literature references, table of contents etc. During the preparation of the text, the candidate should make an effort to produce a well-structured and easily readable report. In order to ease the evaluation of the thesis, it is important that the cross-references are correct. In the making of the report, strong emphasis should be placed on both a thorough discussion of the results and an orderly presentation.

The candidate is requested to initiate and keep close contact with his/her academic supervisor(s) throughout the working period. The candidate must follow the rules and regulations of NTNU as well as passive directions given by the Department of Energy and Process Engineering.

Risk assessment of the candidate's work shall be carried out according to the department's procedures. The risk assessment must be documented and included as part of the final report. Events related to the candidate's work adversely affecting the health, safety or security, must be documented and included as part of the final report. If the documentation on risk assessment represents a large number of pages, the full version is to be submitted electronically to the supervisor and an excerpt is included in the report.

Pursuant to "Regulations concerning the supplementary provisions to the technology study program/Master of Science" at NTNU §20, the Department reserves the permission to utilize all the results and data for teaching and research purposes as well as in future publications.

The final report is to be submitted digitally in DAIM. An executive summary of the thesis including title, student's name, supervisor's name, year, department name, and NTNU's logo and name, shall be submitted to the department as a separate pdf file. Based on an agreement with the supervisor, the final report and other material and documents may be given to the supervisor in digital format.

☐ Work to be done in lab (Water power lab, Fluids engineering lab, Thermal engineering lab)
☐ Field work

Department of Energy and Process Engineering, 15 January 2018

Lars O. Nord
Academic Supervisor

Co-supervisors:
Umberto Desideri, Professor, Università degli Studi di Pisa, Italy
Heiner Schümann, Research Scientist, SINTEF
Luca Riboldi, Postdoctoral fellow, NTNU

ABSTRACT

The primary objective of this work is to evaluate feasible process configurations based on compressed air energy storage system (CAES) in order to reduce the emissions of offshore oil and gas extraction facilities. The main aim is to remove the need for the traditional shared-load gas turbine (GT) operation on the platform, which currently represents a significant source of CO_2 and fuel consumption. Improving the energy management of offshore installations opens up significant opportunities concerning both cost savings and reduction of the environmental impact.

A specific case study, represented by Edvard Grieg and Ivar Aasen installations, has been used to model the components of the system. The model, while tailored for some specific parameters, can be easily adapted to a variety of different situations, and therefore aims to represent a starting point for further optimization work and for the analysis of different site conditions. The models of the various components were defined in MATLAB and EXCEL, and were given particular attention to their off-design operation, in accordance to energy requirements and constrains of the case study. The key investigated parameters were the size of the wind farm, the depth of the sea (which directly affects the sizing of the air storage) and the possibility to recover waste heat from the GT to preheat the air as it is extracted from the underwater storage.

The results show that the integration of a wind farm alone will not allow to remove the need for the 2nd GT, but would provide the system with a significant reduction of CO_2 emissions, ranging between 14% and 40%, depending on the size of the offshore wind park.
The introduction of the CAES system removes the need for the 2nd GT and improves the achieved reduction even further, especially with the use of an air preheater (it is possible to reach a 47% reduction with the best configuration). From an energy point of view, the system looks always promising. On the other hand, when considering the physical space required by the storage, it seems that the available sea depth might be a stringent limitation to an effective applicability, requiring up to 475 vessels in the case study depth of 110 meters. The study of higher depths (400 and more meters) results in a drastic reduction of the required number of vessels, making these sites more attractive for the CAES technology.

ACKNOWLEDGMENTS

I am not very good with words, but I will try anyways, you deserve it.
This five years long journey proved to be incredibly hard, and I would not have finished it without the help of so many amazing people.

First of all, I would like to thank my parents (Luna included, of course), who have always pushed me to do the best I could and always supported me in every way they could.

A very special thank you is also mandatory for Gabriele and Marco. Without our "gruppo studio" I doubt I would have made it through all those incredibly challenging exams. You made all those hours spent on the books much easier and partly "enjoyable". And well, we shared some incredible adventures too throughout the years.

Thank you to "Maltata", my life-long friends and partners in crime. I hope we will go again on those historical summer holidays, and we will keep going on sbocciare like crazy.

Thank you to Agnese and Anna, my oldest friends, who have always been there, both in good and bad moments. You do not know how much I love you and care for you.

These past six months have been a blast, making my decision to work on this thesis in Norway the best thing of my life. Norway really is a beautiful country, full of breath-taking places. I am so grateful to have met some of the best people I know there, and to have created bonds that I hope time will not weaken. No words will ever be enough to describe what we shared in Moholt, but we all know it. Thank you Howmuchdoyourisk crew, I love you all.

This Norwegian experience would not have been possible without the opportunity given to me by prof. Desideri and prof. Nord, thank you so much.

Last, but not least, a big thank you to Luca, who proved to be invaluable for this thesis. I am so glad to have worked with you and I hope to meet you again. If this work is any good, it is thanks to you and your feedbacks.

TABLE OF CONTENTS

LIST OF FIGURES

LIST OF TABLES

1 INTRODUCTION

1.1 Motivation

Oil and gas production in Norway takes place offshore, mostly in the North Sea. Norwegian oil production started in 1971, and the first unit of gas was extracted in 1977. For a country that produces more than 99% of its electric demand through renewable resources (hydropower), the emissions that come from petroleum activities represent a large share of the total. In 2016, for example, greenhouse gas (GHG) emissions from petroleum activities corresponded to about one quarter of Norwegian's aggregate emissions [1].

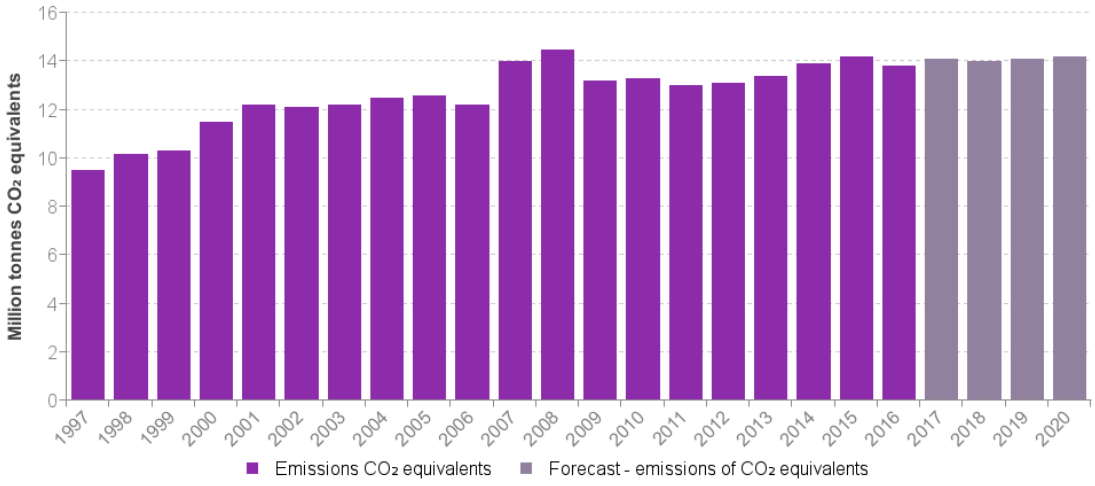

Figure 1-1: Historical Numbers for 1997-2016 and projections. Source: Norwegian Petroleum Directorate

Most of the GHG emissions from Norwegian petroleum production come from the use of gas turbines that generate electricity. These are located on the platforms offshore, and are much less efficient than modern large-scale gas power plants [2]. In 2012, they accounted for 62% of the total GHG emissions from Norwegian oil and gas production. Other sources of GHG are boilers, flaring of natural gas for safety reasons, venting and diffuse emissions of gas, storage and loading of crude oil.

The Carbon Tax and the Greenhouse Gas Emission Trading Act are Norway's most important cross-sectoral climate policy instruments for cost-effective cuts in GHG

emissions. Both these instruments apply to the petroleum industry, while most other sectors either have to take part in emissions trading or pay the carbon tax.

The carbon tax

Norway was among the first countries in the world to introduce a carbon tax, in 1991. This is applied to all combustion of gas, oil and diesel in petroleum operations and on releases of CO2 and natural gas. For 2018, the tax rate is NOK 1.06 per standard cubic metre of gas or per litre of oil or condensate. For combustion of natural gas, this is equivalent to NOK 453 per tonne of CO_2. For emissions of natural gas, the tax rate is NOK 7.30 per standard cubic metre [3].

Greenhouse gas Emission Trading

Norway's Greenhouse Gas Emission Trading Act entered into force in 2005, and Norway joined the EU Emissions Trading System (EU ETS) in 2008. This means that Norwegian installations in the petroleum industry and other industries to which the system applies are subject to the same rules for emissions trading as those within the EU. The EU ETS is now in its third phase, which runs up to 2020.

The combination of the carbon tax and the emissions trading system means that companies on the Norwegian shelf pay up to 55€ per tonne for their CO2 emissions, which is higher than in other sectors in Norway and very high compared with carbon prices in other countries.

It is therefore clear that improving the energy management of offshore installations opens up significant opportunities concerning both cost savings and reduction of the environmental impact.

1.2 Previous works

With the aim of reducing the emissions in the offshore oil and gas industry, several studies have investigated the feasibility of offshore combined cycles [4]. The possibility to introduce a steam cycle for cogeneration of heat and power was studied in [5]. Organic Rankine cycles

were analysed in [6]. Recently, electrification of the offshore facilities was looked into, for both future and existing installations, by the Oil and Gas Department of the Norwegian Ministry of Petroleum and Energy. Another interesting possibility is the integration of offshore wind power facilities with oil and gas platforms and to the onshore grid [7]. An additional option is to integrate renewable energy sources to local power generation: the possibility to operate an offshore wind farm in parallel with the gas turbines on the platform was concluded to be economically and environmentally attractive [8]. Different of these concepts for efficient supply of power and heat to offshore installations were compared, also taking into account off-design simulations and variable demands from the rigs [9].

The work done by He et al [7] regards the integration of a wind farm with an oil and gas platform and will be briefly summarized below.

The study evaluates the effect on the integration of a 20 MW wind farms on an offshore platforms whose power consumption over the year varies between 20 MW and 35 MW. The electric power demand is supplied by two gas turbines of the same type with 23 MW rated capacity. The gas turbines which directly drive the gas compressors are not connected to the electrical grid, and thus are not included in the study. Replacing the gas turbines with electrical motors would allow for a deeper wind penetration and therefore more savings and less emissions. The results carried out by the study show that significant fuel gas consumption and emission reductions could be achieved. Moreover, the amount of wind power able to be integrated into the platform is a function of the power generation strategy. When the base load is maximum, the two gas turbines should both be in operation and the estimated wind power that could be integrated is between 20 MW and 25 MW. When the load reaches its minimum of 19 MW, only one gas turbine should be in operation and the estimated maximum amount of wind power would be between 10 MW and 15 MW. The loss of wind power is critical when the amount of wind power integration is increased, and this fact was used to identify the maximum amount of wind power to be integrated into the stand-alone electrical system, keeping voltage and frequency fluctuations at an appropriate level. Wind power is also dissipated if more is produced than the required amount.

Based on this case of study, an interesting possibility opens up: integrating the wind farm and offshore platform with a CAES system would allow to store the excess energy produced by the wind farm in the form of compressed air and to utilise it during low wind speed periods. Such a hybrid system comes with many complexities. Optimal design of the sub-

systems and their sizing is a function that must consider efficiency, economical constrains, physical constrains. Moreover, the coupling of these different systems must be considered, together with an effective control strategy that must provide the necessary flexibility to ensure continuous extraction of the crude oil.

Master's thesis work [10] aimed to do a cost optimization for an integrated system comprised of a wind farm, a CAES storage system and an oil and gas platform. The results and conclusions will be briefly discussed below.
The platform has a peak demand of 70 MW, and a load variation between 91.4% and 100% over the course of 24 hours. The wind park is sized to ensure 115% wind energy penetration, with the additional 15% accounting for imperfect storage efficiencies. The thesis investigates the feasibility of different scenarios. The base scenario involves the use of back-up generators (standard gas turbines) of 20 MW each, to supplement the base power production to meet the demand profile only when energy storage is not available. Simulations are carried out for a case with no CAES storage and with CAES storage. Results showed that the CAES option yields a cheaper net result than the scenario with no energy storage. In particular, utilising a 2.12 MW CAES with 2,622 MWh storage capacity will be cheaper, as it demands one less GT turbine. This means that without a storage four gas turbines are required instead of the three with the CAES technology.

1.3 Objectives

The primary objective of this work is to evaluate feasible process configurations based on compressed air energy storage system (CAES) in order to reduce the GHG emissions of offshore oil and gas extraction facilities.

The main aim is to remove the need for the shared-load gas turbine operation on the platform, which currently represents a significant source of CO_2.

A variety of parameters are studied:

- Wind farm size (up to 45 MW)
- Storage pressure (11, 40 and 70 bar)

- Heat recovery from the exhaust gases to pre-heat the air extracted from the storage

Most of the works found in the literature regarding this topic focus on design conditions and often only include steady state analyses, therefore do not take into account the inevitable variations caused by the frequently intermittent nature of the wind.

This work aims to account for:

1) The different heat and power demands required by the offshore facility, which vary across its lifetime, in accordance to the evolution of the production profile. The demands are thus described as an annual sequence of steady state conditions, allowing the evaluation of key parameters during a long time span.

2) The variable nature of the wind, which deeply affects the off-design conditions and performances of the system. In particular, the system is described for each year as an hourly sequence of steady state conditions. While this time span does not allow to include the effect of wind gusts (which occur at much smaller time scales), it is accurate enough to reflect the evolution of the wind speed profile during the year, and thus to account for its effects on the equipment (compressors, turbines, size of the storage).

It is therefore important that the models of the various components, defined in MATLAB and EXCEL, are given particular attention to the off-design operation, in accordance to energy requirements and constrains of the case study.

1.4 Thesis organization

This work consists of eight different chapters.

Chapter 2 is the literature review and technological background of the three main subsystems: offshore platforms, wind energy, compressed air energy storage systems.

Chapter 3 introduces the models and the methodology used for the analysis, with particular attention to the off-design behaviour of the components.

Chapter 4 describes and investigates the case study, pointing out the reasons of its inefficiency.

Chapter 5 introduces a renewable source of energy (in the form of an offshore wind farm) into the system and evaluates its effects.

Chapter 6 analyses the introduction of a CAES system and evaluates the performance of the plant concerning different design choices and parameters.

Chapter 7 aims to include a small economic analysis for the studied configurations, in order to figure out the economical attractiveness.

Chapter 8 brings the conclusions and suggestions for further work.

2 TECHNICAL BACKGROUND

This chapter is divided into three main subsections: offshore oil and gas platforms; offshore wind energy and compressed air energy storage systems.

2.1 Offshore oil and gas platforms

2.1.1 Generalities

Oil and Gas platforms cover the upstream component of the oil and gas industry. Upstream is a term commonly used to refer to the searching for, recovery and production of crude oil and natural gas. The extraction is usually carried out through the drilling of wells, and is made possible thanks to the pressure gradient existing between the reservoir and the outer environment. Since pressure is the main driver for the recovery of crude oil, its natural diminishing due to exploitation of the well gives rise to the depletion phenomenon, which consists in the decreasing production of the site.

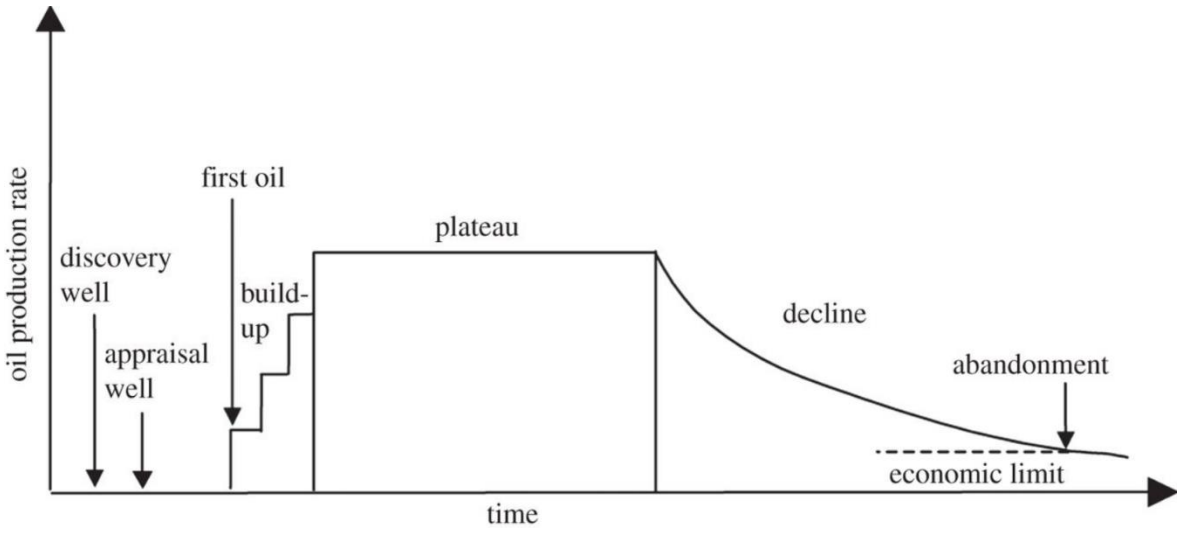

Figure 2-1: Standard production profile for oil and gas extraction [11]

From Figure (2-1), the production period can be divided into three main moments:
The first, commonly short, results in the increase of the rate of production; this behaviour is due to the fact that wells are not fully completed yet, and need time to reach effective productivity. The second is the so-called “plateau”, which lasts for several years, and is the

most important phase of the platform's lifetime. During this period, production rate is kept constant at the maximum planned level, thanks to enhancing oil extraction techniques. The third moment, the production's decline, is the longest phase, and consists in a slow but inexorable decrease of the production rate, due to the depletion of the reservoir. The plant stops operating when the production rate falls under certain limits, which make the recovery and treatment processes not economically feasible anymore.

A peculiarity of the oil and gas sector, in particular for offshore platforms, is the "spare philosophy". A stop in the recovery process will likely cause a huge economical loss, since the products stop being produced and exported. Therefore, the plant has to ensure a continuous production, limiting to the minimum the shutdowns. To fulfil this important requirement, most components have a spare twin, which is kept ready for the times when a breakdown or a maintenance operation occur.

The main equipment is normally designed to perform at peak conditions, even though power and heat demands vary significantly over time. Therefore, for most of its life, the plant is operating in conditions far from design, with a consequent reduction in its efficiency.

Another key aspect is the stringent limitation concerning the maximum space or weight tolerable on-site, so system layouts with low equipment inventory and simplicity are often preferred to more complex configurations.

Oil and gas platforms present similar structure designs, but they process petroleum with different characteristics and operate on fields with different properties. Generally, an oil and gas facility can be divided into two main sub-systems: a processing plant, where oil, gas and water are separated and treated, before being exported to the shore or rejected to the environment; and a utility plant, where the power and the heat required for the processes are produced. Factors such as the well-fluid thermos-physical properties, chemical composition, gas to oil and water to oil ratios, reservoir properties (temperature, pressure, permeability) may strongly differ from one field to another, which implies different technical considerations and technological choices apply for different cases.

For what concerns North Sea oil platforms, although design differences exist, it is worth noticing that gas purification and exportation, waste water treatment and seawater injection,

have become the most preferred gas and water processing routes in this region. Since North Sea's crude oil and natural gas are characterised by a low content of salt, hydrogen sulphite and carbon dioxide, neither desalting nor sweetening units are required. Typical processing platforms consist of eight different sub-systems:

- Production manifolds
- Crude oil separation
- Oil pumping and export
- Gas re-compression and purification
- Gas compression, lifting and exportation
- Wastewater treatment
- Seawater injection
- Power generation

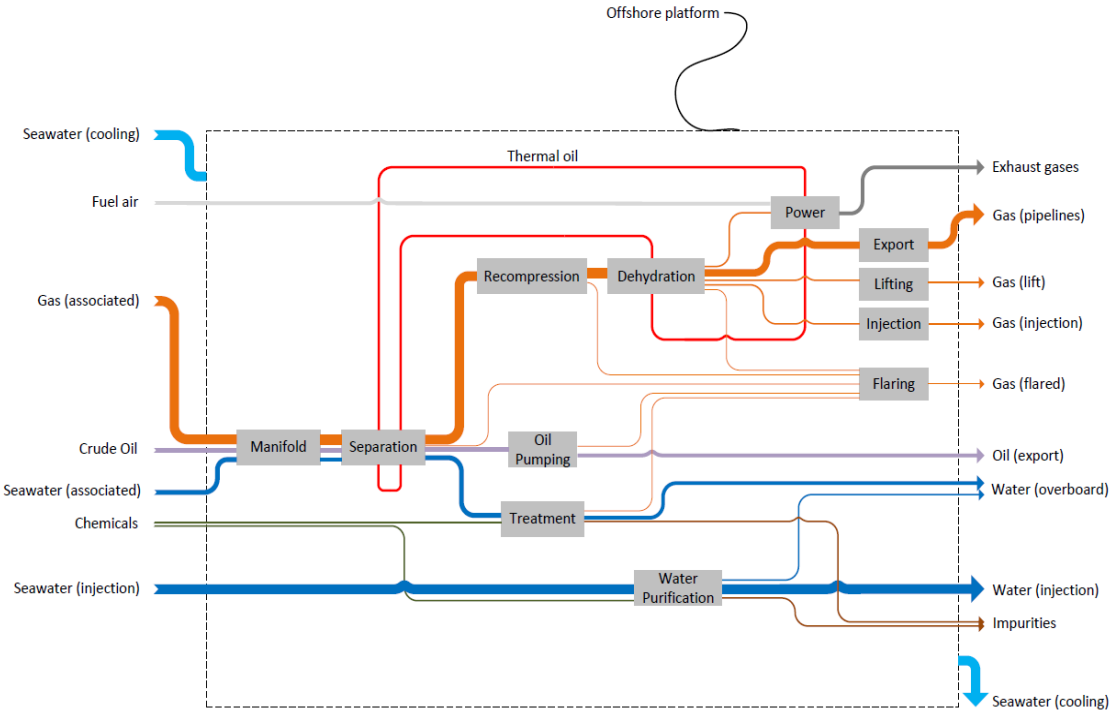

Figure 2-2: Conceptual layout of processes on platforms in the North Sea [12].

Crude oil contains a large variety of multiple chemical compounds such as alkanes, alcenes, and aromatics, ranging from light to heavy, branched to cyclic and saturated to unsaturated hydrocarbons. Complete compositional analyses are rarely carried out, which implies that the exact composition of crude oil (natural chemical compounds and amounts) is usually unknown. In general, crude oil is characterised by conducting a true boiling point (TBP)

analysis, in which crude oil is separated into distillate fractions. Afterwards, molecular weight, viscosity, specific density are measured for each distillate, and thermal properties such as heating values and thermal conductivities are estimated by empirical correlations. Gas may either be mixed with oil and enter the platform system through the same wells (associated gas) or be processed apart via specific wells (non-associated gas). Associated gas is the most common encountered case in offshore processing.

Crude oil treatment and separation

The first treatment process undergone by the crude oil is the physical separation of the three main phases; the purpose is to obtain a gas stream and a stabilized oil stream. Petroleum extracted through the wells is transferred to the platform complex via a network of pipelines and a system of production manifolds. The individual streams are mixed and depressurised by choke boxes, which consist of valves and chokes, and finally fed to the separation train. Crude oil separation is promoted by gravity and takes places in stages operating at different pressure levels. Pressure is decreased along the train by a series of throttling valves and the temperature of the separator is increased by heat exchange with a thermal fluid to increase the separation efficiency. When working under normal separation conditions (the oil has low viscosity and medium-low density and the separation of water does not require special features), it is sufficient to use three-phase gas-oil-water separators. The amount of oil separated and hence the efficiency of the separation process depends on different factors, namely: crude oil composition, temperature and pressure. The oil separation process is the main heat consumer.

Gas purification and recompression

Product gas from the separation processes is recovered and sent to the recompression train (as it has lost most of its pressure during the separation phases). Temperature is decreased to lower the compression work and liquid droplets are separated and removed, resulting in a relatively dry gas ready for re-compression. Once the gas is at the design pressure, there is a need for dehydration unit to prevent corrosion issues in gas pipelines. Dehydration is usually achieved by a glycol absorption/desorption system. A certain fraction of the dry gas is usually recycled to control the volume of the gas entering the compressor and to prevent surge issues.

Wastewater treatment

Downstream cleaning of the produced water is essential for environmental and legislation reason. The water from the separation and purification processes enters a cyclone in which suspended particles and dissolved hydrocarbons are removed. Afterwards, it passes through a series of valves and flows into a degasser, where the last oil and gas traces are recovered before disposal to the sea.

Seawater injection

In parallel with the oil and gas processes, seawater is treated on the platform for further injection into the reservoir, in order to sustain high pressure conditions and to enhance oil recovery. The injected fluid must meet strict quality requirements to prevent corrosion and reservoir degradation: it is thus cleaned before being pumped into the reservoir. The seawater injection train includes a succession of filters to remove solid impurities, deoxygenation towers and high-pressure pumps. As time goes on, a larger seawater volume must be injected into the oil reservoir to keep the recovery of crude oil at acceptable levels, meaning more and more power to pump the water to the needed pressure is required.

Gas lifting

Due to the seawater injection, the density of the fluid in the reservoir increases with time, enhancing the difficulty for an efficient extraction of the crude oil. For this reason, fraction of the dry gas can be used for lifting, which consists in injecting gas at high pressure into the reservoir through the oil wells, in order to increase crude oil recovery, as it artificially lowers the density of the mixture. Lifting gas is cooled and scrubbed to further remove heavy hydrocarbons and to decrease the power requirements of the compressors.

Power generation

Electric power required by the processes is usually produced by gas turbines directly on-site. Turbines are selected considering the maximum expected power requirement over the offshore facility's life. However, for reliability matters and in order to prevent unexpected plant shutdowns, power generation is usually shared amongst multiple gas turbines running part-load, which implies that their maximum thermal efficiency in not reached. GTs are usually aero derivative in the 10-25 MW range. Large facilities have great power demands, from 30 MW upwards to several hundred MWs. If exhaust heat is not needed in the main processes, it can be used to drive bottoming cycles (steam or ORC) by using an HRSG (heat

recovery steam generator). It should be underlined that compressors on offshore platforms are characterized by a relatively low isentropic efficiency, and the use of anti-surge gas recycling has impact on the train power consumption.

Heating and cooling utility systems

Heating is ensured by the waste heat recovery system connected to the gas turbines. In general, the highest temperature level of the platform is found at the reboiler of the desorption column. Heating is often achieved through steam generation, which is widely used and its production is responsible for large amount of energy requirement. Steam is also used as an energy carrier in some separation stages to heat up the crude oil incoming from the reservoir and for minor operations such as heat, ventilation, air conditioning and cleaning operations.

Cooling water is utilised to decrease the amount of heavy hydrocarbons entrained with natural gas and to prevent foaming and low loads in the separation systems. The rejection temperature to the environment is constrained to a maximum of 25°C.

Flaring

Traditionally, flaring took place then it was not economically feasible to treat the gas and commercialized it. Considerable amount of hydrocarbons have been more or less continuously flared. Strong environmental focus has eliminated continuous flaring; vapours and flare gas are normally recovered, and only in exceptional circumstanced does flaring occur.

2.1.2 Energy and Exergy analyses

Several studies and reports have been published regarding this topic [12-15], so the aim of this section is to summarize them and underline the most important results.

Usually, the major electricity consumer is the compression train, which is responsible of around 50% of the total power demand. The seawater injection process ranks second with a share of about 20%. The third greatest power demand of the offshore facility is either the gas recompression process or the oil pumping, depending on the gas-to-oil ratio of the reservoir. Therefore, electric power is mostly required for compression and pumping

processes, while a marginal fraction is supplied to other auxiliary units such as lights system, air conditioning etc.

The produced water and exhaust gases from the power generation system have a small specific exergy content. Operations such as compression and pumping, which aim to increase the physical exergy of the gas and oil flows, have a minor impact on the total specific exergy of these streams. The input and output exergies of the offshore facility are dominated by the chemical exergy content of the oil and gas streams, which is at least a hundred times greater than their physical exergies, and ranges between 43 to 48 MJ/kg. Therefore, most of the exergy found at the outlet of an offshore platform is carried out by these two streams.

The total destroyed exergy, including both the processing and the utility systems, is in the range of several tens of MW, with around 65% of this value attributable to the gas turbines and waste heat recovery systems, while the rest (35%) to the oil, gas and seawater processes. The largest exergy destruction of the overall system lies, in any case, in the combustion chambers of the gas turbine cycles, and amounts to almost half of the total exergy destruction of the rig. In can be split into thermodynamic irreversibility due to mixing of natural gas and compressed air and to the combustion process itself. This shows that the variability of the well-fluid composition has a moderate effect on the output, but has a significant impact on the share of exergy destruction across the processing plant. The results also indicate that the largest thermodynamic irreversibility of the processing section occurs in the production manifolds and in the gas compression system, followed by the recompression and separation modules. In contrast, the contributions from wastewater treatment and the seawater injection processes are negligible, and the exergy destruction taking place in the oil pumping step is moderate in most cases. The exergy destruction in the manifolds is caused by the depressurisation without generation of any useful product. The second largest irreversibility is found at the gas compression train, due to the poor performances of the compressors and to the recycling around these components to prevent surging. Significant exergy destruction also takes place in the recompression step, because the streams flowing out of the separation train are mixed at different temperatures and compositions.

The exergy losses are nearly constant for every platform: they are related to effluent streams rejected into the environment without being valorised, such as flared gases, discharged

seawater, wastewater and exhaust gas from the GT. Approximatively 60% of the total exergy loss is due to the direct rejection of high temperature exhaust gases. About 30% is associated with the flaring and ventilation of natural gas throughout its processing. The remaining 10% is related to the exergy content of cooling and wastewater discharged overboard: these exergy losses are small, as the discharged streams are rejected at nearly environmental conditions. A comparison on the irreversibility ratio suggests that the offshore processing becomes less performant with increasing gas-to-oil and water-to-oil ratios and it also indicates that the total exergy lost and destroyed represents only 0.5 to 1.5% of the total exergy flowing into the system.

The exergy analysis shows that exergy is introduced onsite in the form of raw materials (crude oil, fuel air, seawater and chemicals) and exits in the form of valuable products (oil and gas sent onshore) and waste streams (water, exhaust and flare). The chemical exergy of the reservoir fluid flows through the platform system and is separated into the oil and gas chemical exergies with only minor destruction in the processing section, as no chemical reactions take place. On the opposite, chemical exergy is consumed to a great extent in the utility section, as a fraction of the natural gas produced is used and combusted.

This exergy analysis suggests improvements that could be made to increase the overall performance, reducing or eliminating exergy losses. As discussed previously, the largest thermodynamic irreversibility is found at the combustor. In theory, it could be reduced by decreasing the air to fuel ratio, but this would imply temperatures closer to the adiabatic flame temperature, thus provoking significant thermal stress on the components. The exhaust gases leaving the waste heat recovery system are rejected at high temperature into the atmosphere, leading to a large exergy loss. The excess heat contained in the flue gases could be partially recovered by producing electricity using a bottoming cycle, such as a Rankine or ORC. Another improvement is to avoid continuous flaring: the gases sent for flaring could be recovered in the processing plant. This presents the combined benefits of decreasing the exergy losses, reducing the environmental impact and recovering more gas for sale. The irreversibility taking place in the production manifold could hardly be reduced, as lower pressure of the well-fluid is required at the inlet of the separation train. Higher pressure levels would lead to smaller destruction rates, although this might result in lower gas recovery and conflict with the process constrains of other system section. Substantial exergy destruction is associated with the gas compression train, as the compressors typically used on oil

offshore platforms are featured by a relatively low isentropic efficiency and gas recirculation, since flow variations are expected and surge must be prevented. The compressor's performance could be increased by re-wheeling, implementing variable speed drive systems, using alternative control methods and adjusting the stagger angle of vanes. Another possibility is to integrate compressors of different sizes in parallel so that the majority of them is operated near their optimal operating point.

2.1.3 Gas turbines for the offshore environment

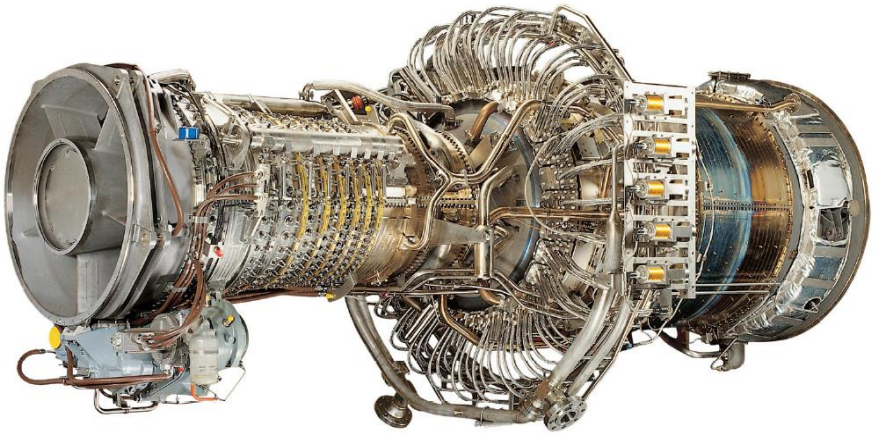

Figure 2-3: GE LM2500+G4 gas turbine [16]

On offshore platforms, relevant and continuous supply on energy is required, and it must be produced taking into account the limited amount of surface available on those kind of plants. Gas turbines offer high reliability, compactness, almost null vibrations, contained weight and most importantly are able to use the fuel as it is extracted by the reservoir. Being able to generate the required power directly offshore removes the need to rely on onshore supply, which can become hard the farther away the platform is and susceptible to weather conditions. Aero-derivative turbines, moreover, have the advantage of being easy to remove and to replace, allowing for onshore maintenance with an expert crew, which may not always be available on the rig. In addition to that, exhaust gas from the turbine's outlet are generally at high enough temperatures (400-500°C) to be used to satisfy other needs, as the desalination of water, heating, etc. It should be underlined that the offshore environment is strongly saline, and can lead to corrosion, especially on the engine's hot spots. For this reason special materials must be used for the realization of those special turbines.

Offshore facilities are usually not connected to the grid, and the demand is met with the use of gas turbines directly on site. It is therefore particularly important to satisfy the power and heat demands in a reliable and continuous way, even in unexpected operating conditions. From this need, the GTs on offshore rigs are traditionally operated in a load-sharing mode: the demand is met by running multiple GTs together (in addition to the extra one needed for the "spare philosophy") in part load conditions. This provides the system with additional flexibility, making it easier to tackle sudden and large variations in the power demand, while at the same time ensuring high reliability and responsiveness. On the other hand, it inevitably leads to higher fuel consumption and lower efficiency, as the turbines are operated far from their design conditions for most of their lifetime.

Common engines found on offshore platforms are the SGT-500 [17] developed by SIEMENS and the LM2500 series by General Electric [16].

2.1.4 Compressors for the offshore environment

Compressors are major components and have a deep impact on the energy request of the whole platform.

Compressors used in the oil and gas industry are divided into groups according to their intended service. For example, lifting and reinjection require compressors capable of providing very high pressure ratios but small flow rates. On the other hand, lower pressure ratios but high flow rates are typical of the air compression for power generation and the gas recompression. The most common compressors found in the offshore oil and gas industry are centrifugal or reciprocating. Axial compressors are less common, as they require very high flow rates and are more susceptible to variations in the incoming flux (steep characteristic).

Compressors in oil and gas platforms are subject to varying flow rates. This can lead to the dangerous phenomena of the surging, which is more pronounced in centrifugal compressors. Set a constant speed, as the flow decreases, the working point shifts towards the surge line. At the left of this line, as flow decreases, pressure decreases as well. This leads to a flux inversion with high frequency and amplitude, which can damage the compressor.

Traditionally, in order to avoid surge, offshore platform recirculate variable amounts of gas in order to keep the flow rate above the surging line. This leads to additional power and fuel consumption. A more efficient approach requires the possibility to change the speed of the compressor. As the flow rate decreases, the speed could be decreased to a proper level and the surge danger avoided, while keeping the wanted isentropic efficiency. Stall and choking are other factors that limit the ratio between outlet pressure and flow rate.

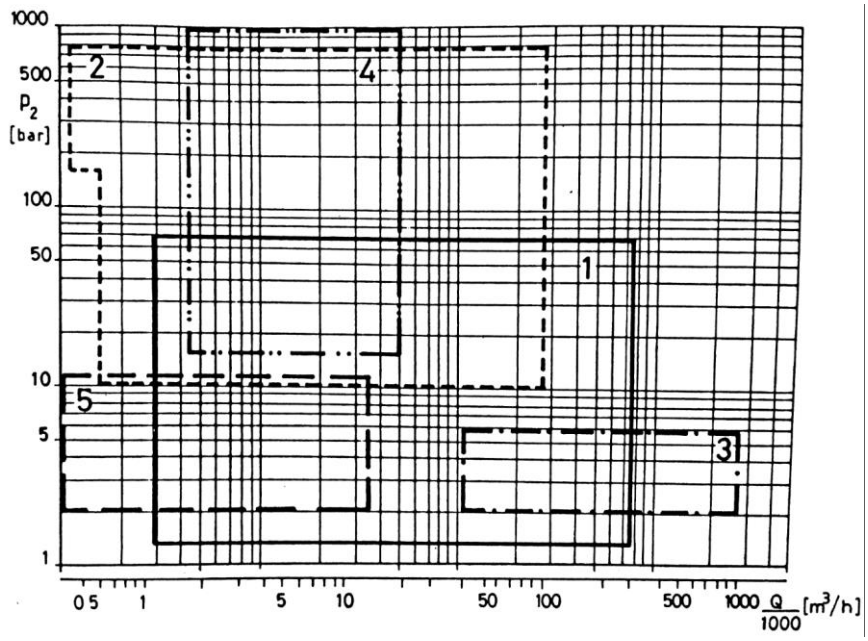

Figure 2-4: Compressor map. It is possible to distinguish 1 as the centrifugal compressor with horizontal opening, 2 as the centrifugal compressor with vertical opening, 3 as the axial compressor, 4 as the reciprocating compressor, 5 as the rotative compressor [18].

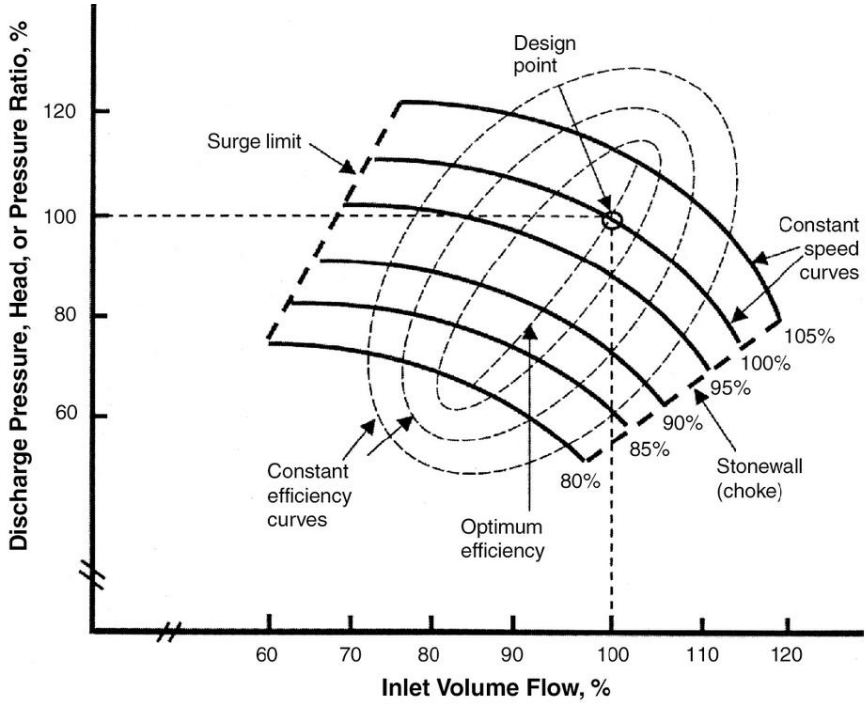

Figure 2-5: Example of a compressor's characteristic curve

2.2 Offshore wind energy

Recent years have seen an exponential growth of wind plants' installed power, and subsequently of the electrical energy produced by wind turbines. In 2015 alone, 63 GW have been installed worldwide, which represents a 22% increment over the previous year, reaching a total installed power of about 430 GW. It is estimated that within the year 2020, 12% of the total world requirement for electricity will be provided by wind energy alone.

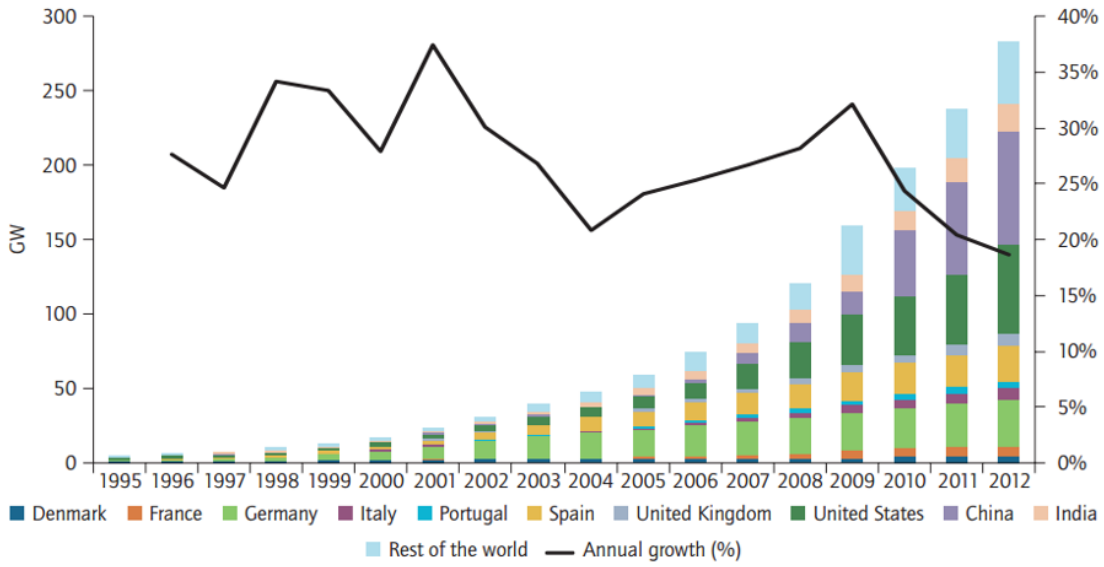

Figure 2-6: Global cumulative growth of wind power capacity [19]

2.2.1 Modern wind turbines

The power output for a wind turbine is given by the expression

$$P = \frac{1}{2} C_p U^3 \rho A \qquad (2.0)$$

Where

ρ is the density of air (1.25 kg/m^3)

Cp is the power coefficient

A is the rotor swept area

U is the wind speed

The density of air is rather low, 800 times less than water which powers hydro plants, and this leads to the large size of a wind turbine. Depending on the design wind speed chosen, a 3 MW wind turbine may have a rotor that is more than 90 meters in diameter. The power coefficient describes that fraction of the power available in the wind that may be converted by the turbine into mechanical work. It has a theoretical maximum value of 0.593 (the Betz limit) and rather lower peak values are achieved in practice. The power coefficient of a rotor varies with the tip speed ratio (TSR), and it has a maximum for a single value of the TSR. Another important parameter is the Capacity Factor (CF)

$$CF = \frac{Nominal\ Power}{Generated\ Power} \qquad (2.1)$$

The capacity factor (2.1) indicates for how much of the time the turbine works at its nominal power. Capacity factors are usually lower than 0.5. Offshore wind farms have higher values compared to the onshore ones.

The three major elements of wind generation are the turbine type (vertical or horizontal axis), installation characteristics (onshore or offshore) and grid connectivity (connected or stand-alone). Most large turbines are upwind horizontal-axis with three blades. With aerodynamic energy loss of 50-60% at the blade and rotor, mechanical loss of around 4% at the gear, and a further 6% electromechanical loss at the generator, overall generation efficiency is typically in the range of 30-40%. The majority of today's turbines are designed and built to utility scale; the average turbine is rated at 2-3 MW capacity. As the power available from the wind increases with the cube of the wind speed, all wind turbines need to limit their power output at very high wind speeds. There are two principal means to accomplish this, with pitch control on the blades or with fixed, stall-controlled blades. Pitch-controlled blades are rotated as wind speeds increase so as to limit the power output once the rated power is reached; a reasonably steady output can be achieved, subject to the control system response. Stall-controlled rotors have fixed blades which gradually stall as the wind speed increases, thus limiting the power by passive means. These dispense with the necessity for a pitch control mechanism, but it is rarely possible to achieve constant power as wind speeds rise. Once peak output is reached the power tends to fall off with increasing wind speed, and so the energy capture may be less than that of a pitch-controlled machine. In the early days of the industry, the merits of the two designs were finely balanced and roughly equal numbers

of each type were being built. Since the turn of the century, however, pitch-controlled machines have become much more popular. This is due to advances in pitch control, which allow larger and lighter machines compared to stall technology. Another reason is the lower efficiencies attained with stall systems when the wind speed is too high and the rotational speed is therefore decreased.

2.2.2 Wind characteristics

Since the energy available in the wind varies with the cube of the wind speed, an understanding of the characteristics of the wind resource is critical to all aspects of wind energy exploitation.

From the point of view of wind energy, the most striking characteristic of the wind resource is its variability; the wind is highly variable, both geographically and temporally. Furthermore, this variability persists over a wide range of scales, both in space and time. On a large scale, spatial variability describes the fact that there are many different climatic regions in the world, some much windier than others. These regions are largely dictated by the latitude, which affects the amount of insolation. Within any one-climate region, there is a great deal of variation on a smaller scale, dictated by physical geography and on an even smaller scale by obstacles such as trees and buildings. Moreover, at a given location, temporal variability can be on a large scale (one year or more), on a medium scale (seasonal, diurnal and hourly variations) and finally on the short scale of minutes to seconds or less (wind gusts). On the shortest timescales, wind speed variations are known as turbulence and have a very significant impact on the design, performance and instantaneous power generation of the individual wind turbine, as well as on the quality of the power delivered and its effect on the consumers.

Turbulence is generated mainly from two causes: friction with the earth's surface and thermal effects which can cause air masses to move vertically as a result of temperature variations and hence in the density of the air. Turbulence intensity is the measure of the overall level of turbulence and depends on the roughness of the ground surface and the height above the surface, as well as topographical features and thermal behaviour of the atmosphere. This means that higher wind speeds are available offshore compared to land.

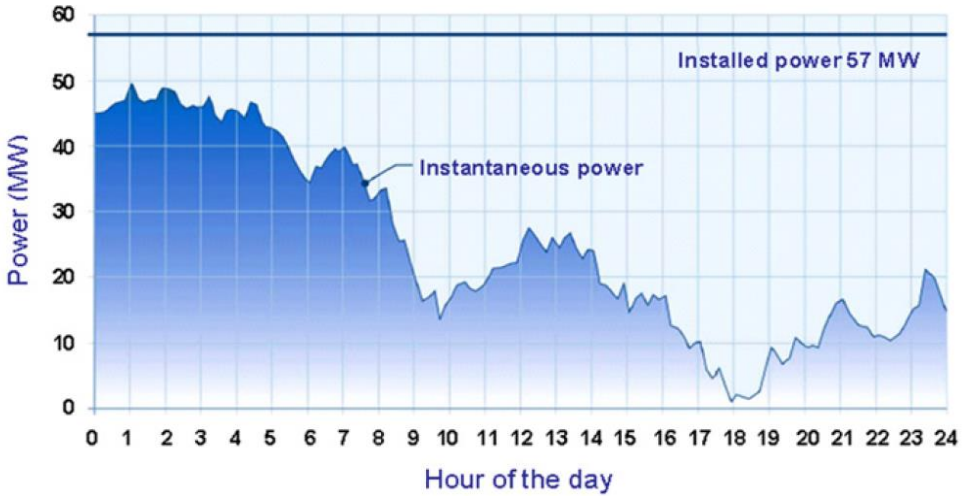

Figure 2-7: Instantaneous power at a wind farm in Canada [20]

2.2.3 Offshore and North Sea

The annual report made by windeurope.org [21] gives an interesting overview on the offshore wind situation. Europe's cumulative installed offshore wind capacity at the end of 2016 reached over 12000 MW, across 81 wind farms in 10 European countries.

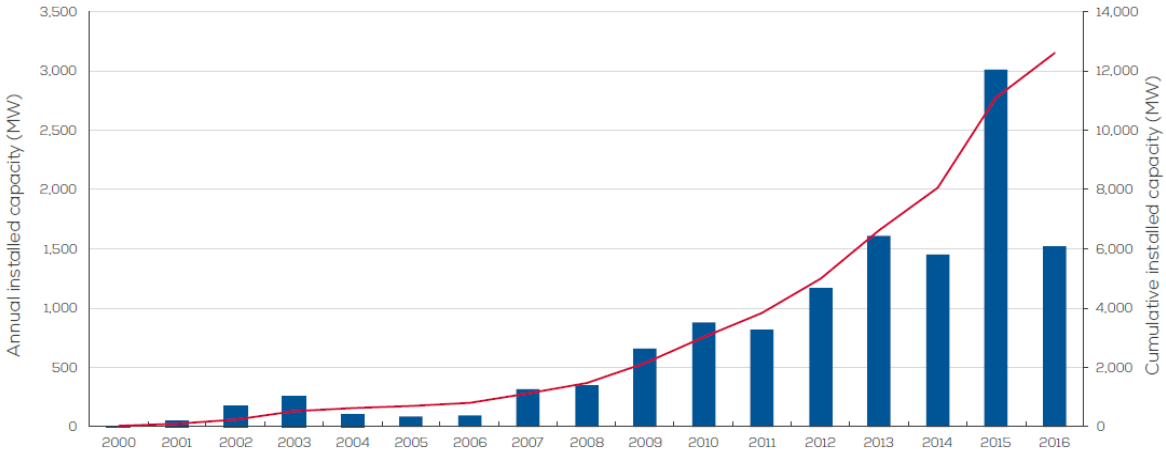

Figure 2-8: Cumulative and annual offshore installations [21]

The rated capacity of offshore wind turbines has grown by 62% over the past decade. The average rated capacity installed in 2016 was 4.8 MW, an increase of more than 15% over the previous year. Moreover, 8 MW turbines were installed for the first time, reflecting the rapid pace of technological development. The size of wind farms has also increased dramatically over the last decade, reaching an average value of more than 370 MW in 2016.

In addition to this, the average depth of offshore wind farms with grid-connection in 2016 was 29.2 metres and the average distance to shore was 43.5 km, both an increase over 2015. The annual load factors of offshore wind in the North Sea region ranges from 33% to 42%, and varies with the country.

Offshore wind resource characteristics span a range of spatial and temporal scales and field data on external conditions. For the North Sea, wind turbine energy is around 30 kWh/m^2 of sea area, per year, delivered to grid. The energy per sea area is roughly independent of turbine size. Necessary data includes water depth, currents, seabed, migration, and wave action, all of which drive mechanical and structural loading on potential turbine configurations. Average wind values are between 8 to 11 m/s, depending on the specific location and hub height.

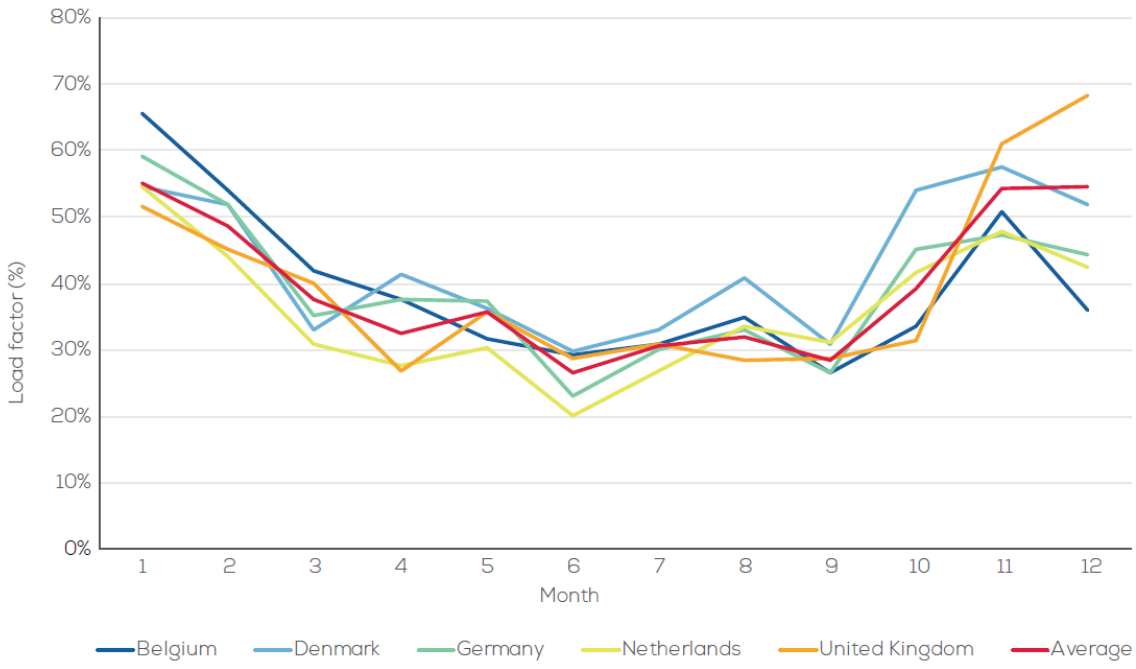

Figure 2-9: Monthly national load factors [21]

2.2.4 Wind energy and electrical energy storage (EES)

Due to the intermittent nature of wind power, the integration into power systems brings inherent variability and uncertainty. The impact of wind power integration on a system's stability and reliability depends on the penetration level. From a reliability point of view, at

a relative low penetration level, the net-load fluctuations are comparable to the existing load fluctuations. As the wind penetration increases, more operating reserves are required, in order for them to have a short enough response time during sudden and large changes of wind power production and load due to random failures and wind gusts. The wind power variation can also degrade the grid voltage stability due to a surplus or a shortage of power. EES has the potential to cover the following aspects: Through time shifting, the power generation can be regulated to match the loads; it can also be used to balance the grid through ancillary services (load following and load levelling). Moreover, it can meet increasing requirement of reserves to manage the uncertainty of wind generation, increasing the system efficiency, enhancing power absorption and achieving fuel cost savings and reducing CO_2 emissions. Additionally, the EES has the potential to smooth out fluctuations, and improve supply continuity and power quality.

The non-guaranteed power production from wind parks can be especially problematic in small autonomous systems, or in those with high wind power penetration. Wind turbines are vulnerable to even slight variations of the system's frequency or voltage amplitude, possibly leading to a total blackout, especially in cases of weak and non-interconnected systems. To avoid this, the wind power penetration is restricted up to a maximum percentage of the power demand; this percentage depends on the size of the system, the available reserve given by thermal plants, and weather conditions. It is usually set at 30% of the total power demand [28]; the excess wind power is wasted. Moreover, the stochastic power production from wind parks cannot follow the power demand variation by itself adequately. This prevents the maximization of wind parks' power production in autonomous systems; in these cases, although the power demand could be totally covered by wind energy, this possibility is not feasible due to the unpredictability of the renewable resource.

The above-mentioned problems can be handled with the introduction of electrical storage systems cooperating with the wind parks. With the support of EES, in fact, the stochastic power production from wind can be adapted to the power demand, through charging and discharging periods, whenever there are wind power surpluses or shortages. This combined system actually converts the stochastic power production into guaranteed power, thus enabling the power plant to follow adequately the varying power demand and to approach higher annual energy production penetration.

Offshore wind parks are always power plants of several tens to hundreds of MW of installed power, as this is the only way to compensate for the increased set up cost of the offshore applications, compared to on shore installations. The storage required for such electricity quantities must exhibit a charging and discharging ability approximately equal to the wind park's nominal power and a total energy capacity which can be between 1% and 3% of the total annual electricity productions, depending on the size of the park and the system connected to it, as well as the operational algorithm of the wind park-storage plant station [28]. This means that, although many EES technologies exist, only CAES and PSS (pumped storage systems) are practically suitable to manage such a large quantity of energy. CAES, with its high reliability, economic feasibility, and low environmental impact, is a promising method for large-scale energy storage. Although there are only two large-scale CAES plants in existence, recently, a number of projects have been carried out around the world, and some innovative concepts have been proposed [22-27]. Existing plants have some disadvantages, such as energy losses due to dissipation of heat during compression, use of fossil fuel and dependence on geological formations.

2.3 Compressed air energy storage (CAES)

2.3.1 Generalities

Recent years have seen an increasing interest in electrical energy storage systems (EES), mostly due to the drastic changes that are undergoing in the electric power generation. The last few decades have seen an increasing shift from the traditional large and centralized fossil fuel power plants to a more decentralized production, which includes different types of renewable energy resources, as a consequence to the growing awareness on climate change. However, this shift represents a major challenge for the power network, mainly due to supply-demand imbalances. Load levelling is initially based on the prediction and forecasting of the daily and seasonal needs, and, when production is not sufficient, it relies on the contribution of secondary reserves, such as hydroelectric plants. The introduction of deallocated production and of variable, fluctuating and often unpredictable renewable resources, increase the difficulty of stabilizing the power network. More than ever then, the storage of electrical energy has become a necessity, as it is convenient to generate the energy, transmit it, convert it and then store it until needed.

There are two types of energy production for which storage is important:

- Conventional energy production, the storage of which could compensate for a temporary loss of production of a generating unit and fulfil a commercial obligation, thus avoiding penalties.

- Renewable energy production, the storage of which adds value to the resource, by making it predictable (for example, allowing to deliver electrical power during peak hours).

Moreover, EES not only is beneficial for the levelling of peaks of the network, but is also interesting for power applications in isolated areas, which are off the grid, because it can increase the maximum penetration level of renewables, otherwise limited by their unpredictability.

Summarizing, electrical energy storage can be attractive for the following reasons, as it:

- Helps meeting peak electrical load demands
- Can be used for peak shaving and load levelling
- Provides time varying energy management
- Alleviates the intermittence of renewable source power generation, thus allowing for a deeper penetration in both on the grid and off the grid applications
- Improves quality and reliability, sustaining frequency and voltage at the required levels
- Supports the realization of smart grids
- Reduces electrical energy import during peak hours
- Helps the management of distributed and stand by power generation
- Reduces the power installed and gets the most out of the existing network. This is made possible by the fact that transmission and production equipment are designed as a function of the maximum demand, thus are oversized for off peaks periods. Storage systems would smooth out the average daily consumption curve, reducing the large disparity between peak and non-peak hours.
- Increases the power systems' efficiency, managing effectively the surplus of power generated by renewables, which would otherwise be lost

There are many possible technologies to accomplish energy storage, found in practically all forms of energy (mechanical, chemical and thermal, as examples). The most important technologies are listed below:

- Pumped Hydro Storage (PHS)
- Thermal Energy Storage (TES)
- Compressed Air Energy Storage (CAES)
- Fuel Cells (FC)
- Flywheel Energy Storage (FES)
- Flow Batteries Energy Storage (FBES)
- Supercapacitators
- Natural Gas energy storage (NGS)

The choice of one technology over another depends on the specific application, and must account for constraints and economic criteria.

Successful CAES implementation first happened in 1949, when S. Laval obtained the patent on using air to store power inside an underground air-storage cavern. The world's first utility-scale CAES plant was installed and commissioned at Huntorf, Germany, in 1978. In 1991, another large CAES plant started operating in McIntosh, Alabama, US.

A CAES system operates similarly to a conventional gas turbine (GT), except that the compression and expansion stages take place at different times. This system can be understood as interrupting the Brayton-Joule thermodynamic cycle: the compressed air is injected into a cavern instead of being sent directly to the combustor. When electricity is needed, the pressurized air is extracted from the reservoir and the cycle is completed. The fact that CAES relies on gas turbines for the generation of electricity is of great importance, as these are energy-converting devices with a very mature technology, outstanding reliability and high efficiencies, ranging between 30% and 40%. Moreover, in conventional gas turbines, almost two thirds of the mechanical output from the turbine itself is required by the compression train; in CAES systems compression takes place during low demand periods, allowing the plant to produce three times the power for the same fuel consumption during peaks (as the power for the compression is taken from the grid). Furthermore, if the electricity used during the compression of air derives from renewable resources, the overall efficiency increases drastically compared to a GT power plant.

Usually, during the compression stage, surplus electricity from the grid powers a compression train to achieve high air pressure (between 40 and 100 bar). The storage involves the injection of such air into an insulated reservoir. While the air is being compressed, it passes through inter-coolers and after-coolers to reduce its temperature, thereby enhancing the compression efficiency, reducing the storage volume requirement and minimizing thermal stresses on the storage walls. However, cooling down air arises problems at the moment of the expansion, as the efficiency of the turbine is strictly related to both air temperature and air pressure. For this reason, fuel is oxidized into air, and the products of the combustion process are expanded through the turbine, generating power. In addition to that, the higher the compression ratio, the more heat is lost due to intercooling. Therefore, a trade-off exists between increasing the pressure ratio to improve turbine performance and minimizing compression heat losses. Finally, the exhaust gas from the turbine contains a significant amount of waste heat, which can be recycled using, for example, a heat recovery unit.

There are three main alternatives for CAES plants layouts:
Conventional CAES, which is the one operating in both Huntorf and McIntosh. Is the simplest layout and may or may not adopt the heat recovery unit.

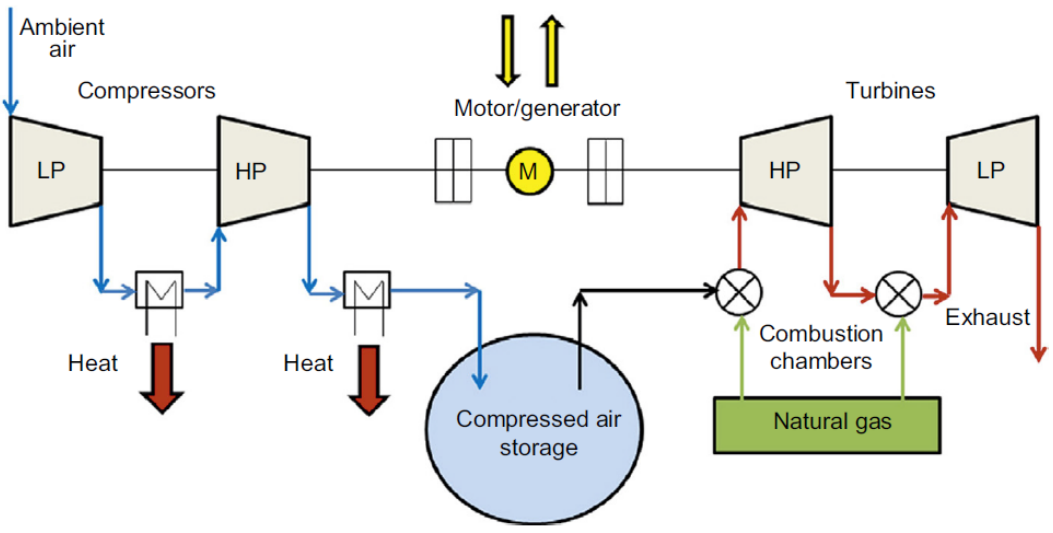

Figure 2-10: Layout of conventional CAES [28]

Using a heat recovery unit allows to increase the total efficiency by up to 10%, as reported by the McIntosh plant. It comes with significant cost, as the heat exchanger itself has a large size due to the low exchange coefficients between two gas streams.

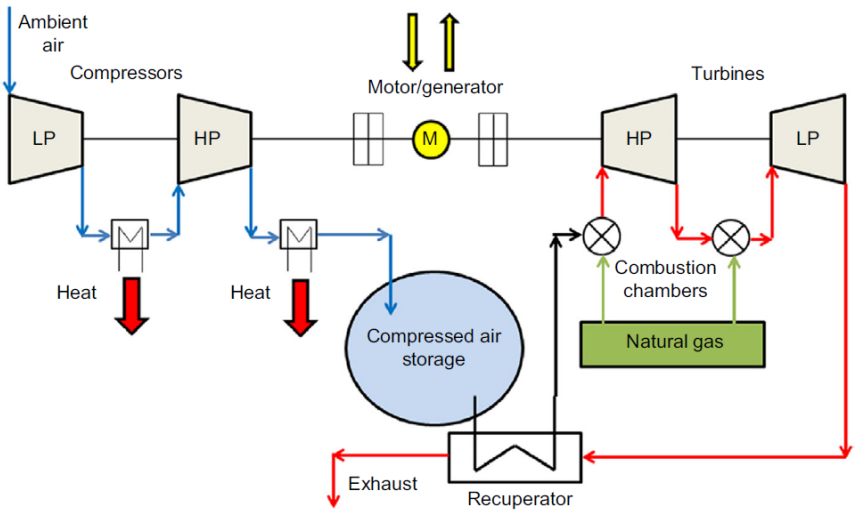

Figure 2-11: Layout of conventional CAES with heat recovery [28]

In the Adiabatic CAES (A-CAES), when a power surplus exists, air is compressed without intercooling and releases its heat in a separate heat storage reservoir before being injected. At discharge periods, the compressed air is heated up to the appropriate turbine inlet temperature (around 600°C) by regaining the heat from the heat storage. Overall efficiencies are expected to reach values up to 70%. The A-CAES eliminates the fuel requirements, thus the CO2 emissions. Moreover, higher outlet temperatures from the compressor are allowed, meaning higher amounts of heat stored. However high capacity storage tanks (120-1800 thermal MWh) need special design to achieve sufficient heat transfer rates and constant outlet temperatures. Minimization of heat losses during charging and discharging of the heat reservoir is also a critical aspect.

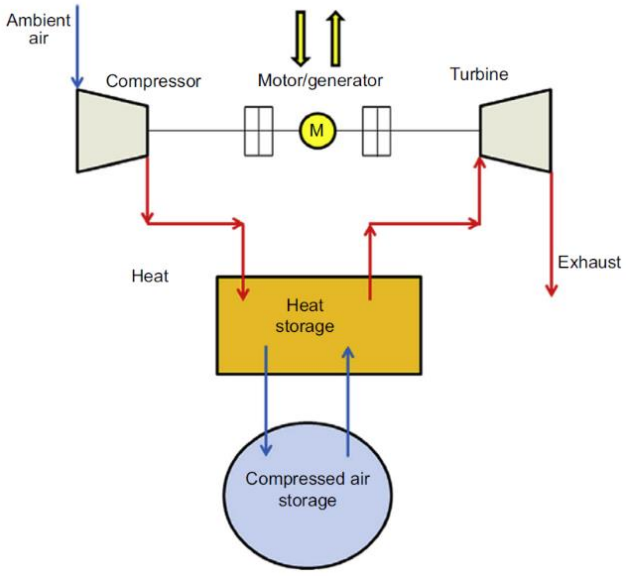

Figure 2-12: Layout for an adiabatic CAES [28]

The third concept is the air injected CAES (AI-CAES). It is based on the injection of the stored and preheated air directly into the compressor discharge plenum to a gas turbine, providing a power increase. Compared to the conventional CAES system, the proposed design patented by Energy Storage and Power Corporation (ESPC) can bring benefits on eliminating the switchover time limitations by decoupling the compression and turbo expander trains, improving energy efficiency.

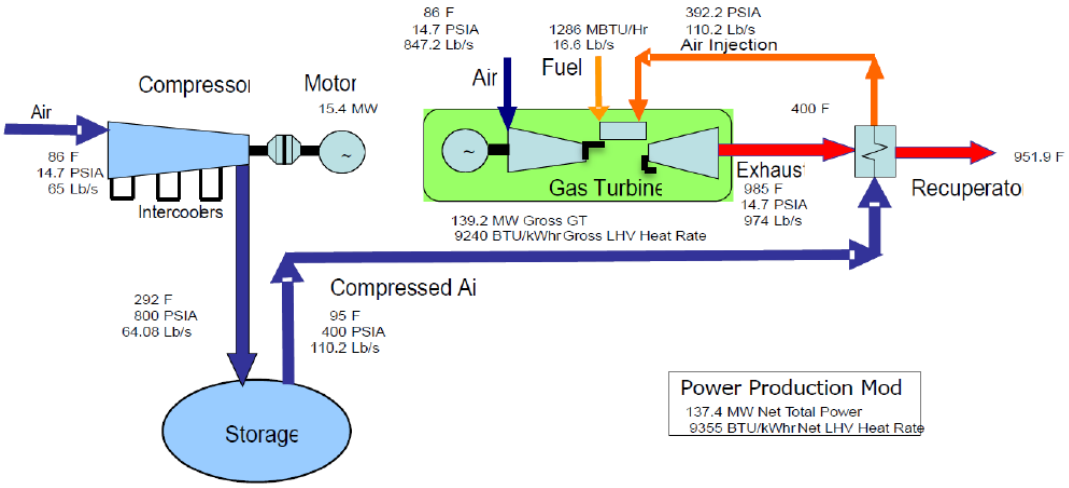

Figure 2-13: Layout for AI-CAES [29]

Comparison between conventional and adiabatic CAES

Conventional CAES has been successfully integrated in the two existing facilities. The compression can be achieved in two or more stages, intercooled and after-cooled. The turbine can be divided into two stages, allowing for reheat, if planned. A regenerator can be used to preheat the compressed air before it reaches the combustion chamber. Conventional CAES is the easiest technology, which require less space. On the other hand, energy is lost due to the cooling down of the air and fossil fuel is required. If there are strict size constrains, the regenerator can be removed, although this further lowers the efficiency. If heat is required for other applications, a heat recovery unit, using a secondary fluid (like water or a diathermic oil), can be used instead of the recuperator. As the exchange coefficients are higher, sizing would be less of a concern. Finally, the energy dissipated in the coolers may be useful for low temperature cogeneration, although additional heat exchangers would be required, increasing cost and complexity.

Adiabatic CAES has the important advantage of not needing fossil fuel to heat back the compressed air for the expansion process, representing an emission-free, pure storage technology with high efficiency. The basic idea is the use of a heat storage; this implies that the energy needed to heat the compressed air for the expansion process is recovered from the compression and stored in the TES unit to eliminate the need for a combustor. The most important parameter of an A-CAES is the chosen storage temperature, as it has direct influence on the system engineering as well as on the operating behaviour of the whole storage plant. In contrast, cycle efficiency is hardly dependent on the absolute storage temperature. A slight decrease in cycle efficiency with lower storage temperature is a result of the exergy losses occurring from additional heat exchange processes.

High Temperature A-CAES (above 400°C)

Ambient air is compressed to a low pressure level of around three bar and then is cooled. To this point, the temperature related part of the exergy is wasted into the environment. This first intercooling is required for two reasons. On the one hand, the inlet temperature of the second compression stage can be adjusted, and this directly affects the storage temperature and furthers decouples the following process from ambient conditions. On the other hand, the cooling lowers the compression work needed to reach the final pressure and actually increases the cycle efficiency. The second compression up to the final pressure is carried out without any additional cooling. This leads to an outlet temperature of around 600°C. The pressurized air flows through the TES unit and loses thermal energy. Afterwards, the air is conditioned by an additional cooler and enters the compressed air storage (CAS) with defined pressure and temperature. During discharge, air flows through the same TSE device in reverse direction and is heated up to around 570°C.

The strength of this concept is the high efficiency of up to 70%. However, to actually build such storage plants two major challenges have to be overcome. First, a high temperature TES must be able to withstand the combination of thermal and mechanical stress, so it requires special materials. On the other hand, there is no electrically driven compressor available off-the-shelf that operates at the high outlet temperature planned in A-CAES.

Medium temperature A-CAES (between 200°C and 400°C)

It requires a two-stage compression, in order to avoid reaching high outlet temperature. Air would transfer heat to the TES twice, lowering the cycle efficiency, but opening up for the

use of existing compressors and for TES media such as molten salt or thermal oil (which are already in use for similar applications). Ambient air is compressed to around three bar in the first stage and is further compressed to an intermediate pressure of 20 bar and about 400°C in the second stage, after intermediate cooling. When the air leaves the second stage, is cooled down again by flowing through a first TES device and an aftercooler. Afterwards, air is compressed to its final pressure and thus is heated up to around 400°C again. Following that, it flows through a second TES device and is stored in the CAS. The discharge process involves two expansion stages with preheating by the two TES devices.

Low temperature A-CAES (below 200°C)

The major advantage of low temperature is the applicability of liquid TES media, which can be pumped and which enable the use of common heat exchangers. To reach low enough storage temperature keeping an acceptable energy density, heat transfer after every single stage must be used. Depending on the state of charge, the liquid is stored inside the hot tank in case of charged storage or inside the cold storage tank otherwise. During charge/discharge process, the liquid is pumped through the heat exchangers to cool or preheat the air, respectively. Such an active TES system requires more advanced control techniques compareing to passive TES systems, but enables enhanced process control.

Medium temperature A-CAES has the advantage of requiring less components than the lower temperature one (which can use up to five compressors and five expanders), thus making the system less complex. On the other hand, a more advanced TES is required. High-temperature storage still requires significant technological advancement in order to become appealing.

Finally, the size and the weight of the required thermal energy storage must be given serious consideration. If, as an example, granite is used to store heat at around 500°C, 100 MWh of thermal storage capacity would require 900 tonnes of rock, taking up to about 550 cubic meters (assuming a packing factor of 60%).

2.3.2 Technological characteristics

The following technological characteristics are important in the design of a CAES plant.

Rated capacity

The total quantity of available energy from the storage system after fully charged, usually in Wh. Currently available CAES plants have a rated capacity up to 2860 MWh; smaller-scale plants can vary from a few KWh to around one MWh.

Specific energy

The total quantity of available energy from the storage system after fully charged, usually in Wh. Currently available CAES plant has a rated capacity up to 2860 MWh; smaller-scale plants can vary from a few KWh to around one MWh.

Energy density

The amount of energy stored per unit volume in a given system, in Wh/m^3 or Wh/L. In EES applications, the energy density is related to the volume of the storage reservoir; the higher the energy density of the storage medium is, the more energy can be stored. Energy density of CAES is around 2-6 Wh/L.

Power density

Is the power per unit volume, expressed in W/L; the power density for CAES is within the range of 0.5 to 2 W/L.

Power rating

The maximum rate at which the system can discharge energy, measured in MW. Typical values for large CAES are up to 1GW.

Part-load

CAES technology has a high part-load operation ability, meaning it is well suited for cooperative work with variable power sources such as wind power generation. CAES output could be controlled by adjusting the airflow rate together with the inlet temperature.

Discharge time

The amount of time the system can provide energy at the power rating without recharging. It is a function of the depth of discharge and operational conditions. CAES can have a discharge time of up to 26 hours (large scale), or up to 2 hours (small scale).

Response time

Large CAES have a faster response time than a typical GT plant; for example, the McIntosh plant can vary its power by around 18MW per minute, which is about 60% higher than the average gas turbine. Small scale CAES is quicker, responding in seconds to minutes.

Heat rate

Indicates the fuel consumed per kWh of output; typical values for CAES without a heat recovery system are around 6000 kJ/kWh (LHV). Using a heat recovery unit this value decreases to around 4500 kJ/kWh. These values come from the existing plants of Huntorf and McIntosh.

Recharge time

The rate at which power can be pushed for storage; regarding CAES, is the quantity of compressed air per unit of time that replenishes the reservoir.

Lifetime and cycle life

The first is the service time of the system (CAES has 20-40 years), the latter is the number of times the system can be loaded and unloaded (12000 cycles).

Reservoir operation method

According to geological conditions, the operation methods for a large scale compressed air energy storage utility mainly consists of two approaches.

- Constant Volume (isochoric): the storage volume is fixed and the reservoir is operated over an appropriate pressure range. In this way, there are two design options to control the reserve output. The first is using a turbine which allows variable inlet pressure; the second keeps the inlet pressure of the turbine fixed with the use of a throttling valve. The two existing plants both make use of a throttling valve.
- Constant Pressure (isobaric): It may be possible to keep the storage reservoir at a constant pressure by using water compensation. Underwater CAES with flexible vessel allows for a constant pressure operation.

Energy transfer

During the compression stage, the surplus electrical power drives the compressors, so it is converted into mechanical power and used to compress air. During the expansion stage, the turbine restores part of the energy carried by the compressed air and utilises the chemical power within the fuel through combustion. For such an energy conversion and transmission process, energy losses are inevitable.

Efficiency

There are two main types of efficiencies that must be considered. The first is the round trip efficiency, which is the ratio between the energy output and the energy input of the storage; it includes charge, discharge, self-discharge and dissipation effects. The second is the cycle efficiency, which is the ratio between the net energy produced by the system and the total amount used. Conventional CAES plant has the presence of two different energy sources, namely the electrical energy from the grid and the chemical energy within the fuel. In order to express the cycle efficiency correctly, it is required to write the energy input as the sum of the electrical power absorbed by the compressors and the equivalent electrical energy produced by the fuel, as if it was generated in a stand-alone plant with its own equivalent efficiency. (Elmegaard).

$$\eta_{cycle} = \frac{E_{out}}{E_{electrical} + \dot{m}_{fuel} LHV \eta_{eq}} \qquad (2.2)$$

In the A-CAES the energy input is just the electrical one, as this system does not need additional fuel consumption.

From the published literature, the efficiencies related do CAES were reported as follows:

- The discharge efficiency (the energy efficiency from the compressed air energy to electric energy) of a conventional large-scale plant is between 70% and 80%.
- The two existing commercial facilities have a cycle efficiency of 42% (Huntorf) and 54% (McIntosh, due to the adoption of the heat recovery unit).
- CAES systems, which avoid fuel combustion, such as A-CAES, may achieve an overall cycle efficiency up to 70%, making it similar to the PHS energy storage.

In order to compare different CAES plants it is often used the simplified efficiency, in which the electrical input and the thermic one are weighted the same.

$$\eta_{cycle} = \frac{E_{out}}{E_{electrical} + \dot{m}_{fuel} LHV} \qquad (2.3)$$

Operating switching time

The turbine is required to produce power for operation at both the compression and the expansion stages; at the Huntorf facility, the switch from one mode to the other requires at least 20 minutes. This switching time may affect and limit the CAES plant application for balancing rapid fluctuations. Redesigning the system structure by separating compression and expansion components, rather than linking them to the same shaft, may solve this problem.

Construction constrains

Are related to geographical and/or environmental requirements. As an example, large CAES require the natural storage reservoir. Moreover, conventional CAES burns fossil fuel, and so emits CO_2, leading to an environmental aspect. To avoid the involvement of fossil fuels, some advanced concepts like the AA-CAES are required.

Limitations

The major barrier to implement underground CAES reservoir is to seek the appropriate geographical locations. So far, it is possible to build CAES plants nearby salt caverns, hard rock and porous rock formations. In practice, however, the mature experience on constructing large-scale plants is only in using mined cavities in salt domes.

2.3.3 Underground caverns and existing plants

In large-scale CAES systems, the reservoirs where the compressed air is stored are always underground, due to the required volumes (hence the name of caverns). The main requirement that needs to be fulfilled is that the geological formation must have sufficient depth to allow safe operation at the required air pressure. There are three main types of geological structures suitable for CAES: salt, hard rock and porous rock.

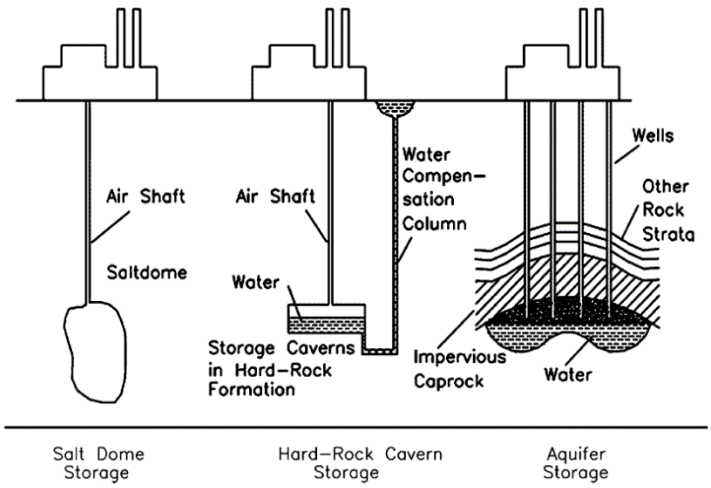

Figure 2-14: Different types of caverns for CAES systems [20]

The salt dome is the most favourable geological structure, also thanks to the knowledge acquired from the storage of high-pressure hydrocarbon products (liquefied petroleum gas and natural gas). Both the two existing commercialized plants use cavities mined into salt domes. Moreover, the elasto-plastic properties of salt pose a minimal risk of air leakage in these underground reservoirs.

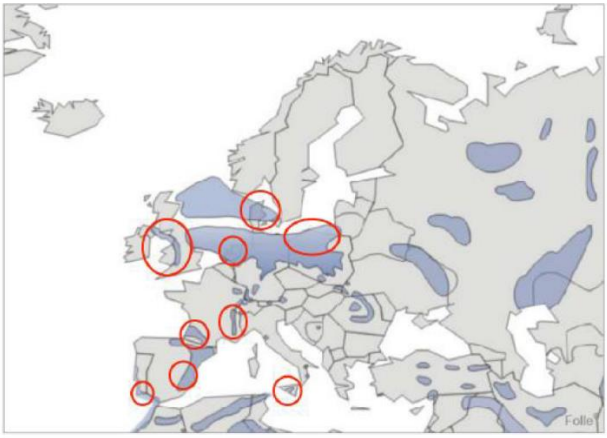

Figure 2-15: Correlation between salt domes and high quality wind areas [30]

Hard rock formations are another option; however, the cost of mining a new reservoir through impervious terrain is relatively high. The available depth for hard rock storage caverns is within the range of 300 m to 1500 m. Several proposed projects plan to use existing mines, which can reduce the cost. The advantage of hard rock storage is the possibility to maintain a constant pressure inside the cavern by using water-compensation ponds. However, this technique has a potential hazard called the “champagne effect”, which is related to water flow instabilities resulting from the release of dissolved air in the upper portion of the water shaft.

Porous rock formations are found in rock aquifers or depleted gas fields. Depending on the permeability of the porous medium, a number of holes has to be drilled into the aquifer. The significant advantage is the low cost, however, in order to design an efficient storage, extensive research into the geologic characteristics of the porous media at the candidate sites are required to determine their feasibility.

The Hunforf plant

The Huntorf plant was commissioned in 1978 and was designed to provide black start services to nuclear and thermal plants near the North Sea. Nowadays it has successfully being levelling the variable power from numerous wind turbine generators in Germany and has operated as a tertiary control reserve. In the Huntorf plant, ambient air is compressed in an intercooled process by two separate turbo-compressors units to a maximum pressure of 72 bar. Before being stored, the air is cooled again in the after cooler; the heat extracted during cooling phases is lost. The storage consists of two mined salt caverns with a total storage volume of about 310000 m^3. Having two different reservoirs allow high availability even during maintenance. The cavern is cycled between 46 and 72 bar, although it can operate at lower pressure if emergencies occur. The expansion is carried out in two separate units in series. The air leaving the reservoir is throttled down to a constant pressure, leading to significant losses, then, it is sent into the combustion chamber inside which is heated to 490°C. The HP turbine expands the gas down to 10 bar; on this pressure level the air is heated again to 870°C and is expanded in the LP turbine. The energy of the exhaust gases leaving the LP turbine at approximately 480°C is wasted, as no heat recovery unit is installed.

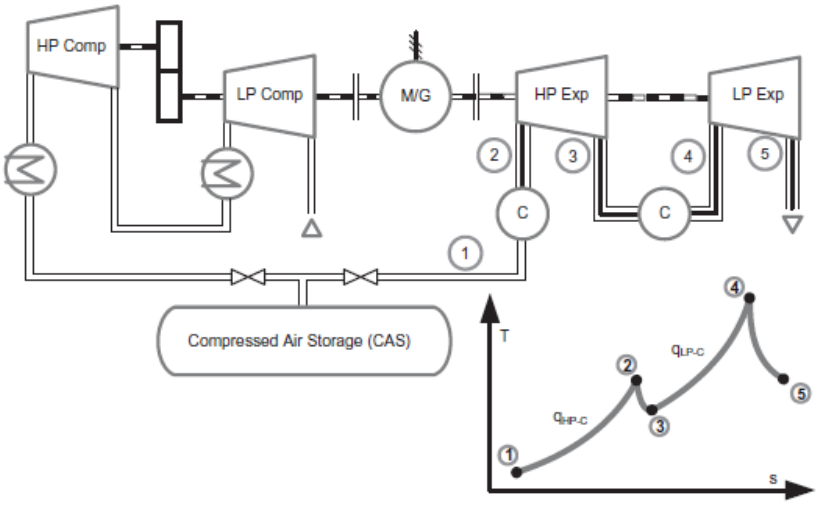

Figure 2-16: Layout and T-s diagram for the Huntorf plant, [30]

The McIntosh plant

The McIntosh plant in Alabama was commissioned in 1991, with only one storage cavern with a total volume of around 560000 m^3. In a similar way to the Huntorf plant, there is no device for heat storage. However, multiple-stage intercooling increases the overall efficiency. Moreover, a heat exchanger is used to recover exhaust gas heat to pre-heat the air from the reservoir. In this way the compressed air is heated up to 295°C before entering the combustion chamber. After the HP expansion the air is reheated to increase the power of the LP section.

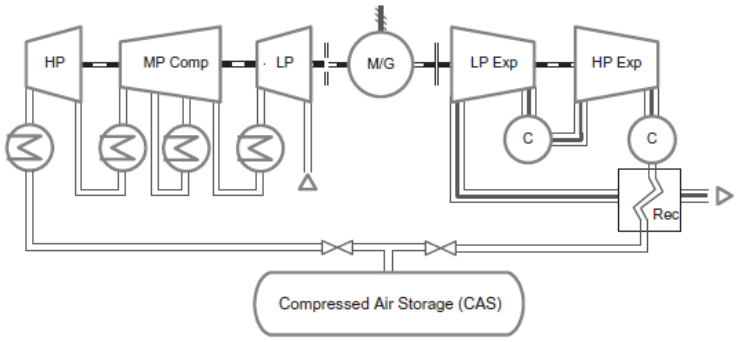

Figure 2-17: Layout of the McIntosh plant [30]

The efficiency of the McIntosh plant, reaching 54%, is higher than the Huntorf's one, which is 42%. Technically this is mainly due to the waste heat recovery unit.

Additional characteristics of the two plants are summarized in Table 1.

Table 1: Comparison between the two existing facilities [30]

CAES plants comparison	*Huntorf plant*	*McIntosh plant*
Equipment Manufacturer	Brown-Boveri	Dresser-Rand
Amount invested (2002 US dollars)	$ 116 million ($400/kWe)	$ 45.1 million ($410/kWe)
Schedule	Commissioned December 1978	Commissioned June 1, 1991
Applications	(1) Peak Shaving (2) Spinning reserve (3) VAR support	(1) Arbitrage (2) Peak Shaving (3) Spinning reserve
Output		
Turbine power [MW]	290	110
Compression power [MW]	60	53
Generation time [hours]	3	26
Compression time [hours]	12	41.6
Ratio Compression/Generation	4	1.6
Reservoir		
Number of caverns	2	1
Geology	Salt	Salt
Air cavern volumes [m^3]	310'000	560'000
Fuel	Gas	Gas/Oil
Air flow rates		
Compression air flow [kg/s]	108	94
Expansion air flow [kg/s]	417	157
air mass flow ratio in/out	0.25	0.6
High pressure expander		
Inlet pressure [bar]	46	43
Inlet temperature [°C]	537	537
Low pressure expander		
Inlet pressure [bar]	11	15
Inlet temperature [°C]	871	871
Heat Rate [BTU/kWh, HHV]	6050	4510
Availability	90%	95%
Starting reliability	99%	99%
Power Requirement	0.82 kWin/kWout	0.75 kWin/kWout
Normal Start [min]	8	10 to 12

2.3.4 Underwater CAES (UWCAES)

The main difference between underground and underwater energy storage (in the form of flexible bags) is that the first one is an isochoric storage, meaning that the pressure of the storage varies and is kept constant at the outlet thanks to a throttling valve (which introduces significant losses). The underwater storage allows for an isobaric storage, in which pressure stays always the same and is the volume of the storage itself that actually changes with operation. The pressure of the stored air is equal to the hydrostatic pressure of the surrounding water. During the expansion processes, the air can be released to drive the expander without having to adjust its pressure, removing the throttling valve. It is important to note that without the throttling valve, the UWCAES can reach higher efficiencies than the underground one, depending on operating conditions [31]. By storing pressurized air in an underwater vessel the pressure in the air can be reacted by the surrounding water, greatly reducing loading at the air/water barrier. This simplifies the design requirements of containment vessels and presents potential for their inexpensive manufacture, relative to the cost of a vessel required to handle full pressure without the support of surrounding water.

The density of seawater is around 1025 kg/m^3, less than half that of the Earth's upper crust (around 2700 kg/m^3), meaning that the storage pressure under a given depth of water is less than half that under the same depth of rock, assuming that compressed air is stored at a pressure roughly equal to the surrounding hydrostatic/geostatic pressure. However, unlike underground stores that require the mining of a cavern, UWCAES stores can be manufactured and installed at potentially low cost, though the method of installing and securing the vessels to the seabed requires some development. Moreover, air in underwater vessel is stored at a lower temperature (around 283 K), so it is denser and occupies less volume. UWCAES vessels are hidden from view, and suitably deep water can readily be found close to many coastlines, not only in saltwater oceans/seas but also in some freshwater lakes.

The load that must be reacted is primarily that of buoyancy, which is proportional to volume, and as a result, the cost of a vessel for UWCAES is roughly independent of depth. Energy capacity storage increases with depth, so it follows that the deeper the vessel is fixed, the lower is the cost per unit of energy storage capacity.

The gauge pressure in seawater at a depth d is given by:

$$p = \rho g d$$

Where ρ is the density of seawater.

Ignoring the mass and volume of the materials (both relatively small for a fabric vessel), the buoyancy force on a flexible vessel is given by

$$F = (\rho - \rho_{air})gV$$

Where V is the volume of the inflated vessel. This buoyancy force must be resisted by some type of anchorage.

It becomes clear that the basic goal is to install the storage at the greatest depth possible, since energy storage capacity increases with increasing depth pressure. Two thermodynamic cases bound the energy density offered by the storages. If both the compression and ultimate de-compressive release of stored air occurs slowly enough to allow the storage to continually adjust to the temperature of the oceanic environment through heat exchange, the process is considered isothermal. Because the significant heat of compression is wasted, this is the least desirable storage option, with an energy density [kJ/kg] of

$$u_{isothermal} = RT_{amb}\ln(\frac{P_{storage}}{P_{amb}})$$

Where R is the gas constant.

If the heat of compression is stored and subsequently re-purposed to heat the air as it is released to drive the energy recovery turbines, the adiabatic energy density can be calculated with

$$u_{adiabatic} = rP_{atm}(r^{\frac{k-1}{k}} - 1)(\frac{k}{k-1})$$

Where r is the pressure ratio and k is the adiabatic index for air.

The isothermal and adiabatic UWCAES energy densities associated with ocean depth are found in Table 2.

Table 2: UWCAES energy density with sea depth, [32]

Depth (m)	Storage pressure (bar)	Energy density (kWh/m^3)		Ratio of adiabatic and isothermal energy densities
		Isothermal	Adiabatic	
50	6.04	0.30	0.39	1.30
100	11.07	0.74	1.05	1.43
200	21.12	1.78	2.84	1.59
300	31.18	2.97	5.04	1.70
400	41.23	4.24	7.55	1.78
500	51.29	5.59	10.32	1.85
600	61.34	6.99	13.30	1.90

Besides the nonlinear increase in storage density with increasing depth in a way that favours greater depths, it is also obtained a very significant depth-related increase by implementing adiabatic capability. For example, increasing installed depth of identical structures from 50 to 500 meters increases stored energy density by a factor of almost 19 in the isothermal case. Optimized adiabatic recovery would theoretically return 26.5 times greater energy density. (Jong, 2014).

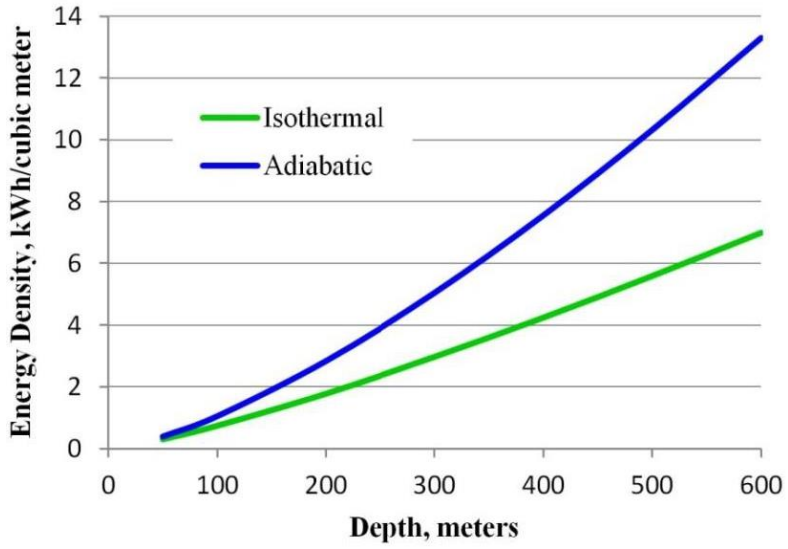

Figure 2-18: Isothermal and adiabatic energy density with sea depth, [32]

An economically efficient target UWCAES installation depth between 400 and 700 meters was loosely identified [32]. Greater depths are preferable due to reduced impact of required ballasted systems on the environment.

3 METHODOLOGY

In this chapter, component's models are introduced and described.

Air is considered to be an ideal and perfect gas, meaning that its state equation is

$$pv = RT$$

Moreover, its enthalpy is a function of temperature only, and k (adiabatic index) is constant too.

It is also supposed that the fuel used is 100% natural gas, with a lower heating value (LHV) of 50.047 MJ/kg. Assuming that the combustion is complete, it is possible to evaluate the CO_2 emissions through the balanced combustion reaction

$$CH_4 + 2O_2 = CO_2 + 2H_2O$$

The molecular weight of methane is 16 g/mol, while the one for the CO_2 is 44 g/mol. This means that for every 1 kg of fuel burned, 2.75 kg of CO_2 are emitted.

3.1 Gas Turbine

The platform is equipped with three GE LM2500+G4, which is an aero-derivative gas turbine specifically designed for marine and industrial applications in an offshore environment. An in depth description of the characteristics of this engine can be found in [16].
The most important parameters are summarized in the Table 3.

It is important to underline that, while the manufacturer certifies that the GT can reach load values as low as 10%, the increased NOx emissions usually do not allow going under 30-35% of the nominal load. For this thesis work, the lower limit will be 36%, as this is the value required to satisfy the heat demand of the platform. The maximum load is set at 95%

of the nominal output: this is a common limit found in most literature, because it gives a flexibility margin in case of unexpected peaks in the power demand.

Table 3: Design parameters of the GE LM2500+G4

Design power [MW]	33.5
Max load [%]	95
Min load [%]	10
T inlet [K]	283.15
P inlet [kPa]	101
Fuel type	CH4
LHV [MJ/kg]	50.047
Air humidity	0.6
DP in [mbar]	10
DP out [mbar]	10

For the off-design performance, data are available from the manufacturer. Figures (3-1) and (3-2) show the correlation between the turbine's power output, its efficiency and the fuel consumption. The relations are not linear, thus low part loads have a much lower efficiency and a higher specific fuel consumption.

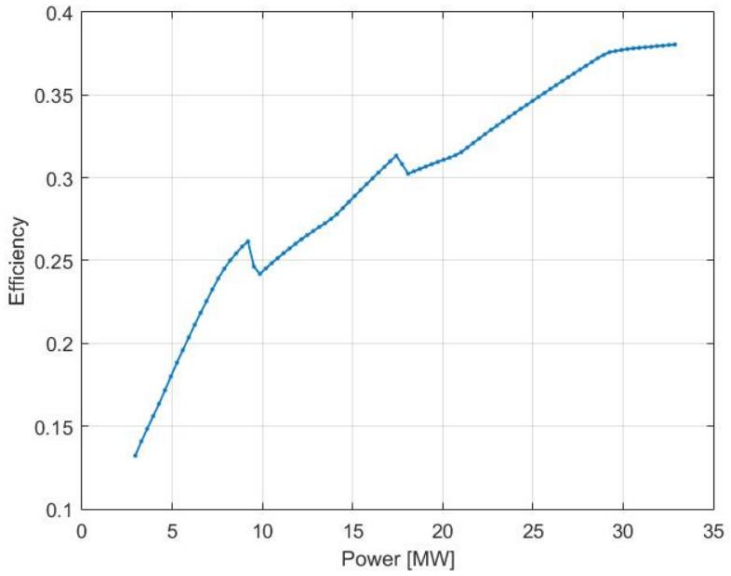

Figure 3-1: Correlation between power output and efficiency

During operation, the GT's load must vary according not only to the platform's power demand, but also to the characteristics of the turbomachinery in the CAES section, namely the compressors (referred to as air compressors) and the turbine (referred to as air turbine).

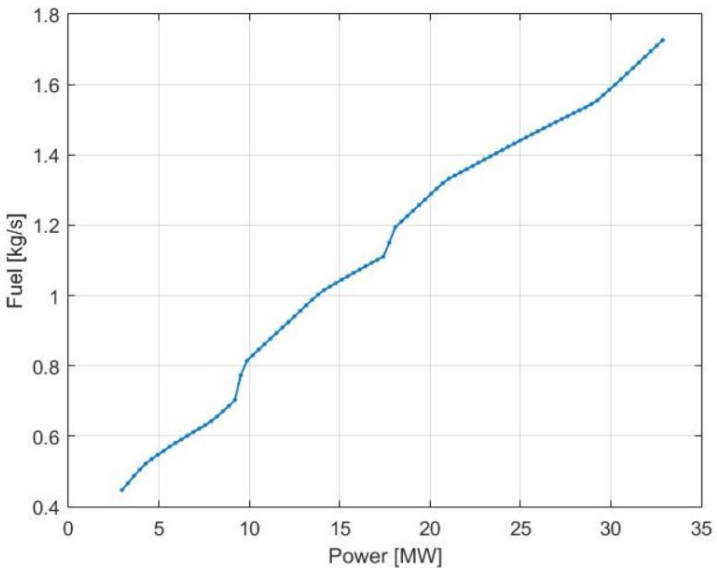

Figure 3-2: Correlation between power output and fuel consumption

Gas turbine adjustments due to the air compressors

If the power available to the air compressor (from the excess wind production) is not enough to reach the minimum load required to start the compression process, the GT can be adjusted as follows:

1c) Reduce the GT's load by the excess power unusable for the compression. This is possible only when the GT is at high enough loads, but it is not feasible when the GT approaches the lower load limit.

2c) Increase the GT's load in order to reach a high enough excess power to start the air compressor. This operation is only possible when the GT is not already close to its maximum load.

Both these strategies are used in this work.

Gas turbine adjustments due to the air turbine

If the power required from the air turbine is lower than the turbine's minimum load, two approaches are possible:

1t) Let the air turbine to work at its minimum and decrease the GT load accordingly, to avoid wasting power.

2t) Increase the GT load to fulfil the power requirements without having to start the air turbine.

The second approach should be used whenever possible. When the GT's load cannot be increased, the first strategy is applied instead.

3.2 Wind Turbine

The default wind turbine's model choice was made taking into account previous works on this topic and recent technological developments [33-35]. Three suitable wind turbine models where identified and compared, as shown in Table 4.

	Rated Power [kW]	Application	Rotor diameter [m]	Nominal output at [m/s]
EnerconE70	2300	Onshore	71	16
VestasV164	7000	Offshore	164	13
NREL	5000	Both	126	12

Table 4: Characteristics of the selected wind turbines

The EnerconE70 was extensively used in previous works, although originally meant to be an onshore only turbine. The Vestas had its first prototype installed in a wind farm in Denmark during 2014 and the first industrial units started operating in 2016 off the west coast of the United Kingdom. The NREL was modelled in [34] with the objective of establishing the detailed specifications of a large wind turbine that is representative of typical utility-scale land and sea-based multi-megawatt turbines, and suitable for deployment in deep waters.

The available data for the power curves of the three turbines were implemented in a MATLAB code, in order to compare them and choose the most performing one.

From Figure (3-3) below, the 5 MW NREL wind turbine resulted with the best power curve out of the three, thus was selected as the default wind turbine for this work. Additional data regarding its power curve are available in Appendix A.

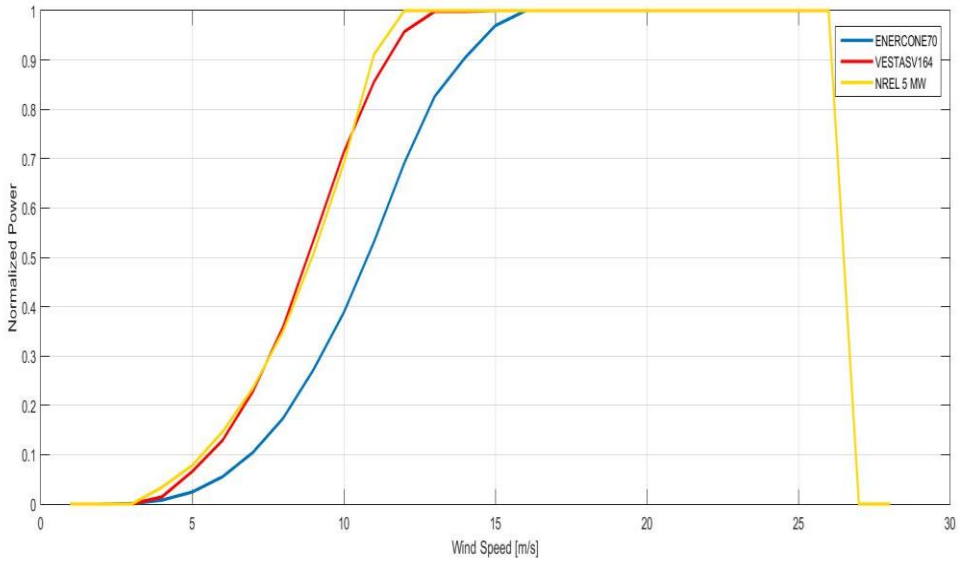

Figure 3-3: Power curves for the three wind turbines

The wind profile is available thanks to the work done by Sleipner: a one-year wind speed time-series with one-minute time-steps from an offshore meteorological measurement station in the North Sea have been used as the default wind speed profile.

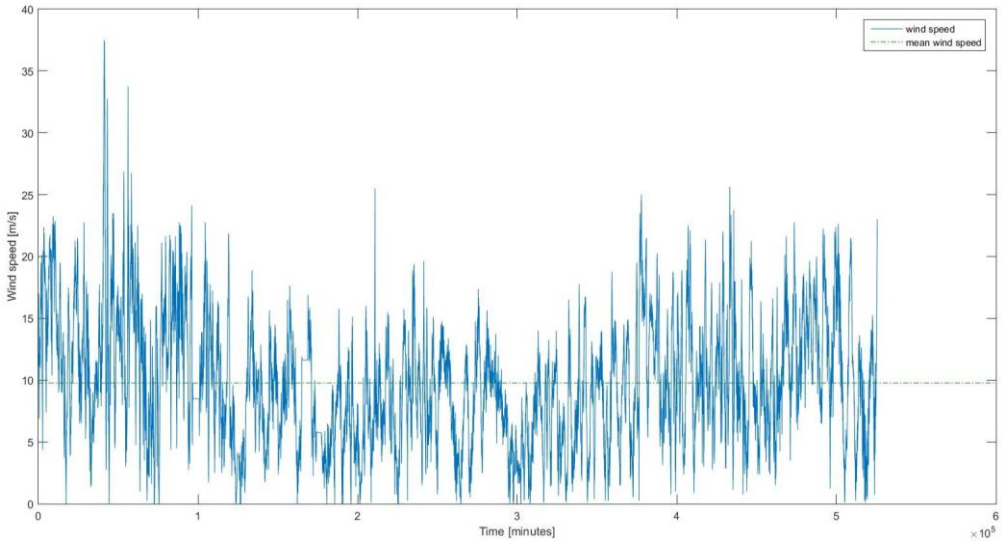

Figure 3-4: Instantaneous and average wind speed profile, with one-minute time-step

Given the default wind speed profile, it is possible to manually adjust the values via the introduction of a wind ratio (WR), which is a multiplicative factor, usually between 1.0 (no adjustments) and 1.5, which has the aim of accounting for different turbine's hub heights or different wind speed values. Three different WRs were tested, with the aim to obtain a wind speed profile that reflects the expected average wind values in the North Sea region (between

8 and 11 m/s) and at the same time gives a capacity factor (CF) for the wind turbine in the range of 0.45 and 0.5.

Results are summarized in Table 5. A wind ratio of 1.1 satisfies the expected results and is therefore used as the default value for this work.

Table 5: Comparison of different wind ratios

Wind Ratio	1.000	1.250	1.100
Average capacity Factor	0.411	0.558	0.474
Maximum annual energy production [MWh]	43800	43800	43800
Annual energy production [MWh]	18002.52	24433.86	20765.34
Average turbine power [kW]	2055.1	2789.3	2370.5
Average wind speed [m/s]	7.815	9.769	8.597

3.3 Air Compressor

For the modelling of the air compressor, an existing map, available in [36], was adopted. The map is of a centrifugal compressor, which perfectly fits the need to operate at relatively high pressure ratios (up to 11) and with small air flows (between 11 and 18 kg/s). Moreover, a centrifugal compressor is more compact than the axial, and therefore easier to install on the platform, given the strict physical constrains on these facilities. It is supposed that the compressor is driven by a variable speed motor: this allows to operate it at constant pressure ratios during off-design periods. Moreover, the isentropic efficiency was increased by a flat 2%, in order to reflect a more modern map in comparison to the one available, which dates back to a 1993 article [37].

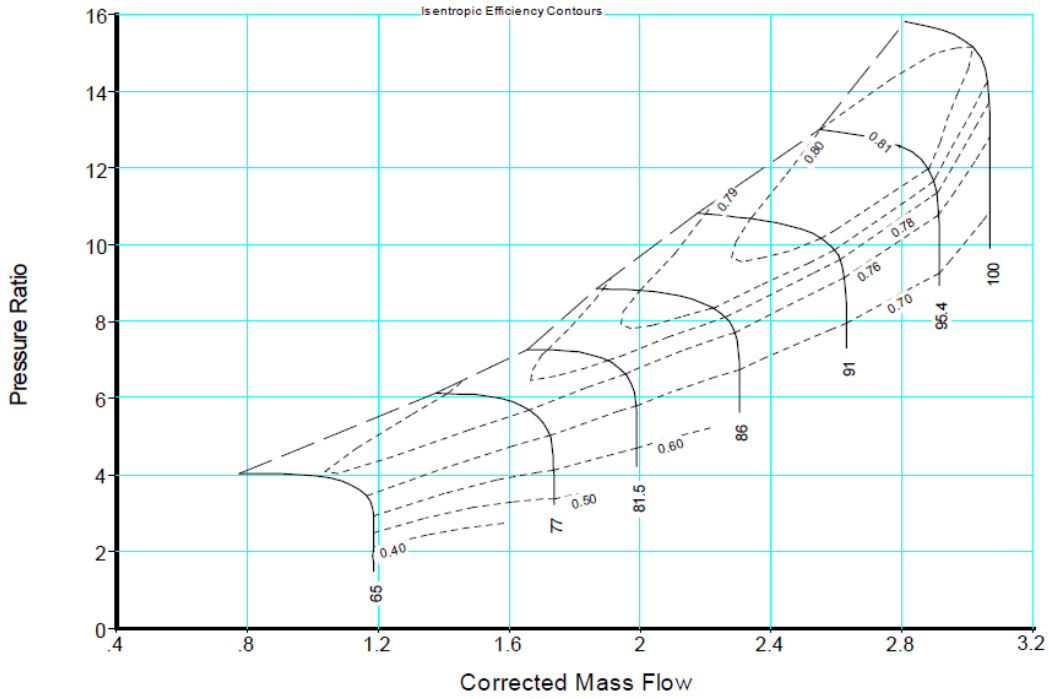

Figure 3-5: Map for the air compressor, [36]

The system requires more compressors to work in parallel. When this happens, the load is shared equally among the active compressors.

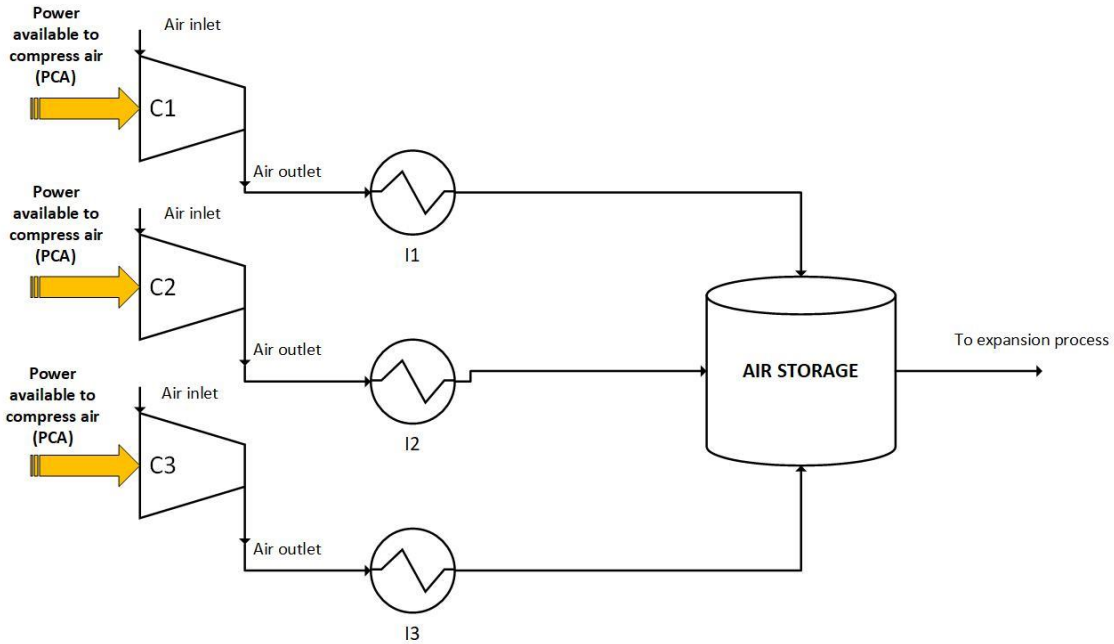

Figure 3-6: Example of three air compressors working simultaneously

As discussed in the Technological background, an aftercooler is always put after the compression phase, before the compressed air is stored into the underwater vessels: this is

done in order to bring the temperature back to ambient conditions (283.15 K) and thus lowering the density, with an advantage for the sizing of the storage.

The compressors are moved by a variable speed motor, therefore the pressure ratio is constant and various points with the corrected mass flow values and isentropic efficiencies are readily available from the compressor's map. Inlet pressure [kPa] and temperature [K] are also known, since the air enters the compressor at ambient conditions. Using the definition of corrected mass flow, it is possible to evaluate the effective mass flow in those points, in kg/s:

$$corrected\ mass\ flow = \frac{\dot{m}\sqrt{T_{inlet}}}{P_{inlet}} \qquad (3.1)$$

For the off-design predictions, a MATLAB code was created. The mass flow values obtained with Equation 3.1 are interpolated and the resulting data fitted to obey the following second grade equation, which allows computing the mass flow in every other point of the map. Coefficients of the data fit are available in Appendix A. Accuracy results to be above 95% in every studied scenario.

$$\dot{m} = Power^2 * p1 + Power * p2 + p3 \qquad (3.2)$$

Where $Power = \dot{m} * \eta_{isentropic} * \Delta h$

The mass flow is read in several points on the map, likewise for the isentropic efficiency. The inlet enthalpy is known, since it is a function of the ambient temperature only (working under the hypothesis of perfect gas); the outlet enthalpy is a function of the outlet temperature, which can be expressed thanks to the pressure ratio:

$$T_{ad_{out}} = T_{in}\left[\frac{P_{outlet}}{P_{inlet}}\right]^{\frac{k-1}{k}}$$

The coefficients p1, p2, p3 are computed by MATLAB.

During the system's simulations, the available power for the compression is known in every condition (since is the excess wind power which is not directly sent to the platform),

therefore, through the use of Equation 3.2, it is possible to evaluate continuously the air flows in the off-design conditions and thus predict the charging pace of the storage.

Using a similar Equation to 3.2, it is possible to evaluate with continuity the compressor's efficiency and thus the effective outlet temperature of the compressed air.

$$efficiency = Power^2 * P1 + Power * P2 + P3$$

Where P1, P2 and P3 are the constant coefficient computed by the software.

In the case study, the available sea depth is around 110 meters. This means that the maximum storage pressure is 11 bar. In this configuration, up to three compressors are required to work together, sharing the load when necessary. Compression is single-staged without intercooling, since this leads to a much simpler and compact system.

The required number of compressors depends on the maximum nominal power of the air compressor and on the maximum excess in wind power production. This is clarified with the following example:
If, for example, the nominal compressor's power is 7 MW, and the maximum excess of wind power is 21 MW, it results that, in order fully exploit the wind power excess, three compressors are required to work simultaneously at full load.

When the storage pressure increases (in other words, when higher sea depths are studied), the single-staged compression, although simpler, would lead to excessive power absorption and very high outlet temperatures for the air stream. Therefore, a two-staged intercooled compression is modelled instead, with benefits regarding the compression work and the outlet temperature. In this configuration, up to two trains of compressors may work simultaneously.

The pressure ratio is divided equally between the two compressors, as the optimal pressure ratio is known to be the squared root of the final pressure level [18, 38-40].

Isentropic efficiencies are included, but the intercoolers are supposed to be with effectiveness of unity. This means that after each intercooler, the air is returned to ambient temperature.

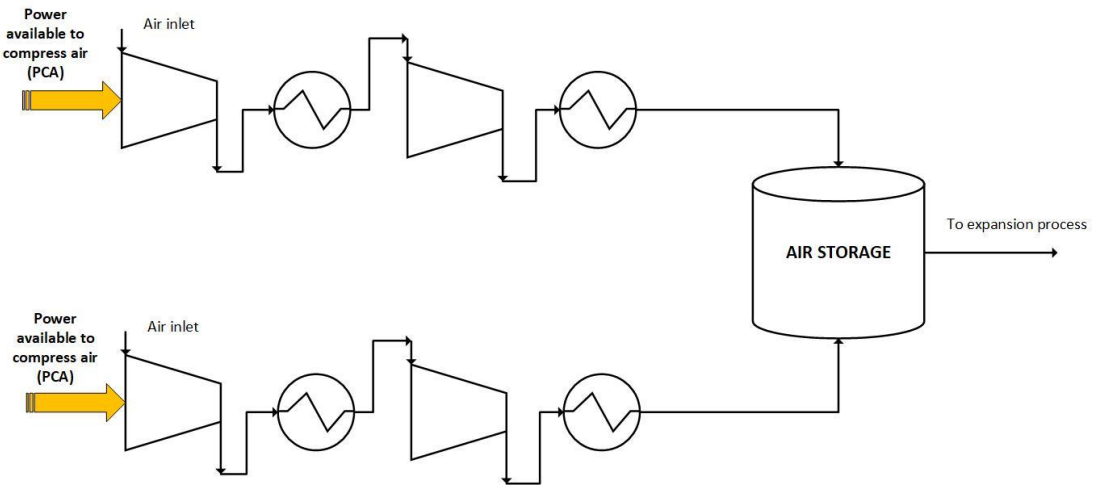

Figure 3-7: Compressor's layout for higher sea depths

If both the compression and ultimate de-compressive release of stored air occurs slowly enough to allow the storage to continually adjust to the temperature of the oceanic environment through heat exchange, the process is considered isothermal, and is therefore well described by the isothermal efficiency

$$\eta_{isothermal} = \frac{RT_{amb}\ln(\beta)}{Power_{compressor}} \qquad (3.3)$$

Where β is the pressure ratio

The isothermal efficiency tells how close the process is to be perfectly isothermal. It is reminded that an isothermal compression requires the least work possible [18, 38-40].

3.4 Air Turbine

The air coming from the storage is at ambient temperature, and therefore has to be sent to a combustion chamber before the expansion in the turbine, in order to reach an appropriate temperature level.

When modelling the air turbine, only a few maps where available, and none of them fitted the system's requirements. Therefore, the design was based on the Stodola's ellipse method. The nominal power output was chosen to be high enough to provide the platform with the necessary power even when the GT is at its minimum and no wind energy is available. The minimum flow was set to be 50% of the nominal value, as suggested in various references [41-47].

The use of Stodola's Ellipse method makes it possible to correlate together the mass flow, the inlet temperature, and inlet and outlet pressure:

$$Ct = \frac{\dot{m}\sqrt{Tinlet}}{\sqrt{Pinlet^2 - Poutlet^2}} \qquad (3.4)$$

Where Ct stays constant in off-design operation.

An empirical expression was used to predict the efficiency in part-load conditions

$$\eta_{off} = \eta_{des}\sqrt{\frac{T_{des_{in}} - T_{des_{out}}}{T_{off_{in}} - T_{off_{out}}}}\left[2 - \sqrt{\frac{T_{des_{in}} - T_{des_{out}}}{T_{off_{in}} - T_{off_{out}}}}\right]$$

This equation is a simplified version of the one used in previous thesis works [41,42], since the turbine speed is supposed to be constant in every condition. Moreover, since the ideal state equation for the air is being used, Cp is also constant and enthalpy is a function of the temperature only.

The adiabatic exhaust temperature can be calculated with the know equation

$$T_{ad_{out}} = T_{in} / \left[\frac{P_{inlet}}{P_{outlet}}\right]^{\frac{k-1}{k}}$$

The non-isentropic exhaust temperature is obtained from the definition of isentropic efficiency

$$\eta = \frac{T_{in} - T_{out}}{T_{in} - T_{ad_{out}}}$$

For the off-design predictions, a MATLAB model was used, similarly to what was done in section 3.3. The available values were interpolated and then fitted.

$$\dot{m} = Power^2 * p1 + Power * p2 + p3 \qquad (3.5)$$

Where, p1, p2, p3 are the coefficients from the data fit (values available in Appendix A).

The power required by the platform from the air turbine (PAT) is known in every condition:

$$PAT = Power\ demand - WP - PGT$$

Where WP is the electric power directly sent on the platform by the wind farm and PGT is the power provided by the GT at the current load. Since the PAT is known, through Equation 3.5 is possible to obtain the mass flows, and therefore predict the discharge rate of the storage.

In Equation 3.4, the Stodola's constant does not vary with operation. Outlet pressure is fixed to ambient conditions (101 kPa). This means that the air turbine can be operated in two different ways:

1) The first one is to keep the ΔP constant. This means that when the mass flow decreases, the inlet temperature increases following a quadratic law. The minimum inlet temperature is fixed at 800 K, in order to limit the air flow required to achieve the desired power output. The maximum temperature is set to be 1100 K, as higher values would require complex and expensive cooling systems such as blade cooling. Therefore, with this approach, the temperature can vary between the above defined range. Once the maximum temperature is reached, it is kept constant and the ΔP is decreased instead. In particular, the inlet pressure is lowered, with the use of a throttling valve.

2) The second one is to keep the inlet temperature constant at its minimum value of 800 K. In this configuration, the inlet pressure is continually adjusted with the throttling valve.

The second approach gives the best results emission-wise and is simpler, thus is the default one for this work. Moreover, since for most of the time the inlet pressure will be lower than the nominal one, it can be thought that the throttling valve responsible for the pressure loss would also include the inevitable pressure losses along the whole process, which would otherwise be unaccounted for. A brief comparison of the two is available in Appendix A.

The effects of different air turbine design parameters were also investigated. Namely, a design with a lower mass flow but a higher inlet temperature (A), was compared to one with a higher mass flow but a lower inlet temperature (B). Design (B) resulted with a steeper discharge curve due to the increased mass flow required by the turbine. This is a negative effect, because the steeper the discharge curve, the harder is to balance the energy level between initial and final level (this is explained better in section 3.5). For this reason, design (A) was preferred, even though it leads to slightly higher CO_2 emissions. This comparison was done to prove that the design parameters of the air turbine have a deep effect on the performance of the overall system. Design (B) parameters are available in Appendix A.

3.5 Underwater Storage

The UWCAES takes advantage of the hydrostatic pressure associated with water depth as its motive force. The compressed air is stored in a fabric balloon-like vessel that is anchored to the seabed. Since the intent is to use the hydrostatic pressure to resist the pressure of the stored air, the structural requirements of the vessel essentially disappear. The vessel is relegated to provide a membrane boundary between air and water and to restrain the buoyancy of the air bubble. Another benefit is that the stresses experienced by the materials remain essentially independent of the depth. Moreover, the pressure within the bag remains constant regardless of the filled volume of the vessel.

Air is stored when the compressors are working, charging the storage. On the other hand, when the air turbine is active, air is extracted from the vessels, discharging the storage. Mass flows in both directions are known for every operating condition, thanks to the models introduced in the previous sections.

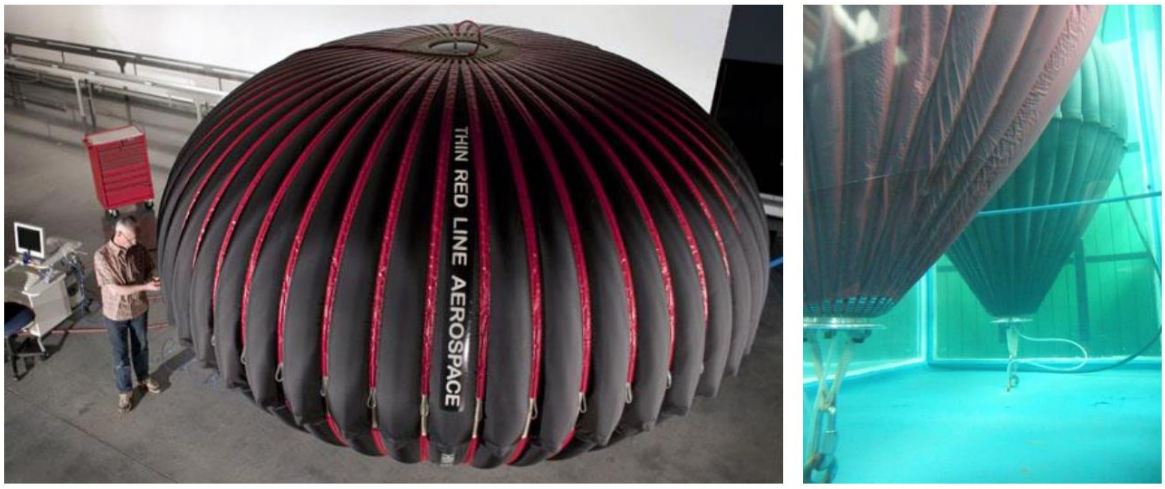

Figure 3-8: Images of vessel prototypes, [32]

The energy density, expressed in kWh/m^3 is given by

$$u = RT_{amb}\ln(\beta)$$

Which is the upper term of Equation (3.3) and represents the mechanical exergy of the air stream.

Using together the mass flows [kg/s], the energy density [kWh/m^3] and the air density at a given pressure [kg/m^3] allows to express the storage's energy level in MWh, and to follow its charge and discharge curve. Once a peak is identified, it is possible to compute the required maximum storage volume for that year. Doing this for the platform's lifetime makes it possible to identify the global maximum required volume and therefore the number of fabric vessels needed.

It is important to note that the energy level between the beginning and the end of each year has to be the same: if the level at the end is lower, the storage is not large enough to meet the platform's demand; if it is higher, a fraction of the stored wind energy is not usable and therefore goes wasted. This will be further explained with the following example.

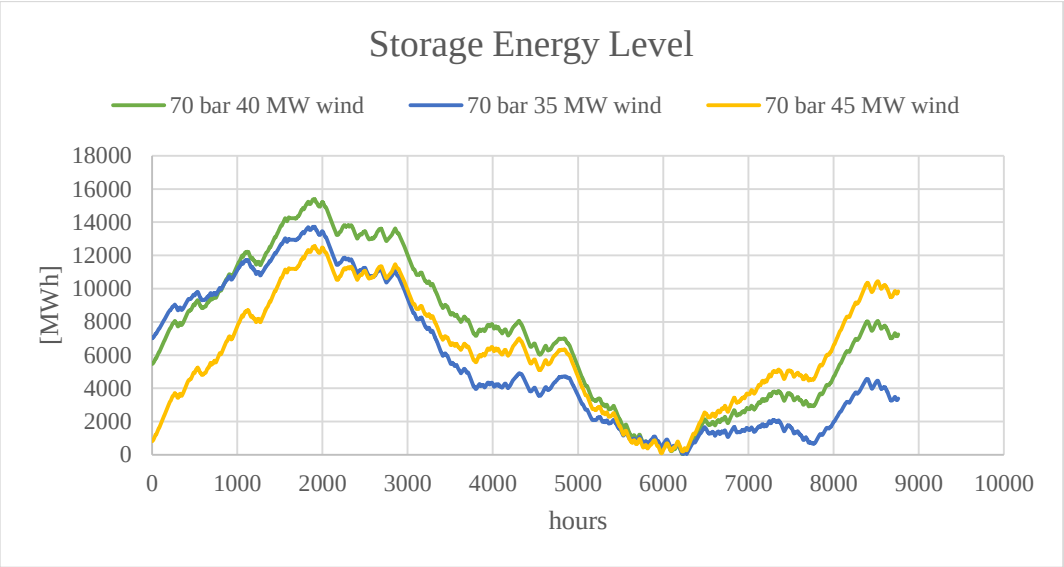

Figure 3-9: Example of storage energy level for different wind farm sizes. 70 bar pressure and 30 MW demand from the platform

Figure (3-9) shows the storage energy level for a platform's demand of 30 MW, a storage pressure level of 70 bar and different wind farm sizes. The 40 MW case leads to a balanced profile, with an energy level at the beginning of the year roughly equal to the one at the end of the year. The 45 MW case ends up with an excess of stored energy, which is not usable since the GT on the platform is at its minimum load (36%), and therefore represents a wasted fraction of wind energy. The 35 MW case on the contrary ends up with a lower energy level compared to the one at the beginning of the year, meaning that the CAES needs more energy than what is available. It is theoretically possible to balance the profile by increasing the load of the GT, meaning that more energy from the wind is stored into the CAES.

Taking now into consideration Figure (3-10): In this case, the platform's power demand is 44 MW, and the GT works close to its nominal rated power (95% of the load). This time the wind farm size is fixed at 35 MW and the storage pressure varies between 11, 40 and 70 bar. The 11 bar case is perfectly balanced, while the remaining two end the year with a lower energy level compared to the beginning. The GT's load cannot be further increased, since it is already approaching its maximum value. This means that, in this case, the 35 MW wind park is too small for the 40 and 70 pressure level scenarios. The above discussed examples make it clear that the wind farm size has an important influence on the behaviour of the system and on the storage energy level profile.

In addition to this, it is interesting to focus on the results achieved in the two examples for the 70 bar 35 MW wind case: when the platform's demand is maximum (44 MW), the wind park is too small to provide the storage with the necessary energy. On the other hand, it could work when the platform's demand is minimum (30 MW), but it would require an increased power output from the gas turbine. Since the storage energy profile has to be balanced around the whole lifetime of the platform, the 35 MW installed wind power is not enough, even though it seemed initially applicable. This means that, when looking at the lifetime performance, scenarios that look promising in particular years may end up not being feasible. This fact will be further discussed in chapter 6.

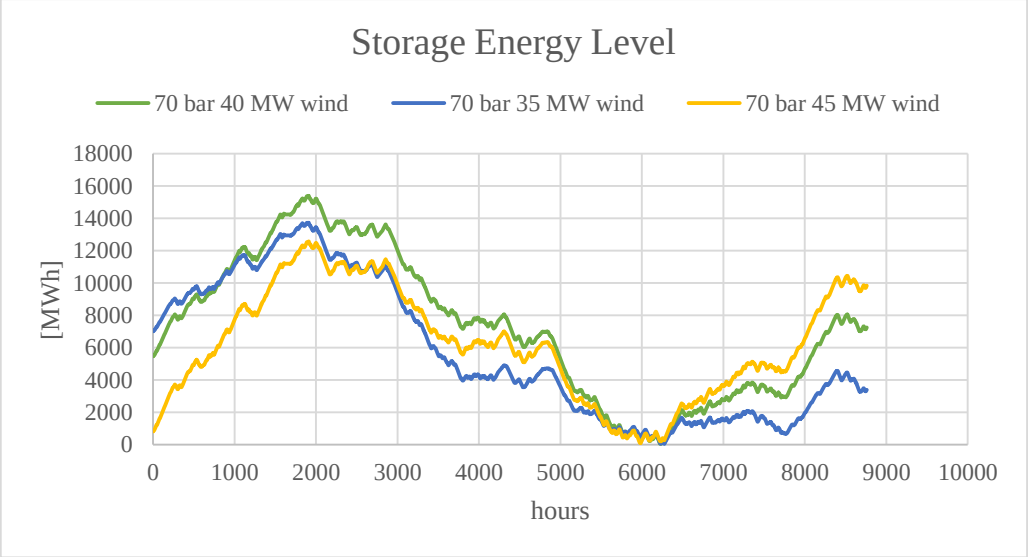

Figure 3-10: Example of storage energy level for different pressure levels. 35MW wind farm and 44 MW platform's demand

Another important aspect is the relationship between the wind profile and the storage energy level. Consider, as an example, the profile of the 70 bar 45 MW wind case shown in Figure (3-10):

In the interval between hours 0-2000, the average wind speed is high, and this leads to an excess of wind power and to a steep charging curve for the storage. From hour 2000 to hour 6000, the average wind speed is lower, and the storage starts to discharge, reaching its minimum. From hour 6000 to the end of the year, the average wind increases again, and the storage keeps charging. This trend is the result of the available wind speed, and is a common feature for all the studied scenarios. In order to reduce the excessive energy stored past hour 6000, it would be necessary to decrease the GT's load on the platform. In this way, the air turbine would work at a higher part load, extracting more air from the storage and discharging it until reaching the initial energy level, therefore balancing the profile. In this

case though, the GT is already working at its minimum load (36%), thus there is no opportunity to utilize the remaining stored wind energy. This also means that, the steeper the discharge profile is between hour 2000 and 6000, the smaller the regulation margin for the GT past hour 6000 is, so the harder it becomes to balance the profile. This could be partially solved by increasing the GT's load between the beginning of the year and hour 2000. However, doing so would increase the energy level peak, with a negative effect on the sizing of the storage (which is dimensioned based on the maximum peak).

Focusing now on Figure (3-11), which shows the storage energy level for 44 MW power demand, 45 MW installed wind power and a storage pressure of 11 bar. The energy profile is roughly balanced, and the reason behind this is the reduction of the GT's load past the energy minimum level, as shown in Figure (3-12).

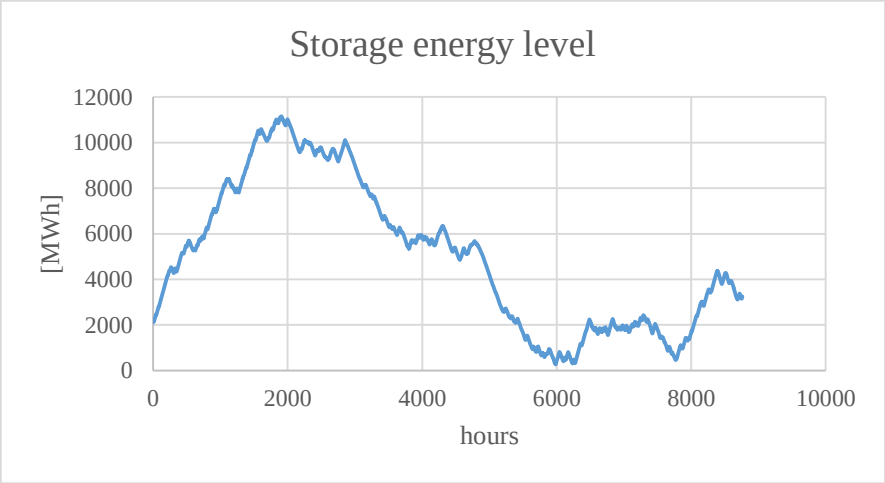

Figure 3-11: Example of storage energy level. 44 MW demand, 45 MW wind and 11 bar pressure

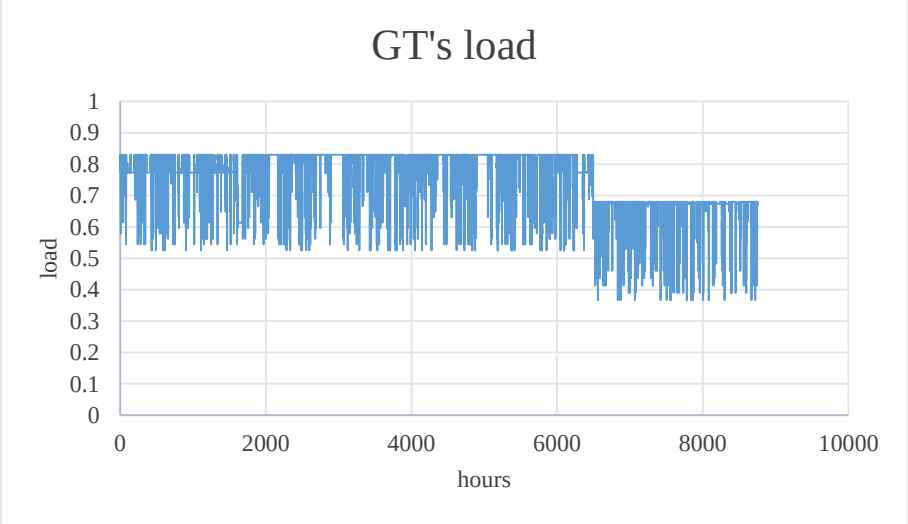

Figure 3-12: Example of GT's load. 44 MW demand, 45 MW wind and 11 bar

The frequent load changes are a result of the GT's adjustments 1c) and 1t) described in section 3.1 and will be explained with more detail in a following chapter. The default GT's load however is set to 0.8 (the lower the load in the first part, the smaller is the energy peak and the smaller is the size of the storage), and is reduced to 0.68 immediately after reaching the minimum energy level, in order, as discussed above, to balance the energy level.

Concerning the sizing of the storage, it is supposed that the required volume is divided into a number of vessels, each of them with a radius of 20 meters. The effect to the pressure gradient between top and bottom of the vessels is not considered.
If the vessel is thought to have a spherical shape, then the number of required units can be easily obtained

$$N_{vessels} = \frac{3}{4\pi}\frac{V}{r^3}$$

Where V is the maximum volume required and r is the vessel's radius.

3.6 Heat Exchanger

The platform's heat demand is met through the recovery of heat from the waste gas exiting the GTs. Mass flows and outlet temperatures are known in each off-design condition, thanks to the data given by the manufacturer.

The heat is sent to the processing unit of the platform using pressurised water at 22 bar, which enters the heat exchanger at 120°C and exits at 170°C.
Design parameters of the heat exchanger are presented in the Table 6.

The effectiveness is a dimensionless quantity between 0 and 1, and expresses the ratio between the actual heat transfer rate and the maximum possible heat transfer rate:

$$\varepsilon_{exchanger} = \frac{\dot{Q}}{\dot{Q}_{max}}$$

$\dot{Q}_{max}$ is the maximum heat that could be transferred between the fluids per unit time.

$$\dot{Q}_{max} = C_{min}\Delta T_{max}$$

Where

C_{min} is the lowest specific heat between the two fluids, and must be used as it is the fluid with the lowest heat capacity rate that would, in this hypothetical infinite length exchanger, actually undergo the maximum possible temperature change. The other fluid would change temperature more quickly along the heat exchanger length. The method, at this point, is concerned only with the fluid undergoing the maximum temperature change.

ΔT_{max} is the largest temperature differential experienced by one of the two fluids.

Table 6: Heat exchanger design parameters

Thermal Power [MW]	22
Gas flow required [kg/s]	88.3
Gas inlet temperature [K]	536.5
Gas outlet temperature [K]	313.6
UA [kW/K]	81.22
Water flow for cooling [kg/s]	102.5
Exchanger effectiveness	0.52

The effectiveness is a function the two types of fluids and their properties, the arrangement (cross-flow, counter-flow etc.) and the NTU (number transfer unit). NTU is a dimensionless coefficient, which links together the surface of exchange, the global heat transfer coefficient and the specific heat. Moreover, the exchanger's efficiency varies with operation, as the temperatures and the mass flows can vary, and because of fouling.

For the off-design calculations, a MATLAB routine was implemented, in order to obtain the gas outlet temperatures and flows, the water flows and the global exchange coefficient (UA). The exchanged heat is expressed through the following equations

$$Q_{exch} = \dot{m}_{gas}\, Cp_{gas}(Tin_{gas} - Tout_{gas})$$

$$Q_{exch} = \dot{m}_{water}\, Cp_{water}(Tin_{water} - Tout_{water})$$

$$Q_{exch} = UA\Delta T_{ln}$$

Where

$\Delta T_{ln} = \frac{\Delta T_2 - \Delta T_1}{\ln(\frac{\Delta T_2}{\Delta T_1})}$ is the log-mean temperature difference

And $$\begin{cases} \Delta T_2 = T_{hout} - T_{cout} \\ \Delta T_1 = T_{hin} - T_{cin} \end{cases}$$

In which T_h and T_c are the temperatures of the hot and of the cold fluids, respectively.
The UA values for the off-design operation can be computed through the commonly used relation [48-51].

$$\frac{UA_{off}}{UA_{des}} = \left(\frac{\dot{m}_{off}}{\dot{m}_{des}}\right)^{0.6}$$

3.7 Air preheating

The air coming from the storage enters the combustion chamber at ambient temperature; this means that a significant amount of fuel needs to be burned to heat the air at the required inlet temperature for the expansion in the air turbine (800 K). Introducing an air preheater in the form of a heat exchanger makes it possible to reduce fuel consumption and the subsequent emissions. The layout is shown in Figure (3-13) below.

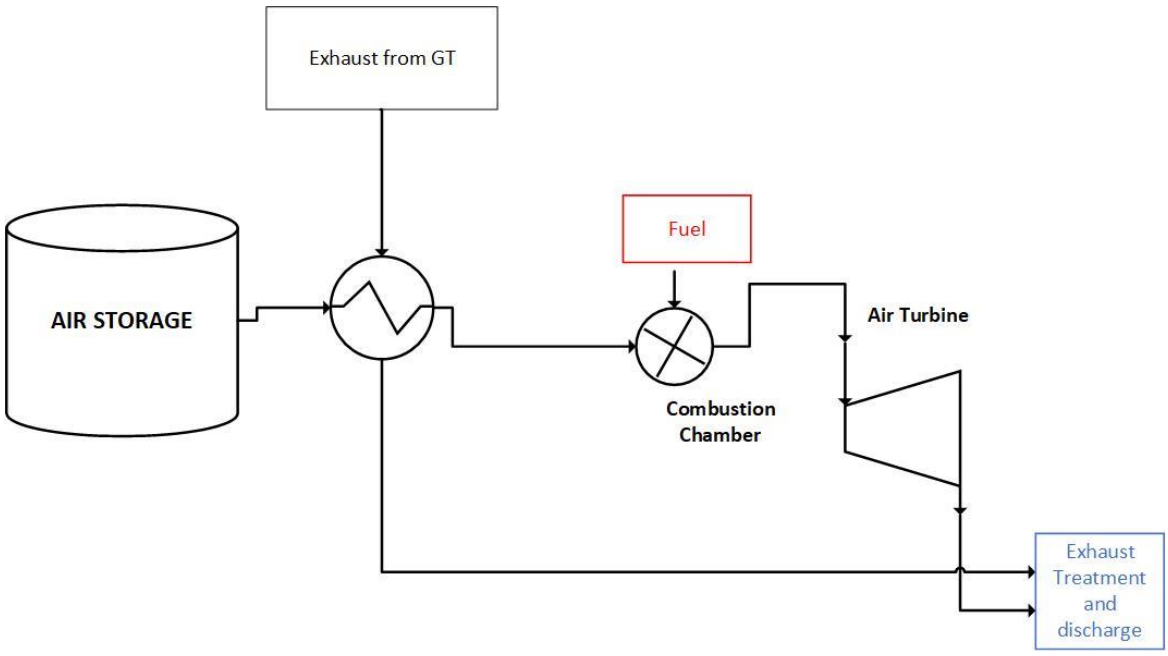

Figure 3-13: Layout scheme for air preheat integration

The GT on the platform operates continuously in order to provide the necessary heat and power. The minimum load of the GT is 36%, which means an exhaust flow of 60.1 kg/s, and is enough to satisfy the heat demand of the platform in every condition. In Table 7 are shown the heat demands for the lifetime of the platform and the required exhaust flows to meet these demands. The maximum flow is 60.1 kg/s, while the minimum is 26.2 kg/s. The minimum exhaust temperature is 774 K. The unused exhaust is the difference between the exhaust flow at 36% load and the exhaust flow required to meet the platform's power demand. During normal operation, the GT often works at higher loads, therefore the actual available exhaust flows are higher. However, for precautionary reasons, the available exhaust flow that can be used to preheat the air is thought to be the one in the Table below. This means that for the years 2016-2018, no air preheat is possible. From 2019 to 2022, the available flow is the one in Table 7, and varies between 11 and 20.2 kg/s. For the remaining years, the exhaust flow sent to preheat the air is limited 33.9 kg/s: in this case, depending on the storage pressure level, it may be required to lower the exhaust flow used to preheat the air down to 27.5 kg/s, in order to keep the minimum pinch point (this is done for 40 and 70 bar pressure, but not for the 11 bar scenario).

Table 7: Heat demand and exhaust flows

Year	Heat demand [MW]	Required exhaust flow to meet heat demand [kg/s]	Exhaust T [°C]	Unused exhaust [kg/s]
2016	15	56.5	518.0	3.6
2017	15	60.1	501.3	0.0
2018	15	57.9	511.3	2.2
2019	14	49.1	532.4	11.0
2020	13	45.0	529.7	15.1
2021	12	44.9	501.3	15.2
2022	11	39.9	503.1	20.2
2023	10	35.3	503.1	24.8
2024	9	30.5	506.8	29.6
2025	8	26.2	508.6	33.9
2026	8	26.2	508.6	33.9
2027	8	26.2	508.6	33.9
2028	8	26.2	508.6	33.9
2029	8	26.2	508.6	33.9
2030	8	26.2	508.6	33.9
2031	8	26.2	508.6	33.9
2032	8	26.2	508.6	33.9
2033	8	26.2	508.6	33.9
2034	8	26.2	508.6	33.9

The air enters the exchanger at ambient conditions (283.15 K) and is heated up to a maximum of 730 K. The maximum inlet temperature for the exhaust gas is 805.5 K, while the minimum is 774 K. This ensures a minimum pinch point of 44 K in every operating condition. The exhaust gases leave the exchanger at a temperature of 370 K. These values are summarized in Table 8.

Table 8: Extreme temperatures for the air preheat exchanger

Min exhaust inlet T	[K]	774
Exhaust outlet T	[K]	370
Air inlet T	[K]	283.15
Max air outlet T	[K]	730
Min pinch point	[K]	44

The heat exchange diagram for the values found in Table 8 is shown in Figure (3-14) below. The available heat from the exhaust stream varies between 14 MW and 0 MW, depending on the available exhaust flow rate (maximum 33.9 kg/s, minimum 0 kg/s). No calculations regarding the design and sizing of the heat exchanger are done, but only a thermodynamic analysis to quantify the available heat, the flows and the temperatures. Moreover, the sizing requirements for the additional equipment required for the integration of the air preheat may conflict with the stringent physical constrains of the offshore facility. Preheating the air up to 730 K means that less fuel has to be burned in the combustion chamber in order to reach the wanted inlet temperature in the air turbine (800 K).

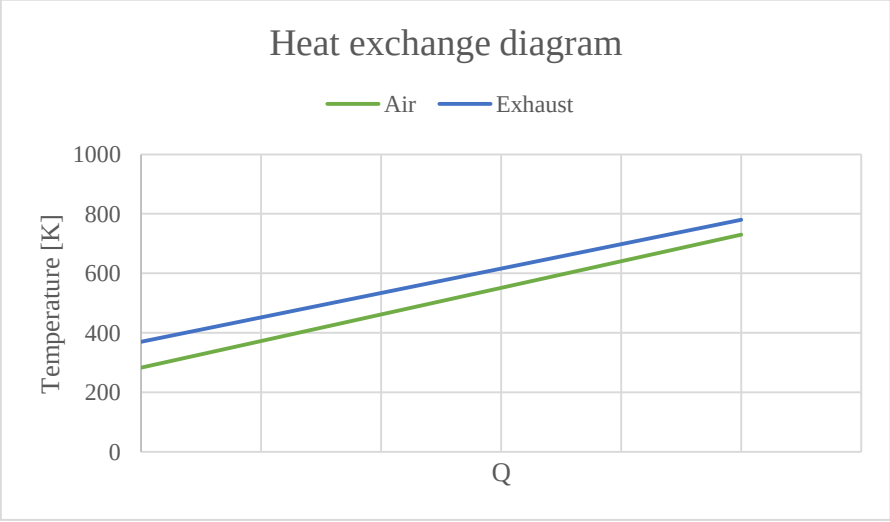

Figure 3-14: Heat exchange diagram between air and exhaust gas

4 CASE STUDY

Edvard Grieg and Ivar Aasen are two offshore installations located in the North Sea [52,53]. Edvard Grieg is equipped with two gas turbines in order to provide the necessary power to the system. An alternating current cable connects the two platforms, allowing the GTs on Edvard Grieg to supply the power demand of Ivar Aasen too.

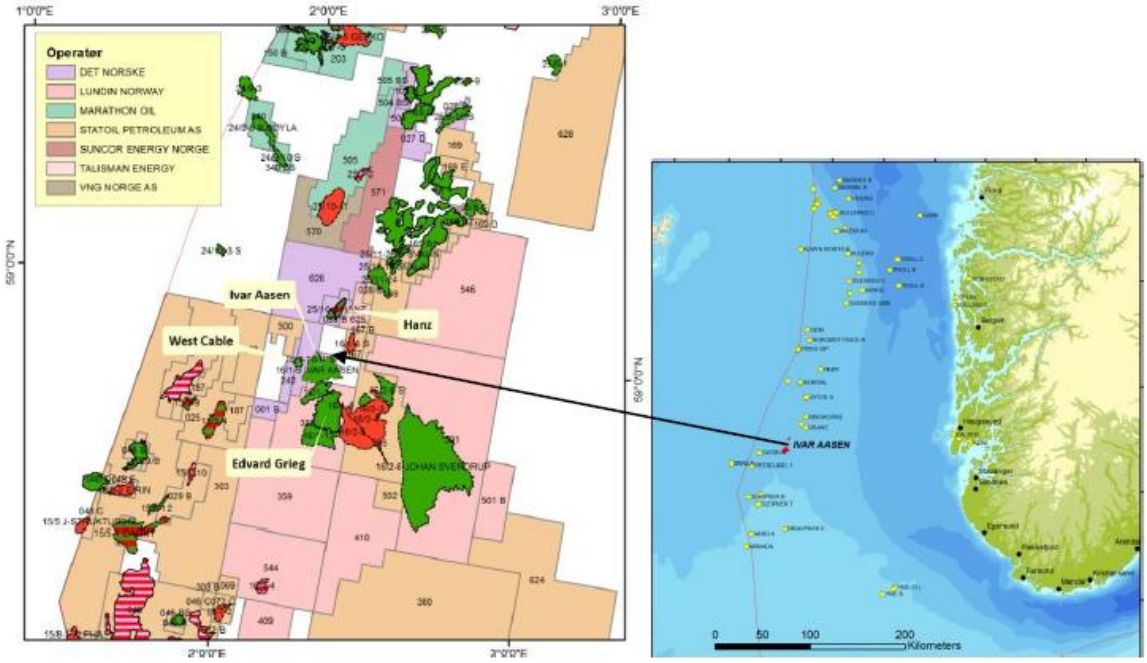

Figure 4-1: Location of the two platforms, [2]

The first oil was delivered during 2015 for Edvard Grieg and during 2016 for Ivar Aasen. The processing system for both plants consists of the following sections: production manifold, crude oil separation and stabilization, oil and gas condensate treatments, gas re-compression, oil pumping and water treatment.

Heat and power are required continuously to operate such facilities. The demands are shown in Figure (4-2). The maximum power demand occurs for the year 2019 and is 44 MW, while the minimum is during 2016 at 30 MW. From 2024 to 2034, the power demand stays constant at 33 MW. For what concerns the heat demand, it peaks at 15 MW during the period from 2016 to 2019, then it slowly decreases down to 8 MW (2025-2034). The heat and power

demand profiles reflect the typical evolution for offshore facilities (described in 2.1.1): Initially, there is an increased rate of production, therefore the power demand increases from 30 MW to 44 MW, and the heat demand is at its maximum of 15 MW. After this initial and brief phase, both the power and heat demands decrease, reaching the effective productivity level. The years from 2024 to 2034 cover the long timespan of the production plateau, during which both the heat and the power demands are practically constant. Moreover, the power and heat demands are averaged on an annual basis. The plant's lifetime was thus described as an annual sequence of steady-state conditions.

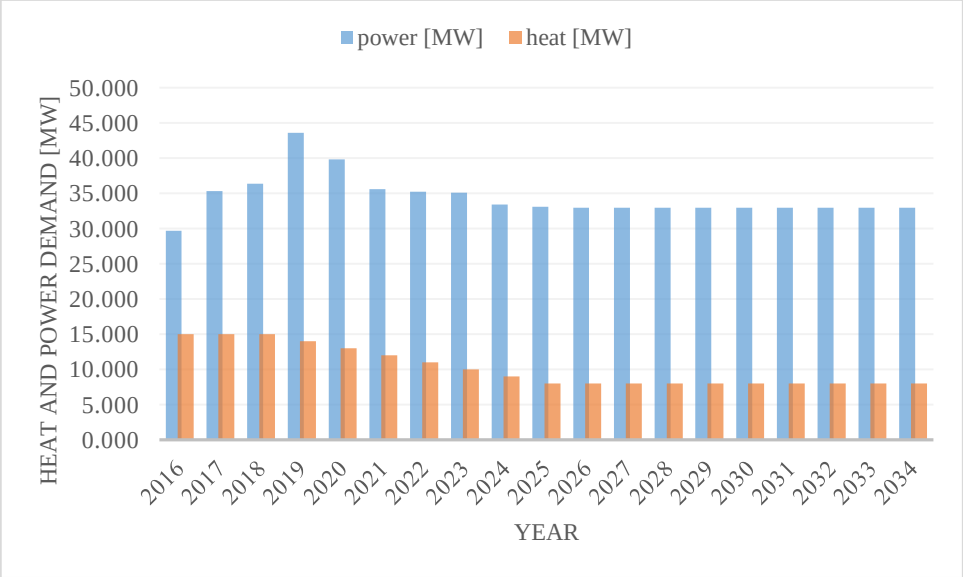

Figure 4-2: Platform's lifetime heat and power demands

Additionally, it is approximated that power is mainly needed for pumps and compressors, while only a marginal fraction is supplied to the other auxiliary functions. The main heat consumer is the oil separation and stabilization process. Additional heat is required for utility demands.

Oil and gas are sent from Ivar Aasen to Edvard Grieg for further processing and export. Therefore, process heat requirements are located almost exclusively on Edvard Grieg, while Ivar Aasen's heat demand can be considered to be negligible.

The current operating strategy is to provide the process heat via heat recovery from the exhaust gases of the two GTs. The recovered energy is transferred to a heating medium (pressurized water) in a separate heating circuit.

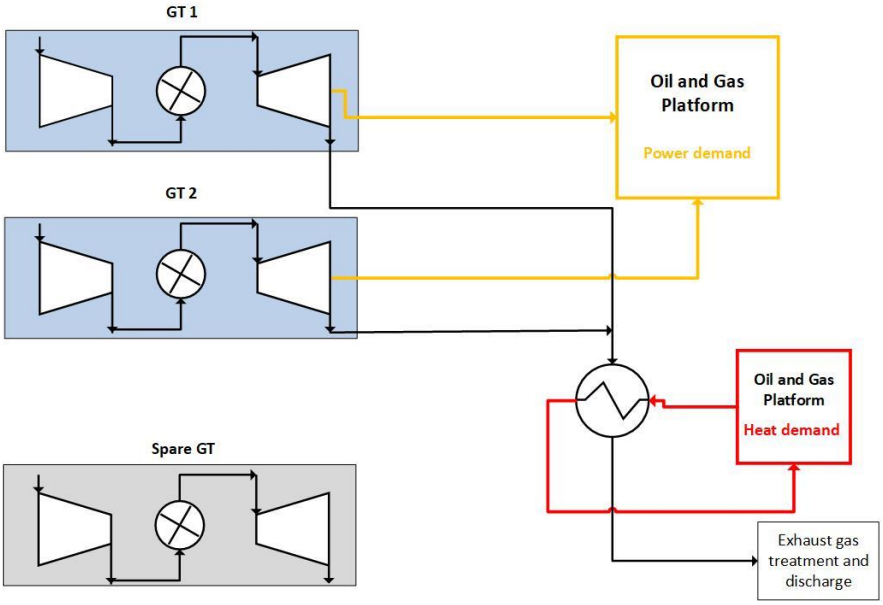

Figure 4-3: Case of study system layout

The offshore plants were simplified into two main blocks, the processing one and the power generation block, as shown in Figure (4-4) below. The power generation block includes the necessary equipment to provide power and heat to the offshore system. Depending on the specific operating conditions, the processing block has certain heat and power demands that must be met by the power generation section. For different heat requirements, the heating medium is adjusted by varying the amount of circulating water, assuming that the same temperature is requested by the processing unit.

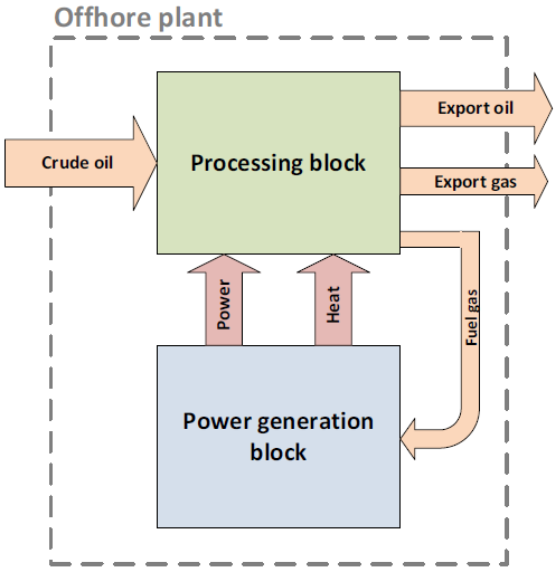

Figure 4-4: Processing and power generation units [9]

Site conditions and modelling assumptions are listed in Table 9 below.

Offshore facilities are usually not connected to the grid, and the demand is met with the use of gas turbines directly on site. It is therefore particularly important to satisfy the power and heat demands in a reliable and continuous way, even in unexpected operating conditions. From this need, the GTs on offshore rigs are traditionally operated in a load-sharing mode: the demand is met by running multiple GTs together in part load conditions. This provides the system with additional flexibility, making it easier to tackle sudden and large variations in the power demand, while at the same time ensuring high reliability and responsiveness. On the other hand, it inevitably leads to higher fuel consumption and lower efficiency, as the turbines are operated far from their design conditions for most of their lifetime. Therefore, two GTs operate continuously in part load, and an additional spare GT is kept on the platform for emergency reasons. The model used is GE LM2500+G4, an aero-derivative turbine specifically developed by General Electric for marine and industrial applications. The rated power at full load (ISO conditions) is 34.3 MW and the efficiency is 41.3%. Adjusting the values for the case study ambient conditions, the maximum shaft power decreases to 33.5 MW and the efficiency to 38.6%.

Table 9: Case study key parameters

Site	
Ambient T [°C]	10
Ambient P [bar]	1.013
Cooling water system	direct sea water cooling
Cooling water T [°C]	10
Sea depth [m]	110
Gas Turbine	
Fuel	CH4
LHV [MJ/kg]	50.047
GT ΔP inlet [mbar]	10
GT ΔP outlet [mbar]	10
Design power [MW]	33.5
Design efficiency	0.386
Water Loop	
Pressure [bar]	22
Inlet temperature [°C]	120
Outlet temperature [°C]	170

Part load and efficiency of each GT are evaluated for each year, by dividing equally the platform's power demand, as described above. Results are shown in Figure (4-5). The average load is around 50%, with a minimum at 45% during the year 2016 and a peak of 66% in 2019. Efficiency averages around 30%, value that is way lower than the design one (38.6%).

These results clearly show that the shared-load strategy leads to low turbine efficiency, low loads and therefore higher fuel consumption and CO_2 emissions.

The system's efficiency is obtained with the known relation

$$\eta_{global} = \frac{Output}{Input} = \frac{Power\ Demand}{\dot{m}_{fuel} LHV} \qquad (4.0)$$

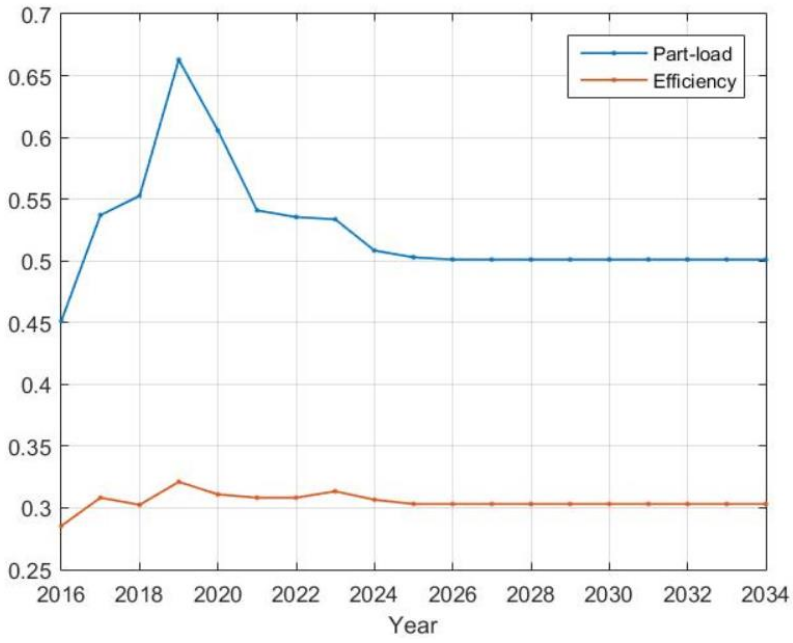

Figure 4-5: GT's efficiency and load in the case of study. years 2016-2034

Regarding the CO_2 emissions, as described in the beginning of chapter 3, it is supposed that the combustion is complete and that the fuel composition is 100% methane (CH_4). Therefore, using the balanced combustion reaction, it is possible to estimate the lifetime's emissions, which amount to 3.65 million tonnes.

$$CH_4 + 2O_2 = CO_2 + 2H_2O$$

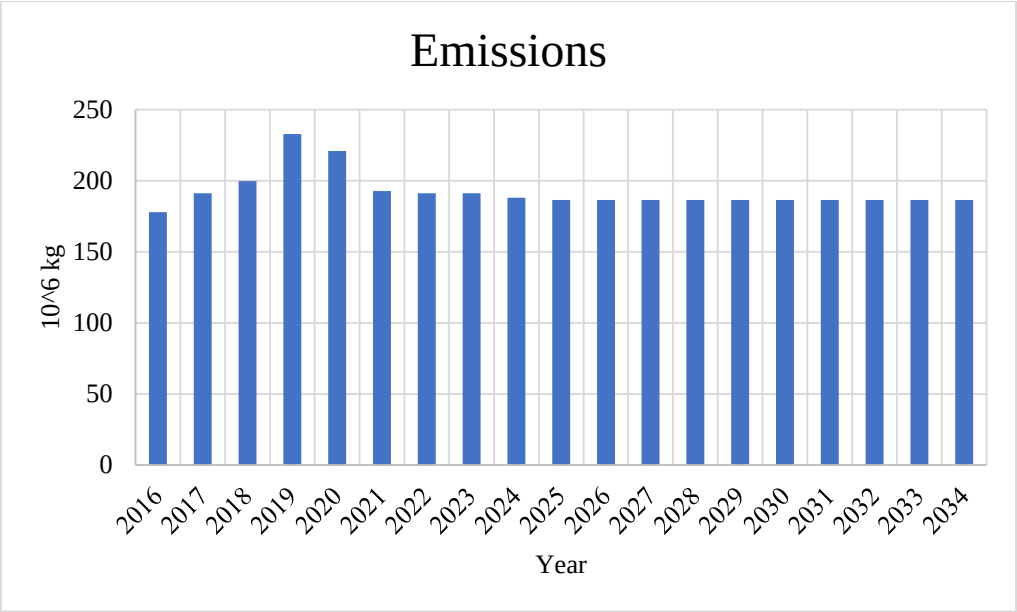

Figure 4-6: Annual CO_2 emissions for the case of study

The heat demand peaks at 15 MW. Therefore, the minimum GT's load has to be enough to provide the necessary exhaust gas flow to provide this heat. The model of the heat exchanger was described in section 3.6. The main result is that one GT at 36% load is able to satisfy the 15 MW heat demand alone. This means that in the case study, a significant amount of heat is wasted, since both the GTs operate at the same time. When the heat demand decreases, it would theoretically be possible to lower the GT's load even further; however, mostly due to NOx emissions, it is rarely possible to decrease the GT's load under 35%. For this reason, the lower limit was set to be 36% in every operating condition, regardless of the particular heat demand.

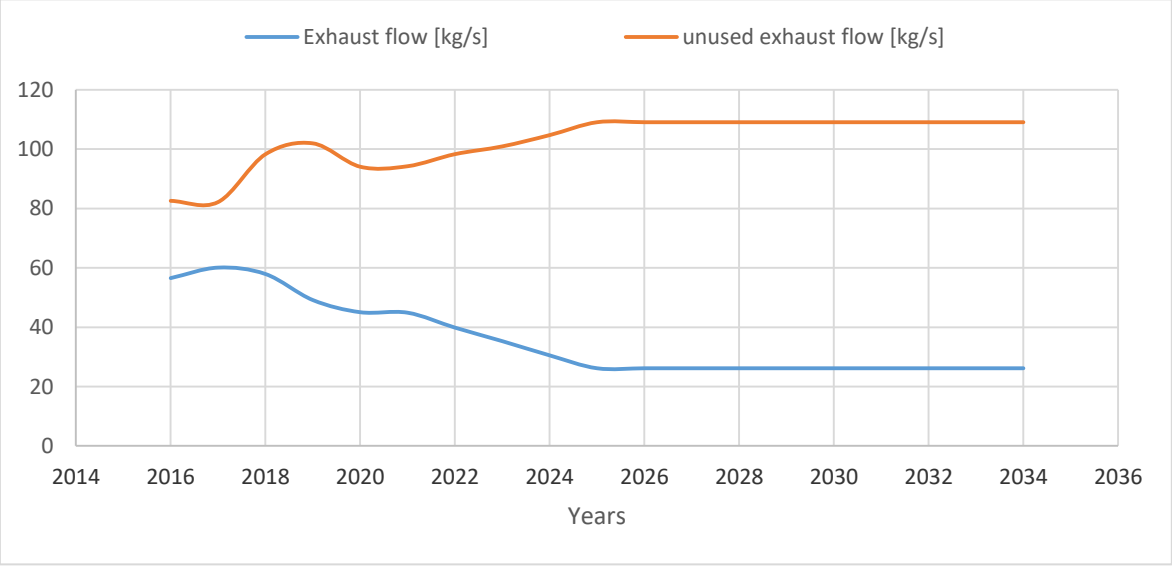

Figure 4-7: Exhaust flow and unused exhaust flow for the years 2016-2034

From Figure (4-7), it can be seen that the exhaust gas flow exiting the GTs diminishes, thanks to the lower power demand of the platform. The unused exhaust flow, which is the fraction of the total exhaust flow that is not needed to meet the platform's heat demand, increases instead, because of the large decrease of heat demand, especially during the production plateau. This means that, for a long time-span, a significant fraction of the available exhaust heat is wasted, leading to energy and exergy dissipations.

A decreasing trend can also be seen in the heat exchanger's effectiveness (described in section 3.6). The design value is 0.52, but it rapidly reaches values under 0.2, meaning that the exchanger is over-sized for the case of study. The effectiveness profile is shown in Figure (3-8).

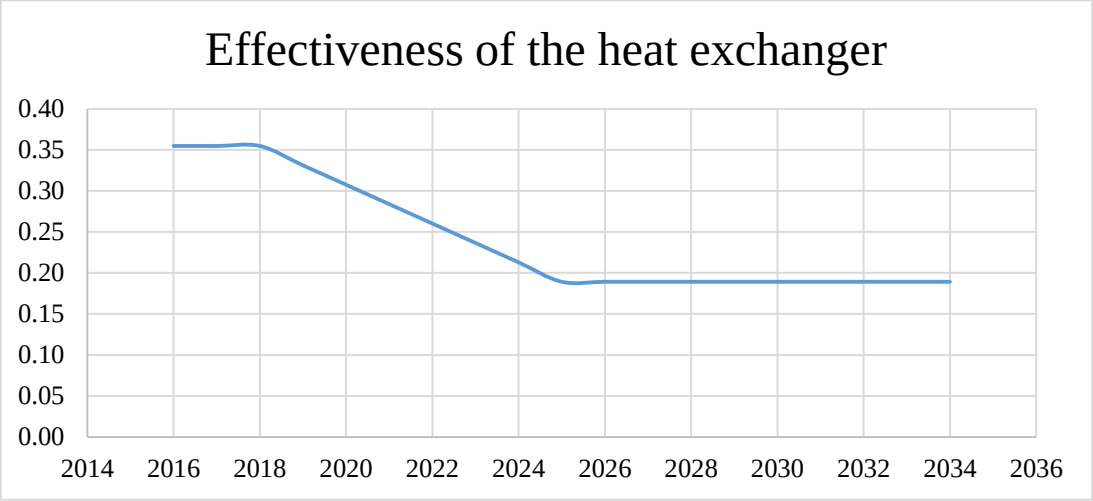

Figure 4-8: Effectiveness of the heat exchanger. Years 2016-2034

This study clearly shows that the high CO_2 emissions are caused by the shared load operation for the GTs on the platforms. Moreover, this operating strategy also results in far from optimal heat exchange, with a significant fraction of exhaust gases at high temperature that is wasted.

Both these problems could be partly addressed with the removal of the 2nd GT, which is possible with the integration of a wind farm and a CAES system.

Another interesting opportunity is presented by the integration of a wind park together with a different operating strategy for the GTs on the platform, without the implementation of a CAES system. Both these ideas will be developed in the following sections.

5 INTEGRATION OF A WIND FARM

5.1 Introduction and operating strategy

The first step to reduce the CO_2 emissions is to build a wind farm in the proximity of the platforms, and connect it to the platform with electric cables. In this way, the extracted energy from the wind is directly sent on the platform in the form of electric energy, and therefore can be immediately used to partially cover the power demand of the offshore rig.
In this chapter, a detailed analysis of how different installed wind powers affect the case study is carried out. The results that are obtained here are useful when investigating the system including the CAES section. In particular, the performances of the system with only the integration of the wind farm represent an important benchmark to understand if the CAES brings a large enough improvement to justify such a complex configuration.

As introduced in section 3.2, a 1-year wind profile with a 1-hour time-step is available (the wind profile had 1-minute time-steps, and was down-sampled to a 1-hour one). The default wind turbine was chosen to be a 5 MW NREL. Coupling these two with a 1.1 wind ratio allows to compute the wind turbine's electrical power output, averaged hourly. This means that the following analyses are considered as an hourly sequence of steady-state conditions. A 2% transmission loss was included in the computation too.

In this configuration, the system's efficiency can be expressed by adjusting Equation (4.0): the power demand is the same, but the energy input becomes the sum of the energy released by the fuel during combustion and the electric energy sent from the wind park.

$$\eta_{global} = \frac{Output}{Input} = \frac{Power\ Demand}{\dot{m}_{fuel} LHV + Power\ from\ wind} \qquad (5.0)$$

The layout of the system is shown in Figure (5-1) below.

The integration of a wind farm does not allow for the removal of the 2nd GT. This fact is independent on the wind farm size, and the reason behind this is that the maximum GT load

(95%) is 31.9 MW. Therefore, if there is no wind blowing, the platform's power demand simply can not be met with the use of 1 GT only. The only exception is the 30 MW demand year, since a single GT close to full power can provide the necessary power alone.

The GTs can operate, as described in previous sections, between 36% and 95% of their nominal output.

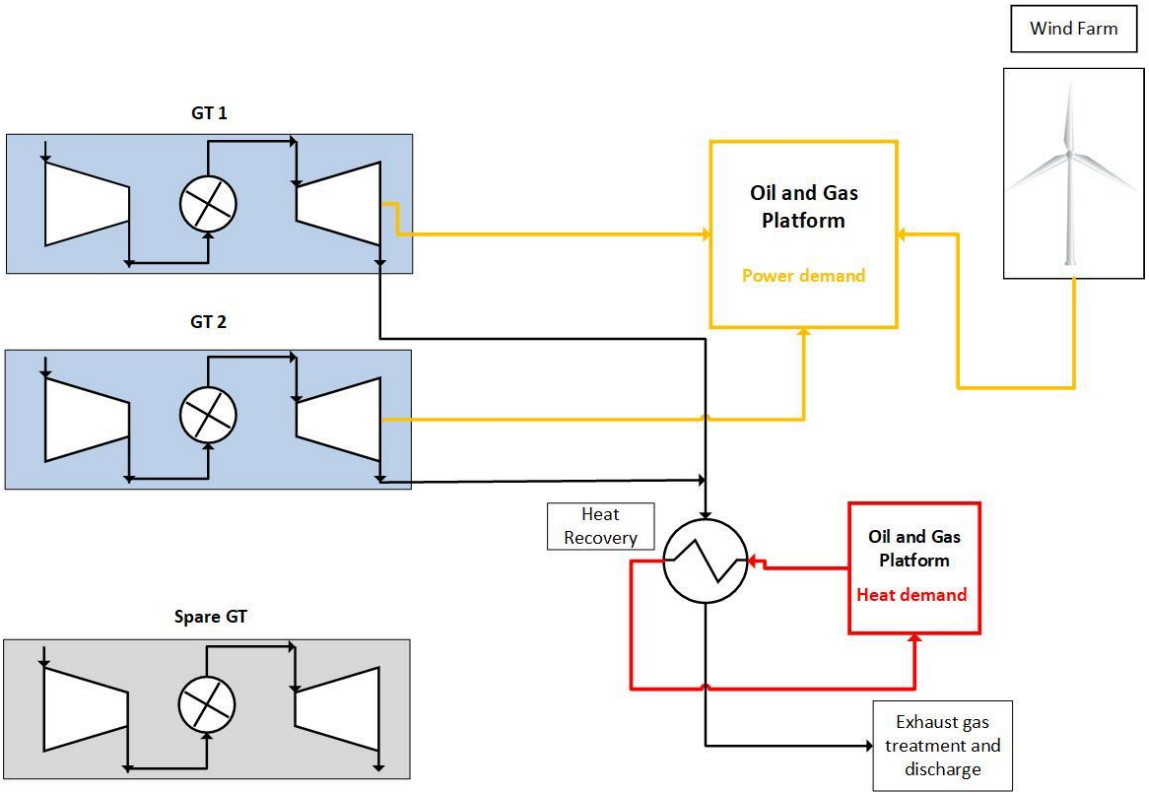

Figure 5-1: Layout of the system with wind integration

Operating strategy

The aim is to exploit as much as possible the energy contribution that comes from the wind turbines. The wind power (WP), which is sent directly on the platform in the form of electric energy through the cables, is immediately used, as it represents an "emission free" source of energy. This leads to the fact that the GTs have the objective of covering the remaining power demand that is not met by the WP, adjusting their loads. As discussed in chapter 4, the traditionally used shared-load operating strategy has the disadvantages of low part loads and high specific fuel consumption (and therefore, high CO_2 emissions). For this reason, the shared-load operation is limited as much as possible in this configuration.

The idea is to meet the power demand of the platform (PP) with a combination of power from the wind farm and power produced by a single gas turbine (PGT). When this is not enough, for example during periods without wind, the 2nd GT is started, and the power demand is divided equally among the two turbines.
The following scenarios are possible:

- If $WP + PGT\_\min > PP$

  The available power from the wind and the minimum power output (36%) produced by a single gas turbine are enough to meet the power demand of the platform. This means that any excess in the wind power production is not usable (the GT's load cannot be lowered any further), and therefore goes wasted

- If $WP + PGT\_\min < PP$

  The available power from the wind and the minimum power output produced by a single gas turbine are not enough to meet the power demand of the platform. In this case, the GT's power output must be increased accordingly to reach the power demand. This is possible until reaching the GT's maximum power output (95%). No wind energy is wasted.

- If $WP + PGT\_\max < PP$

  The available power from the wind and the maximum power output produced by a single gas turbine are not enough to meet the power demand of the platform. The 2nd GT is started, and the load is shared equally among the two. If both the GTs are working at their minimum power outputs, any excess in WP is wasted.

The above described strategy maximizes the wind utilization, makes the single GT work at higher part loads (so, closer to its nominal conditions) and leads to the shared-load GTs operation only when there is no other way to provide the platform with the necessary power. On the other hand, this strategy comes with inevitable disadvantages: wind energy is often wasted, the 2nd GT incurs in frequent starts and stop and the 1st GT is subjected to rapid and variable load changes, required to match the unpredictability of the wind profile. Frequent starts and stops, and sudden load variations, affect negatively the turbines, and can lead to a lower lifetime, increased wear and additional maintenance operations.

5.2 Discussion of the results

The introduction of wind energy into the system reduces the fuel consumption on the platform and leads to lower CO_2 emissions into the atmosphere. Different wind farm sizes are compared, and their lifetime results are summarized in Table 10 (averaged values for the whole lifetime).

Table 10: CO_2 reduction and wasted wind energy for a different number of installed wind turbines

	CO2 [10^6 tonnes]	Reduction from base case [%]	Reduction from case above [%]	Wasted wind [%]
Base case	3.65			
5 MW	3.13	14.20	14.20	0.00
10 MW	2.92	20.06	6.83	0.00
15 MW	2.74	24.91	6.06	0.00
20 MW	2.60	28.65	4.98	0.33
25 MW	2.47	32.30	5.11	7.72
30 MW	2.39	34.57	3.36	16.20
35 MW	2.31	36.66	3.19	23.73
40 MW	2.24	38.70	3.22	30.14
45 MW	2.17	40.58	3.07	35.56

The integration of a wind farm with the operating strategy discussed in the section above looks highly beneficial, reducing the CO_2 emissions significantly even with the 5 MW case. A single wind turbine reduces the emissions, compared to the case study, by more than 14% alone, and fully exploits the wind production. This value is particularly high because of the effects of both the integration of the wind resource and the different operating strategy of the GTs on the platform. Increasing the number of wind turbines keeps improving the reduction, from the 20% of the 10 MW installed wind power to the 40.6% of the 45 MW wind farm. It

is interesting to point out that increasing the wind farm's size by 450% (from 10 MW to 45 MW), only doubles the CO_2 reduction (20% to around 40.6%). This fact is more evident when considering that an increase of 50% of the number of turbines (from 6 to 9, meaning from 30 Mw to 45 MW), only results in an additional 6% decrease in CO_2, compared to the case study. Therefore, there is a sort of diminishing effect: increasing the installed wind power gives smaller and smaller benefits, as clearly visible by looking at the "reduction from case above" of Table 10. This effect is partially explainable by the increased fraction of wind energy that goes wasted (the values in Table 10 are the lifetime averages). Installing one to three wind turbines allows to fully exploit the wind resource, while increasing this number leads to higher and higher fractions of wasted energy, from 0.33% of the 20 MW case, to the 35.56% of the 45 MW scenario. The reason behind this increasing amount of wasted wind energy can be found in the operating strategy of the system: the larger the wind penetration, the lower becomes the average load of the gas turbines. But, as described above, once the GT is at its minimum, any additional wind power is simply not usable and goes wasted. Table 11 below adds more interesting results.

Table 11: Working hours and loads for the GTs. Wind farm size between 5 MW and 45 MW

	Working hours single GT	Working hours in shared-load	Average load for single GT	Average shared-load	System's efficiency
Base case	0	8760	0.00	0.51	0.310
5 MW	4313	4447	0.79	0.48	0.355
10 MW	5422	3338	0.76	0.48	0.370
15 MW	6105	2655	0.73	0.48	0.382
20 MW	6424	2336	0.65	0.48	0.389
25 MW	6617	2143	0.60	0.48	0.396
30 MW	6809	1951	0.57	0.48	0.397
35 MW	6912	1848	0.55	0.48	0.396
40 MW	7021	1739	0.53	0.48	0.395
45 MW	7105	1655	0.52	0.48	0.394

The introduction of the wind farm and the adoption of the different operating strategy compared to the one used in the case study, immediately results in higher system's efficiency, from 31% to 35.5%. The shared-load strategy operates for only 4447 hours, compared to the 8760 of the case study. The remaining hours are covered by the single GT plus the wind integration, as explained in the operating strategy of the system. This reduces significantly the fuel consumption for two reasons: the first one is the reduced time in which two GTs work simultaneously, and the second one is that the higher the average load is, the smaller is the specific fuel consumption, accordingly to what described in Figure (3-2). It is interesting to note that increasing the number of wind turbines has no effect on the average shared-load of the two GTs, but reduces the working time of the shared-load strategy. The second effect is easy to explain, since a higher wind penetration reduces the need to start the 2^{nd} GT more often. The 2^{nd} GT only starts when the sum of the power from the wind and the power from the single GT at its maximum power output (95%), do not match the power demand of the platform. This leads to two results: the first is that no wind energy is wasted during the shared-load mode, since all the available wind energy was already being used. The second is that the load is shared only when the single GT would go above the 95%, leading to a shared value between 47.5 and 60%, depending on the specific demand for that year. However, the values in Table 11 are lifetime averages, in which the contribution of the production plateau is predominant, leading to that 48% shared load for every wind farm size. When considering the behaviour of the single GT, an increase in the installed wind power means more working hours, in accordance to the reduced working time of the part load strategy (at least one GT always operates, in order to provide the platform with the necessary heat for the processing of the crude oil). On the other hand, it reduces the average GT's load. While this effect should be considered negative when considering the GT only, since low loads mean lower efficiencies and higher specific fuel consumption, it becomes a positive effect when considering the whole system. A low GT's power output means that a higher fraction of the platform's power demand is met with "emission free" energy from the wind park, therefore the total CO_2 emissions decrease.

Efficiency-wise, up to 30 MW of installed wind power have a beneficial effect. This is particularly true for the scenarios in which the wind energy is fully exploited and the fuel consumption is reduced. After this point, the efficiency starts to slowly decrease. This is because the positive effect of the reduced fuel consumption is counter-balanced by the increasing fraction of wasted wind energy, as understandable with Equation (5.0).

It is now interesting to focus on the 30, 35, 40 and 45 MW wind sizes, which are the promising when considering the CAES integration in chapter 6 (smaller wind sizes would not allow the removal of the 2nd GT, which is the main objective of the CAES, as will be discussed later).

Table 12: Lifetime results for significant wind farm sizes (30-45 MW)

	CO2 [10^6 tonnes]	Reduction from base case [%]	Reduction from case above [%]	Wasted wind [%]
Base case	3.65			
30 MW	2.39	34.57		16.20
35 MW	2.31	36.66	3.19	23.73
40 MW	2.24	38.70	3.22	30.14
45 MW	2.17	40.58	3.07	35.56

Moving from the lifetime average to a year-by-year average, the CO_2 emissions are shown in Figure (5-2). When the power demand from the platform is low (30 and 33 MW), increasing the farm size results in smaller improvements compared to the ones achieved for high power demand years (40 and 44 MW). This is again one of the results of the operating strategy: when one GT operates at its minimum output, the excess wind energy is wasted. Therefore, the lower the power demand and the larger the wind farm, the faster the GT reaches its minimum (36%), resulting in a lower CO_2 reduction and a higher fraction of unused wind energy, as can be seen in Figure (5-3).

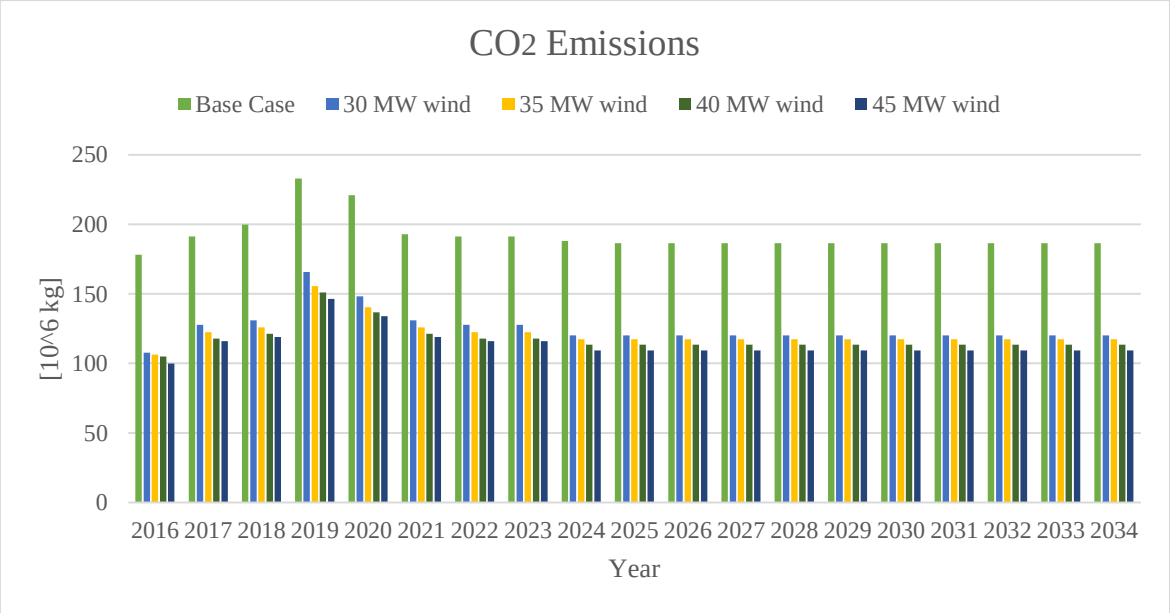

Figure 5-2: Emissions on a yearly average for 30-45 MW wind

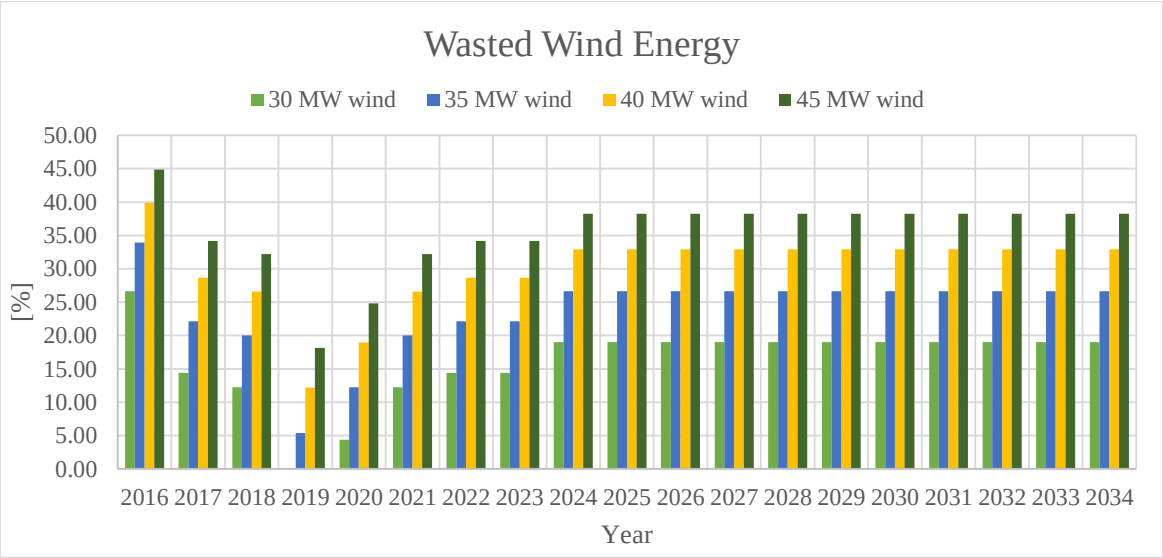

Figure 5-3: Unused wind fraction for wind farm size between 30 and 45 MW

This also means that during low demand years, a smaller wind park has a better overall system's efficiency, while on high demand years the opposite happens, as can be seen in Figure (5-4). In any case, the achieved efficiency is always much higher than the one of the system without wind integration, increasing from around 30% to almost 40%.

Regarding the working hours of the single GT, shown in Figure (5-5), a wind farm increase means a higher operating time, as discussed above. It is however interesting to point out that, while for the 30 MW demand the single GT works without the need for the 2nd GT, during the remaining years the higher the power demand is, the less time the single GT works.

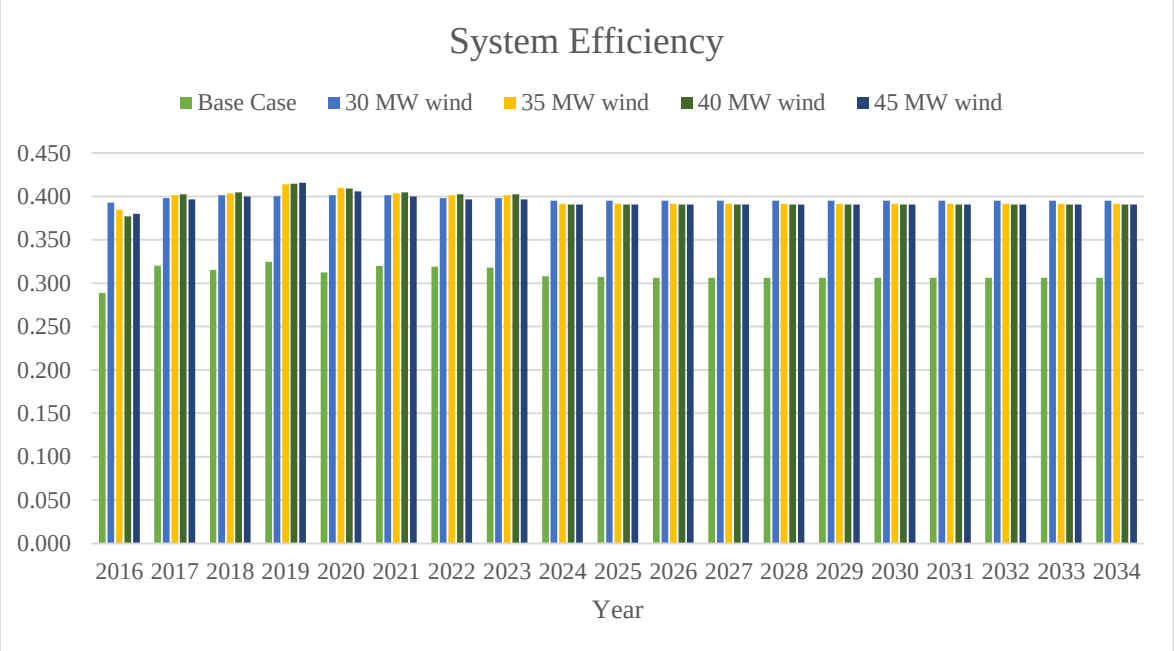

Figure 5-4: System's efficiency. Values are yearly averages

This agrees with the operating strategy: higher demands are more likely to need the integration of the second gas turbine in shared-load with the first. This fact is confirmed by the operating hours of the shared-load strategy, shown in Figure (5-6), which decrease for low demand years and high wind farm sizes.

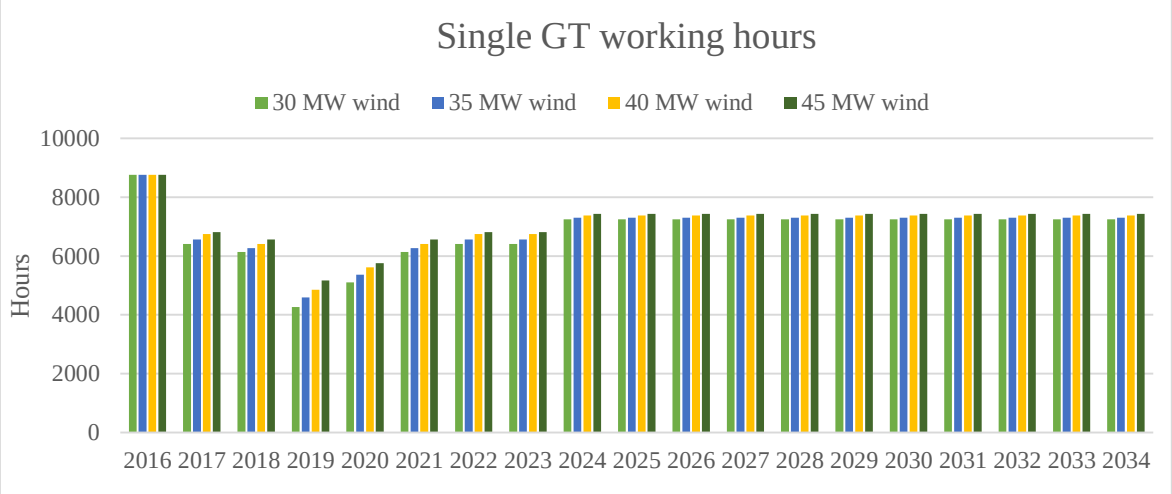

Figure 5-5: Working hours for single GT operation. 30-45 MW installed wind power

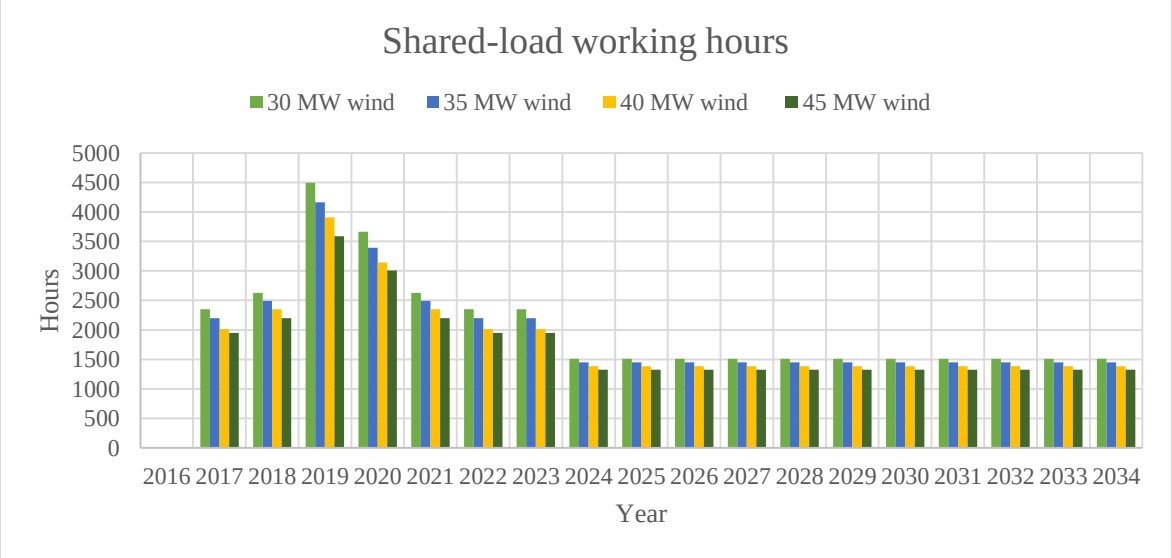

Figure 5-6: Working hours for both the GTs sharing the same load.

Summarizing:

- Increasing the wind farm's size has a beneficial effect on the CO_2 emissions, but leads to an increased waste of wind energy. This beneficial effect however becomes smaller and smaller the larger the wind farm is.
- Increasing the wind farm's size reduces the working hours of the shared-load GTs operation, with a beneficial effect on the fuel consumption. However, the average load is not affected by the number of wind turbines.

- Increasing the wind farm's size also reduces the fuel consumption for the single GT, as more of the platform's power demand is satisfied with the wind energy. An average load of 0.52 for 7100 hours (45 MW installed wind) ends up using less fuel than a load of 0.79 for 4300 hours (5 MW installed wind). This is of course advantageous when considering the CO_2 emissions.

From this analysis, it would seem that, when considering only the CO_2 emissions, the 45 MW wind farm gives the best results and therefore should be pinpointed as the most promising configuration. However, nor the economical aspect neither the electrical balance of the system are taken into account. Both these aspects are of fundamental importance: increasing the number of wind turbines comes with additional cost (investment, operation, maintenance), therefore it could result that a larger wind farm is less economically attractive than a smaller one. This fact will be introduced in the Economic section, further in this work. Concerning the electrical balance of the facility, as introduced in section 2.2.4, the non-guaranteed power production from wind parks can be especially problematic in small autonomous systems, or in those with high wind power penetration. Wind turbines are vulnerable to even slight variations of the system's frequency or voltage amplitude, possibly leading to a total blackout, especially in cases of weak and non-interconnected systems.

6 CAES INTEGRATION

6.1 Introduction and operating strategy

The objectives of this system are to remove the need for the 2nd GT on the platform and exploit in a more effective manner the wind power. The effect would contribute to reduce the emissions even further, while at the same time improving the overall efficiency of the energy system. Moreover, integrating a storage with a wind farm, especially in an off-the-grid system like the offshore environment, would bring a series of advantages from the point of view of the electrical balance and stability, as discussed in more detail in section 2.2.4.

The CAES is of the conventional type, with a post-refrigerated compression and additional fuel needed to heat the air, which is stored at ambient temperature. The A-CAES was not studied, since this technology is not mature yet. Moreover, the strict physical constrains on the offshore platform would make it particularly difficult, if not impossible, to size a thermal storage with the appropriate capacity.

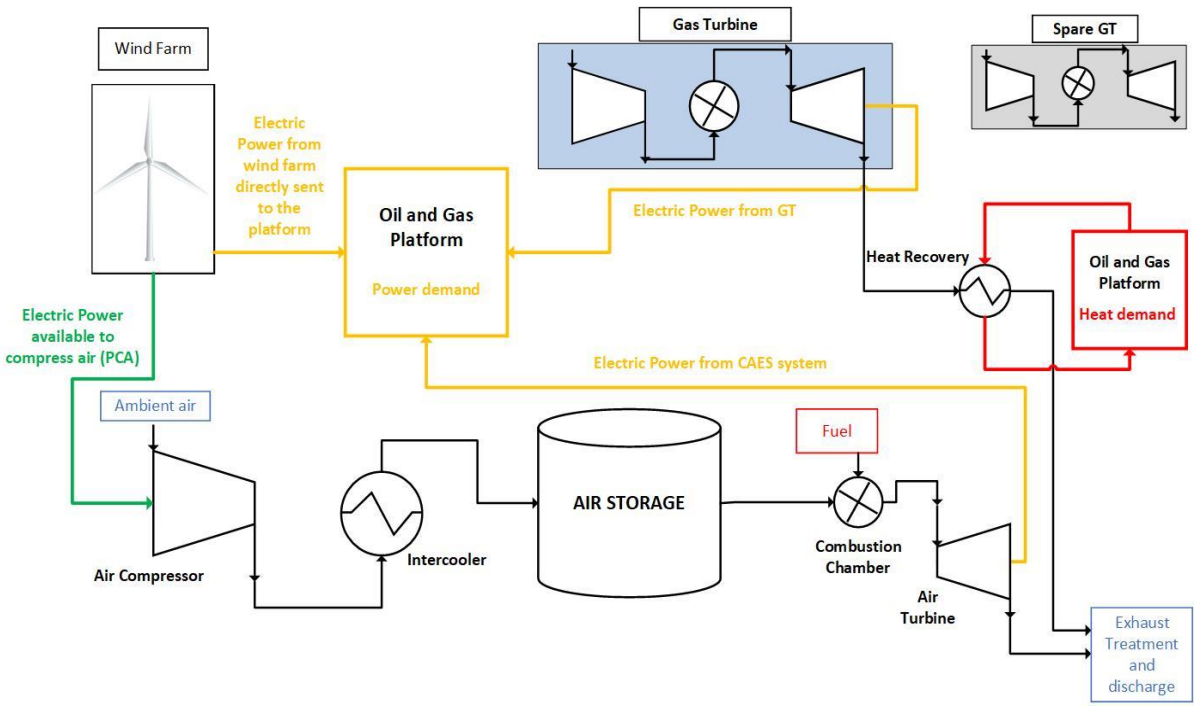

Figure 6-1: Layout of the system with CAES integration

The layout of the system is shown in Figure (6-1) above. The models of the various components have already been introduced and described in chapter 3.

A variety of key parameters are investigated, from the size of the wind farm (in a similar way to what was done during chapter 5) to different storage pressure levels, to the possibility to recover some of the exhaust gas from the gas turbine to preheat the air coming out of the storage, before its entrance into the combustion chamber.

For each scenario, simulations are carried out for two significant platform's power demands: 30 MW (the minimum) and 44 MW (the maximum). Those extreme values provide useful information regarding the performance of the system, the charging-discharging of the storage and its sizing. It is important to investigate both these scenarios before proceeding to simulate the lifetime's performance of the system for a given configuration. This is better explained with the following example, shown in Figure (6-2), which represents the storage energy level for the two extreme demands of the platform in the case of a storage pressure of 11 bar and a wind park of 30 MW.

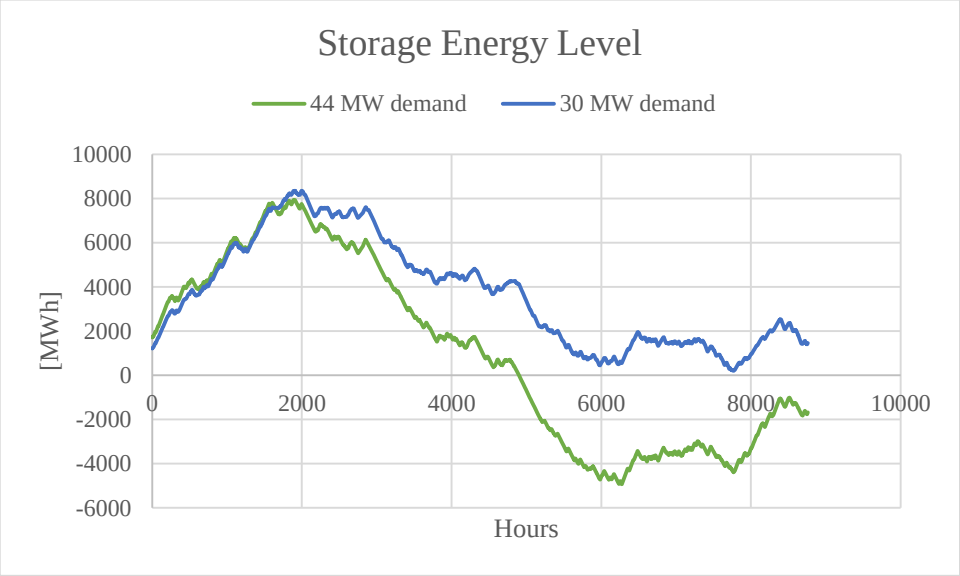

Figure 6-2: Energy storage level for min and max demand of the platform. 11 bar storage and 30 MW installed wind

It can be seen that the 30 MW demand results in a balanced profile, while for the 44 MW demand the storage empties around hour 5000, meaning that the system is not able to provide the required power to the platform, since the GT is already working close to its full power. The result is that the 30 MW wind farm is not a feasible option, since it does not satisfy the requirement of making it possible to remove the need for the 2nd GT in every operating condition. This fact only emerged because both the extreme demands were studied.

Therefore, if a configuration works for both these demands, it will also work for the other power demands, which are in between these two extreme values. Moreover, from the simulations that were carried out in this work, it is also possible to state that the maximum volume required by the storage is always found for one of these two demands.

After comparing the different configurations for these demands, the most promising scenarios are pinpointed and calculations for the CO_2 emissions during the whole platform's lifetime executed, allowing to compare the obtained results with the benchmarks represented by the base case of study and by the system including the integration of the offshore wind farm.

The key investigated parameters are summarized in Table 13 below.

Table 13: Key investigated parameters for the CAES introduction

Wind Farm Size [MW]	Storage Pressure Level [bar]	Air Preheat	Air Turbine Design
30	11	YES	A
35	40	NO	B
40	70		
45			

The size of the wind farm directly affects the emissions, the average load of the gas turbine and the energy storage requirements. Sizes below 35 MW do not allow to remove the need for the 2nd GT, as shown from the example of Figure (6-2). Sizes above 45 MW were not investigated, given the decreasing trend linked to the size of the wind farm discovered and discussed in the previous chapter.

The pressure level of the storage mostly influences the volume's requirements, and therefore the number of the required underwater vessels. Moreover, it has a direct effect on the air compressor design, leading to preferring a single-staged compression without intercooling for the 11 bar scenario, or a two-staged compression with intercooling for the other two pressure levels. The different configuration for the air compressor section leads to different power consumptions and therefore different elaborated air flows and CO_2 emissions, as will be discussed in the following. The 11 bar case was studied because it is the maximum possible storage pressure given the limited sea depth in the surroundings of the platforms

used as case of study. The 40 and 70 bar were chosen as significant examples because of the results achieved in (Jong, 2014), were it was found that sea depths between 400 and 700 meters are particularly attractive for the UWCAES technology.

Simulations of the performance of the system are also carried out for different air turbine designs. Namely, a design with a lower air consumption but a higher inlet temperature (A) is compared to one with higher elaborated flows but a lower inlet temperature (B). A steeper discharge curve and a marginal reduction in CO_2 emissions are achieved with the second design. This was already introduced in section 3.4, and additional details can be found in Appendix A. Design (A) is the one chosen for this work.

Finally, the air turbine design has to be adjusted when studying different sea depths, as the mass flow elaborated in the air compressors are different, leading to different charging profiles for the underwater vessels. In particular, while the inlet temperature is assumed to be constant in every condition, the minimum and maximum output powers of the turbine vary according to the different discharge capabilities of the compressed air storage.

Operating strategy

The general strategy is to exploit as much as possible the wind resource, therefore trying to utilize as little as possible the gas turbine on the platform (which still has to operate at least at 36% of its nominal power due to the heat requirement of the processing section of the offshore facility). The preferred option is to send the electric power produced by the wind turbines directly on the platform through the underwater cables that connect the offshore rig to the offshore wind farm. Another possibility is to use the power generated by the wind to produce compressed air and store it into underwater vessels for future use. Both these option can occur at the same time. In particular, the power extracted from the wind is sent to the CAES system in the situations during which it could not be sent directly on the platform.
It is important to underline that the gas turbine on the platform is continually adjusted depending on several parameters:

- The wind power output (WP)
- The range of powers in which the air compressors can operate (AC)
- The range of powers in which the air turbine can operate (AT)
- The energy storage level (ESL)

First of all, the load of the GT is lowered if there is an excess of wind power or increased if there is a reduction in the wind power output, in a similar way to the operating strategy described during chapter 5, in order to exploit the wind resource as much as possible.

The adjustments required by the gas turbine due to the behaviours of the AC and AT have already been described in section 3.1, and will be recalled below:
If the power available to compress the air (from the excess wind production) in not enough to reach the minimum power required to start the compressor, the GT can be adjusted following one of the two strategies:

1c) Reduce the GT's load by the excess power unusable for the compression. This is possible only when the GT is at high enough loads, but it is not feasible when the GT approaches the lower load limit.

2c) Increase the GT's load in order to reach a high enough excess power to start the air compressor. This operation is only possible when the GT is not already close to its maximum load.

Both these strategies are used: approach one is more appropriate for platform's demands of 40 and 44 MW, since during these years the gas turbine works at high average loads, while the second approach is applied for the remaining demands, during which the load of the gas turbine is lower.
If the power required from the air turbine is lower than the turbine's minimum load, two approaches are possible:

1t) Let the air turbine to work at its minimum and decrease the GT load accordingly, to avoid wasting power.

2t) Increase the GT load to fulfil the power requirements without having to start the air turbine.

The second strategy is more favourable, since the gas turbine has a higher efficiency compared to the air turbine, and is applied whenever possible, with the exclusion of the years during which the power demand is close to the maximum (40 and 44 MW). During those two years, the first approach is used instead.

Finally, concerning the ESL, and reminding that it can never go below zero, the power output of the gas turbine can be increased or decreased according to the trend of the storage energy level. More in detail, the load of the GT has to be increased if the storage is close to be empty, while can be decreased if the energy level is sufficiently far from zero. This fact have already been introduced in section 3.5 but will be further explained with the following two examples.

The first one is shown in Figures (6-3) and (6-4) below.

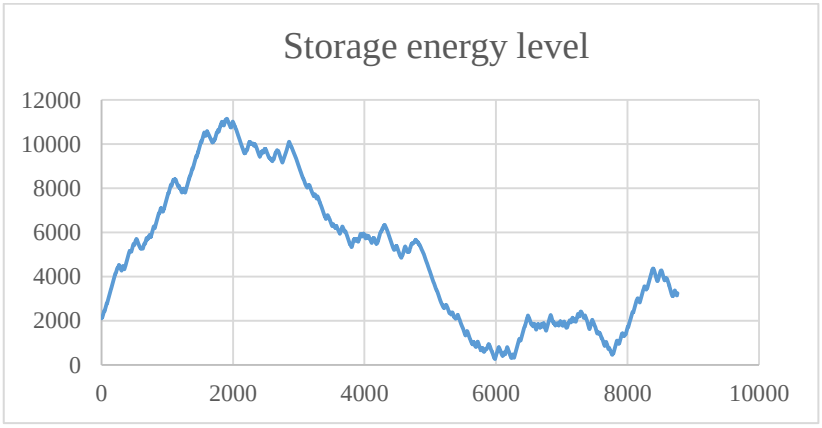

Figure 6-3: Example of storage energy level. 11 bar, 45 MW wind and 44 MW demand from the platform

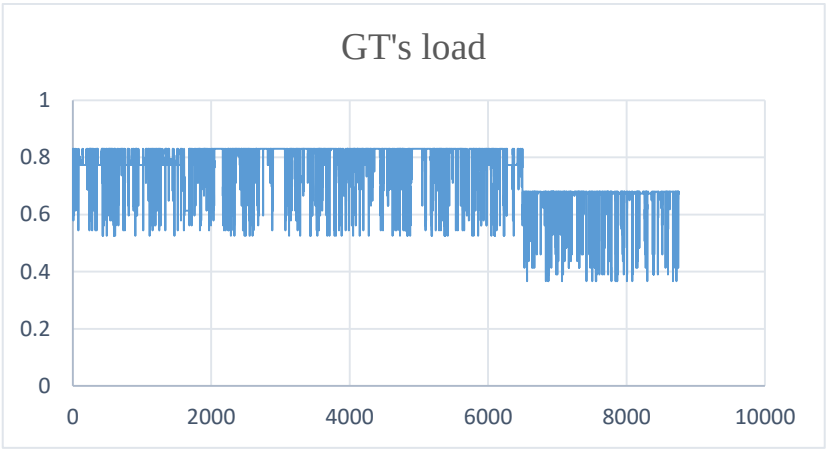

Figure 6-4: Example of GT's load. 11 bar, 45 MW wind and 44 MW demand from the platform

The first figure shows the energy storage level, the second one the load of the gas turbine for the case of a storage pressure of 11 bar, a wind park of 45 MW and a power demand from the platform of 44 MW. The first thing to point out is that the profile is balanced, meaning

that the energy levels at the beginning of the year and at the end are close to be the same. Moreover, the sudden load reductions that are seen in Figure (6-4) are the result of the approaches 1c) and 1t) discussed above.

This balanced energy profile is achieved by adjusting the turbine according to the energy storage level: a default value of 0.8 is kept from the beginning of the year to hour 6500. After this point, it is possible to reduce the GT's power output by lowering the load to a default value of 0.65. This is strongly linked to the wind speed profile, as described in section 3.5: In the interval between hours 0-2000, the average wind speed is high, and this leads to an excess of wind power and to a steep charging curve for the storage. From hour 2000 to hour 6000, the average wind speed is lower, and the storage starts to discharge, reaching its minimum. From hour 6000 to the end of the year, the average wind increases again, and the storage keeps charging. This means that, overall, the gas turbine load is usually higher in the first part of the year (0-6000), while it can be lowered (compatibly with its minimum value of 36%) after this point, in order to balance the energy profile. It is reminded that the importance of having a balanced profile lies in the fact that no wind energy goes wasted at the end of the year.

The second example is shown in Figures (6-5) and (6-6), which represent a scenario with the same pressure level and installed wind power as the one above, but with a power demand required by the platform of only 30 MW.

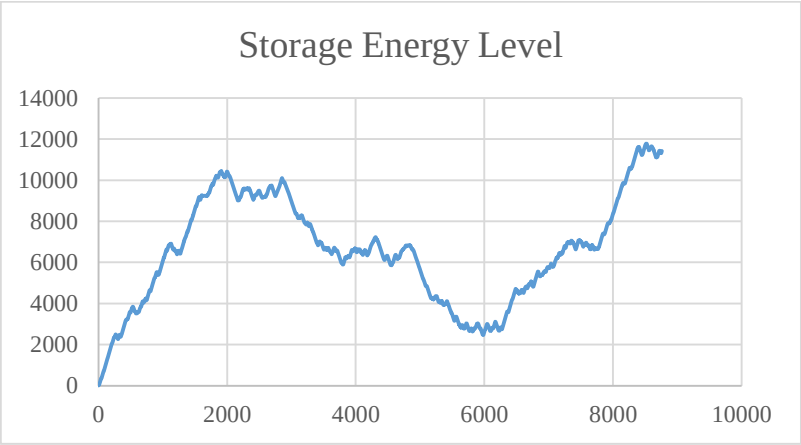

Figure 6-5: Example of energy storage level. 30 MW demand, 45 MW wind, 11 bar

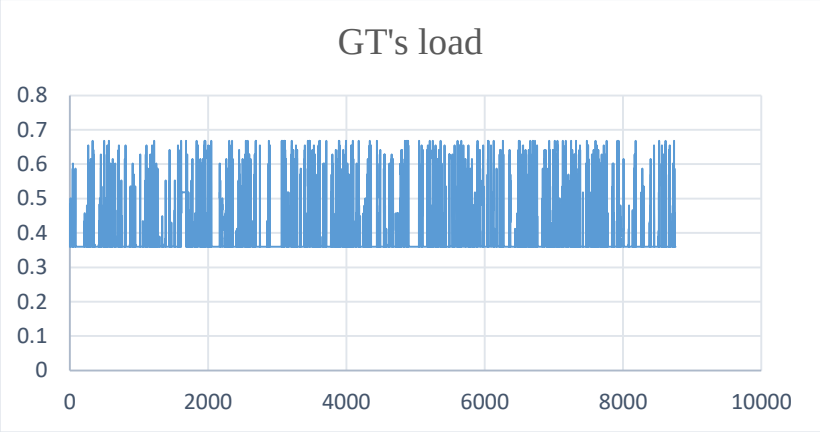

Figure 6-6: Example of GT's load. 30 MW demand, 45 MW wind, 11 bar

In this case, the energy profile results to be completely unbalanced, leading to a significant excess of stored energy at the end of the year. From what discussed above, the first idea to reduce this energy excess and try to balance the profile would be to lower the default load of the GT. However, when looking at Figure (6-6) it appears clear that this is not possible, since the default load is already at its minimum of 36%, and only increases when approaches 2c) and 2t) require it. The result is that, in these conditions, the wind farm is oversized for the platform's power demand and this leads to an inevitable loss of stored energy.

When considering all the factors described above, the operating strategy results to be the following:

- If $PGT + WP > PP$

  In this case, the sum of power provided by the gas turbine and the power directly sent to the platform from the wind park is higher than the power demand of the platform. This means that any additional power produced by the wind turbines is sent to the air compressor in the CAES section, thus is used to produce compressed air which is sent to the underwater vessels, charging the storage.

- If $PGT + WP < PP$

  In this case, WP represent all the power produced by the wind farm, and is sent, in the form of electric energy, to the platform. This means that the power provided by the gas turbine and the WP sent to the platform are lower than the power demand of the platform. The missing power to meet the power demand is thus produced by the air turbine. Air is extracted from the storage (discharging it),

heated up in the combustion chamber with the use of additional fuel and then sent to the air turbine for the expansion.

The overall system's efficiency can be expressed with Equation 5.0, in which, in this case, the fuel flow accounts both the natural used in the gas turbine on the platform and the additional fuel burned in the combustion chamber of the CAES section.

6.2 CAES application to the case study

The depth of the sea in the surroundings of Edvard Grieg and Ivar Aasen is around 110 meters, limiting therefore the storage pressure to 11 bar. The effects of the different number of installed wind turbines are investigated, for the extreme power demands of the platform, namely 30 MW and 44 MW. The most promising configuration, CO_2-wise, would require a 45 MW installed wind power. Lifetime simulations are thus computed for this scenario, with and without the integration of an air preheat system. The obtained results are compared to the benchmarks that were set in chapters 4 and 5.

With this pressure level, the compression is single-staged, without intercooling and with an aftercooler, as explained in section 3.3. Up to three compressors are required to work simultaneously at their maximum loads, as shown in Figure (6-7).

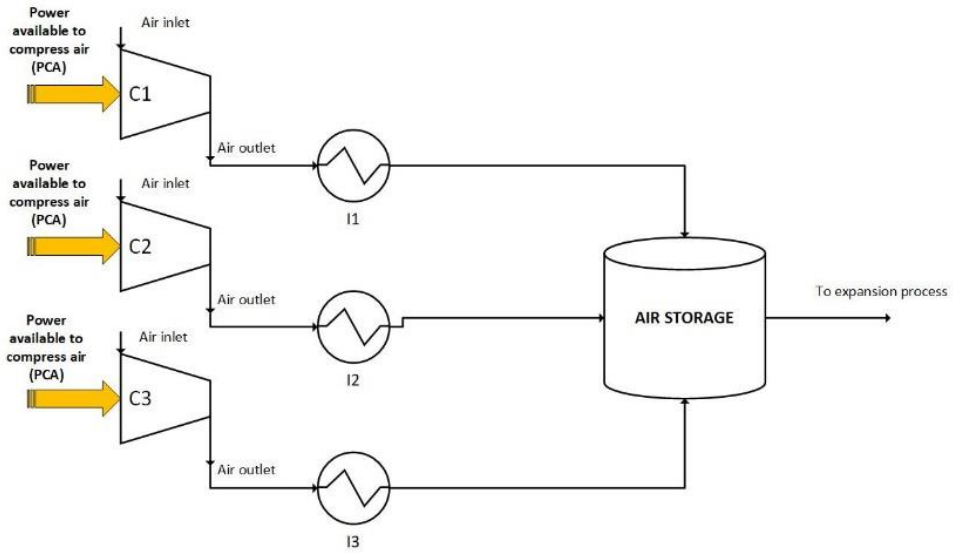

Figure 6-7: Layout for the compression section of the CAES

The design parameters for the air compressor and for the air turbine are summarized in Tables 14 and 15 below.

Table 14: Air compressor design parameters. 11 bar storage pressure

T amb	[K]	283.15
P amb	[kPa]	101
h amb	[kJ/kg]	562.14
T outlet adiab	[K]	562.15
P outlet	[kPa]	1111
h outlet adiab	[kJ/kg]	862.3
Compressor min power [kW]		4780
Compressor max power [kW]		7400
Design isentropic efficiency		0.82

Table 15: Air turbine design parameters. 11 bar storage pressure

Mass flow [kg/s]	50
T inlet [K]	880
P inlet [kPa]	1111
P outlet [kPa]	101
Min outlet power [kW]	10750
Max outlet power [kW]	18750
Design efficiency	0.85

6.2.1 Platform's maximum power demand (44 MW)

The storage energy trend for different wind farm sizes is shown in Figure (6-8). With this power demand requirements from the platform, the 30 MW case (and all the other smaller wind farms) is not sufficient to remove the need for the second gas turbine, and therefore will not be considered in the following analyses. 35 MW up to 45 MW of installed wind power lead to balanced energy profiles.

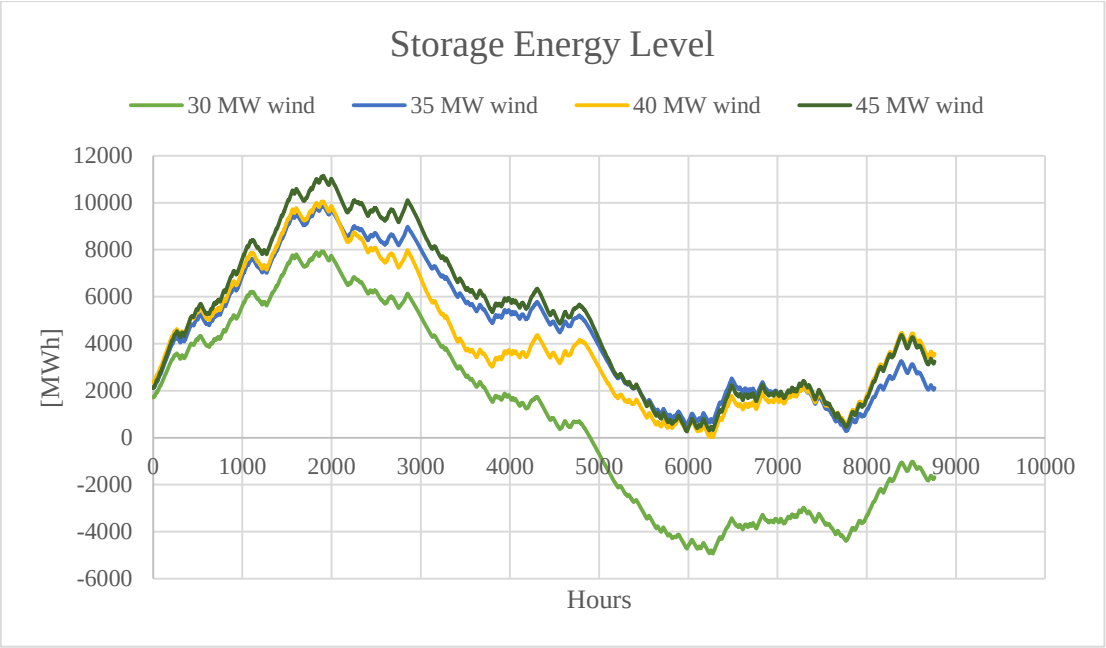

Figure 6-8: Storage energy level for different wind farm sizes. 44 MW demand, 11 bar storage pressure

Increasing the size of the wind farm leads to higher energy peaks, and therefore in larger volumes required by the underwater vessels, with a negative effect on the sizing. However, it also results in a smoother and less steep discharge curve, with the benefits described in the previous sections, allowing more flexibility in the regulation of the power output of the GT on the platform, thus making it easier to balance the energy profile between the beginning and the end of the year. Figure (6-9) shows the average values for the load of the gas turbine for different installed wind powers. In the 30 MW case, the GT is very close to its maximum output (95%). This fact confirms that it is not possible to operate the system using only one GT, as the storage inevitably empties around hour 5000. As expected, increasing the wind farm's size leads to reduced loads from the GT, lowering the fuel consumption and the CO_2 emissions.

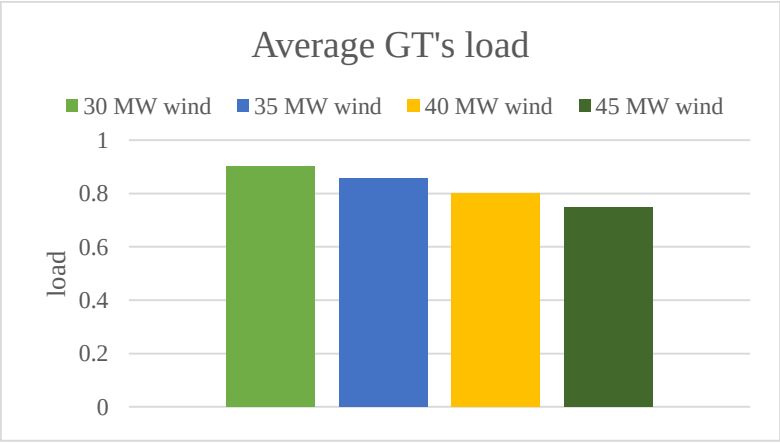

Figure 6-9: Average loads for the GT with different wind powers. 44 MW demand, 11 bar storage pressure

Concerning the CO_2 emissions, the achieved results are summarized in Table 16.

Table 16: Comparison of the emissions. 44 MW demand, 11 bar storage pressure

	CO_2 emissions [10^6 kg]	Reduction from Base Case [%]	Reduction from wind only [%]
Base Case	233		
CAES system			
35 MW	152	34.76	2.56
40 MW	149	36.05	1.32
45 MW	146	37.34	0.00
wind farm only			
35 MW	156	33.05	
40 MW	151	35.19	
45 MW	146	37.34	

The emissions in the base case, which utilizes the traditional shared-load operating strategy, amount to 233 million kilograms. Introducing a wind farm reduces the emissions by 33-37%, depending on the number of installed wind turbines. Approximatively, adding an extra wind turbine reduces the emissions by around 5 million kilograms. The integration of the CAES system further improves this reduction, cutting the emissions by 34.8-373.%, depending once again of the size of the wind park. Anyways, the improvement becomes smaller and smaller with any additional wind turbine, reducing only by three additional million kilograms instead of the almost 5 possible in the wind only scenario. This means that the increased reduction obtained with the introduction of the CAES system becomes less relevant the larger the installed wind power is. This is confirmed by the fact that for the 35 MW scenario, the improvement is around 2.6% compared to the wind farm without CAES, while for the 45 MW case, this improvements quickly goes to zero, meaning that the addition of the CAES would seem not to bring any useful advantage.

It is important to understand why, even though one GT has been removed with the integration of the CAES system, the emissions are not significantly reduced. The CO_2 in the CAES configuration is produced both by the GT on the platform and by the combustion chamber

in the CAES section. The different contributions, for the various wind sizes, are listed in the Table 17.

Table 17: CO2 contributes for different wind powers. 44 MW demand and 11 bar storage pressure

	CO_2 from GT [10^6 kg]	CO_2 from CAES section [10^6 kg]
35 MW	132	20
40 MW	128	21
45 MW	124	22

As expected, as the installed wind power increases, the GT on the platform works at lower loads, therefore burns less fuel and produces less CO_2 emissions. This positive effect is however partly counteracted by the increased emissions coming from the CAES's combustion chamber, which are caused by the higher average load of the air turbine (working hours are more or less the same), as shown in Table 18.

Table 18: Loads and working hours for GT and AT. 44 MW demand, 11 bar storage pressure

	GT average load	AT average load	AT working hours
35 MW	0.86	0.78	4426
40 MW	0.8	0.85	4396
45 MW	0.75	0.91	4416

If increasing the wind farm size allows on one hand to reduce the average utilization of the GT on the platform, on the other hand it results in averagely higher output powers for the air turbine in the CAES section, therefore partly counteracting the positive effect of the reduced fuel consumption on the platform. It is clear that, in order to improve the system, it is of fundamental importance to find ways to reduce the fuel consumption in the CAES section. Efficiency-wise, the results are summarized in Table 19.

The improvement between the introduction of a only wind farm and the system including the CAES seems rather small. Increasing the wind farm's size has the same effect introduced in chapter 5, leading to a lower overall efficiency of the energy system. However, this reduction is very small.

Table 19: System's overall efficiency. 44 MW demand, 11 bar storage pressure

	Efficiency [%]
Base Case	0.324
CAES system	
35 MW	0.421
40 MW	0.419
45 MW	0.416
Wind only	
35 MW	0.414
40 MW	0.415
45 MW	0.416

6.2.2 Platform's minimum power demand (30 MW)

Figure (6-10) below shows the energy storage level for the studied platform's power demand.

Increasing the number of wind turbine results into higher storage peaks and therefore a higher number of underwater vessels. It is interesting to point out that all the three studied scenarios lead to an unbalanced energy profile, with an excess of stored wind energy at the end of the year that, for the reasons discussed so far, is not usable, since the gas turbine is already working at close to minimum power outputs, as seen in Figure (6-11).

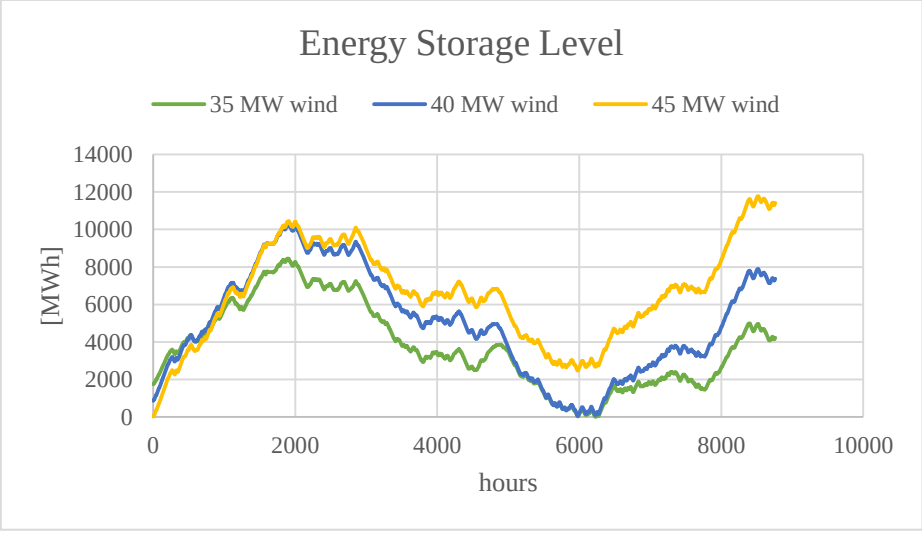

Figure 6-10: Energy storage level for different wind farms. 11 bar pressure and 30 MW demand from the platform

The stored energy that represents an unusable excess and therefore goes wasted is however much smaller than the wasted wind fraction for the system with only the integration of a wind farm but without a CAES, as shown in Table 20 below.

Table 20: Comparison of the wasted wind fraction with and without CAES. 30 MW demand, 11 bar storage pressure

	Wasted wind energy [%]
Wind only	
35 MW	33.92
40 MW	39.88
45 MW	44.87
CAES system	
35 MW	1.71
40 MW	3.92
45 MW	6.11

Moreover, since this case is the one for which the platform's power demand is minimum, is also the one that results with the higher amount of unusable energy at the end of the year. This means that, at maximum, only 1.71% of the total produced energy goes wasted in the 35 MW installed wind power scenario. This value increases to 6.11% for the largest wind farm, but it still much lower than the 44.87% of the introduction of only the wind farm. Table 21 below summarizes the results regarding the CO_2 emissions.

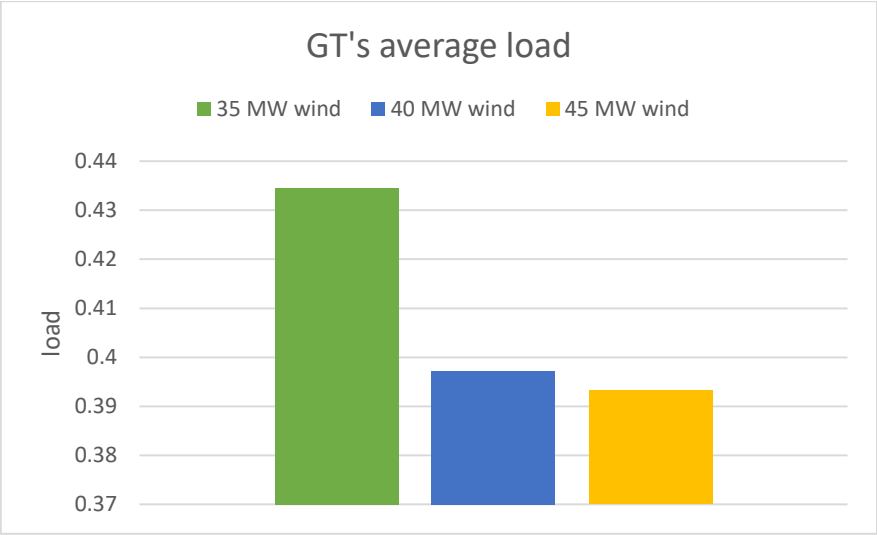

Figure 6-11: Average load for the GT for different wind scenarios. 30 MW demand and 11 bar storage pressure

Table 21: Emissions' comparison for 30 MW power demand, 11 bar storage pressure

	CO_2 emissions [10^6 kg]	Reduction from Base Case [%]	Reduction from wind only [%]
Base Case	178		
CAES system			
35 MW	104	41.57	1.89
40 MW	102	42.70	2.86
45 MW	99	44.38	1.00
wind farm only			
35 MW	106	40.45	
40 MW	105	41.01	
45 MW	100	43.82	

Similarly to the 44 MW demand case, the introduction of the CAES gives better results compared to the ones achieved with the integration of only the wind farm. Moreover, it is interesting to point out that the reduction percentage from the base case is, for all the studied cases, higher for the minimum platform's power demand than for the maximum's. This is because the shared-load strategy is less efficient the lower the power demand of the platform is, since the average loads of the two gas turbines are lower. Therefore, the operating strategies discussed in chapters 5 and 6 are more beneficial when the platform's power demand is at or close to its minimum (30 MW and the 33 MW demand during the production plateau).

Dividing the emissions between the ones generated in the GT and the ones generated in the combustion chamber of the CAES, makes it is possible to notice that increasing the number of installed wind turbine reduces the emissions caused by the gas turbine, but has little to no effect to the ones coming from the CAES, as shown in Table 22.

Table 22: CO2 emissions from the GT and the AT. 30 MW demand, 11 bar storage pressure

	CO_2 from GT [10^6 kg]	CO_2 from CAES section [10^6 kg]
35 MW	88	16
40 MW	84	17
45 MW	83	16

This is because the GT on the platform is less utilized, in accordance to the results obtained so far. For what concerns the CO_2 emissions from the air turbine, it is possible to see, in Table 23, that the working hours and the average loads are similar in the three investigated scenario, thus the similar emissions found in Table 22.

Table 23: GT and AT average loads, 30 MW demand and 11 bar storage pressure

	GT average load	AT average load	AT working hours
35 MW	0.43	0.67	2949
40 MW	0.4	0.73	3078
45 MW	0.39	0.7	2930

When considering the overall system's efficiency (Table 24), the values achieved for the 30 MW power demand are lower than the ones of the 44 MW demand. This is because of the larger amount of unused wind energy due to the unbalanced profiles of the energy level of the storage, and due to the lower utilization of the GT (a gas turbine working at lower loads has a lower efficiency compared to the same GT working close to its nominal power).

Table 24: System's efficiency, 30 MW demand and 11 bar storage pressure

	Efficiency [%]
Base Case	0.289
CAES system	
35 MW	0.392
40 MW	0.387
45 MW	0.381
Wind only	
35 MW	0.385
40 MW	0.377
45 MW	0.38

6.2.3 Lifetime analysis, results and implementation of air preheating

From the results obtained for the minimum (30 MW) and maximum (44 MW) power demands required by the platform, it appears that, when considering the CO_2 emissions, the best results are achieved with the integration of a 45 MW wind farm into the system. Since

the aim of this work is mainly the one to identify and analyse the most promising configurations that allow the more pronounced reduction of the emissions, the 45 MW wind farm is chosen as the default size for all the power demands, and is used to predict a variety of interesting parameters, from the CO_2 emissions, to the sizing of the underwater storage.
In addition to this, the 45 MW results in a penetration level of more than 100% of the power demand, in accordance to the work developed by (Lazerte, 2014). Moreover, the 45 MW wind park leads to the largest number of underwater vessels required. Therefore, if a reasonable number of vessels is obtained for this scenario, a better result would be achieved with lower installed wind powers.
On the other hand, as already discussed, nor the economical aspect nor the electrical balance are considered. Therefore, it may be possible that this chosen wind farm size is not the best one from these points of view.
Table 25 shows the performance of the three systems studied, with particular regard to the CO_2 emissions.

Table 25: Emissions comparison, 45 MW wind power, 11 bar pressure storage

	CO2 [10^6 tonnes]	CO2 savings [10^6 tonnes]	CO2 savings [%]	Reduction from wind only [%]
Base Case	3.65			
45 MW wind	2.17	1.48	40.55	
45 MW wind + CAES	2.11	1.54	42.09	2.60

The total CO_2 emitted during the platform's lifetime was estimated to amount to 3.65 million tonnes in the current two-GTs shared load operation. The integration of a wind farm made up of nine 5 MW wind turbines would allow to cut the emissions by 40.5%. Introducing the CAES system would improve the results by 2.6%, achieving an overall 42.09% reduction compared to the base case.

The adoption of a complex CAES system seems questionable when it ensures such little performance improvement over a simpler configuration represented by the integration of only the offshore wind farm. In addition to this, due to the limited depth of the sea in the surroundings of the platforms (110 meters), a high number of underwater vessels would be required. With the hypothesis of vessels of 20 meters of radius each, a total of 475 units would be necessary.

However, it is interesting to investigate the possibility to reduce the fuel consumption in the CAES by recovering waste heat from the exhaust of the GT. This otherwise wasted energy could be used to preheat the air coming out from the storage, before its entrance into the combustion chamber. The next section will analyse this possibility.

Results with the integration of the air preheating system

The model was descripted with great detail in section 3.7. For this reason, this section is only dedicated to the analysis of the results.

From an energy point of view, the only effect of the integration of a system to preheat the air coming from the underwater storage is to reduce the amount of fuel needed in the combustion chamber of the CAES. Therefore, the total CO_2 produced in the CAES with and without the heat recovery is shown in Table below.

Table 26: CO2 emissions comparison with and without air preheat

CO2 CAES [10^6 tonnes] Without preheat	CO2 CAES [10^6 tonnes] With preheat
0.38	0.24

The introduction of the air preheat system reduces the emissions in the CAES section by a significant 36.84%.

The overall effect on the emissions for the whole system is visible in Figure (6-12).

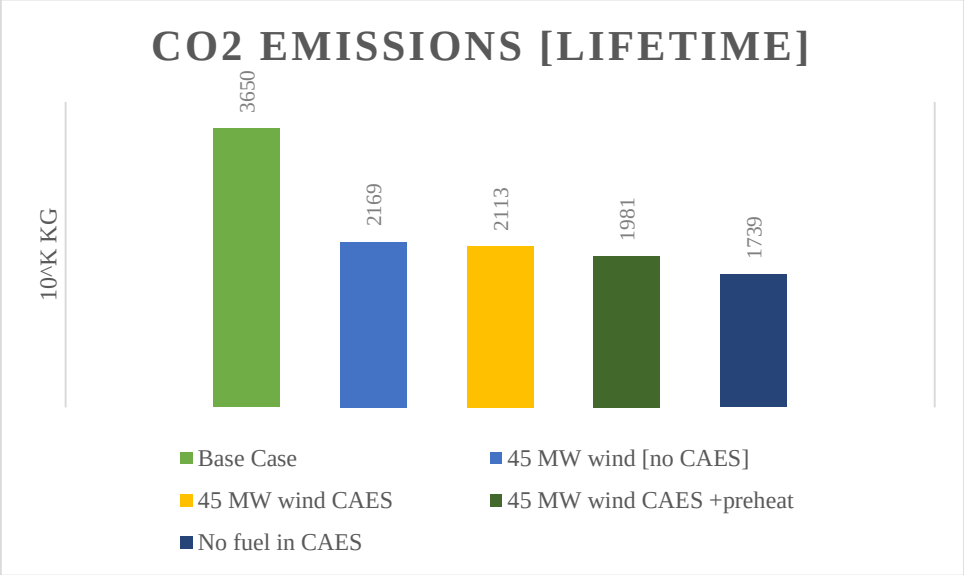

Figure 6-12: Comparison of the emissions for the different configurations

The implementation of the air preheating strategy reduces the emissions from 2113 kilograms down to 1981, resulting in an additional 6.25% reduction. Compared to the scenario with the wind farm only, the reduction increases to 8.67%. The “no fuel in CAES” is a case that could be in theory approached with some form of thermal storage, heating up the air to the desired temperature of 800 K without the use of any additional fuel. While this represents an interesting benchmark to evaluate how good was the heat recovery with the air preheat, the possibility to integrate a thermal storage in the system was ruled out in this thesis because of the already stringent physical constrains on the offshore platform.

It is also interesting to evaluate in which years and for which demands the air preheat is particularly effective in reducing the need for additional fuel in the combustion chamber of the CAES section. The results are shown in Table 27 below.

Table 27: Year by year comparison of the reduction of emissions achieved with air preheat

Year	Power demand [MW]	CO2 emissions without preheat [10^6 kg]	CO2 emissions with preheat [10^6 kg]	Reduction with preheat [%]
2016	30	99	99	0.00
2017	35	111	111	0.00
2018	36	113	113	0.00
2019	44	146	142	3.04
2020	40	137	131	4.29
2021	36	113	109	3.88
2022	35	111	105	5.78
2023	35	111	105	5.78
2024	33	107	97	8.99
2025	33	107	97	8.99
2026	33	107	97	8.99
2027	33	107	97	8.99
2028	33	107	97	8.99
2029	33	107	97	8.99
2030	33	107	97	8.99
2031	33	107	97	8.99
2032	33	107	97	8.99
2033	33	107	97	8.99
2034	33	107	97	8.99

The results in Table 27 agree with what was described in section 3.7: for the first three years, no heat recovery is performed, due to the lack of extra exhaust gases from the GT (almost all the exhaust are needed in the heat exchanger that heats up the water used to satisfy the heat demand of the platform). After this point, the CO_2 reduction achieved with the air preheat increases, reaching a maximum of 9% during the years of the production plateau.

Summarizing the results:

- The 45 MW wind farm was the default size chosen for the analyses of these sections. The reason of this choice is that it gave the best CO_2 reductions, while still being at the penetration level found in other works. As already stated, this might not be the best configuration, since no economic nor electrical balance points of view are included.

- In the configuration without air preheating, the CAES system only achieve an additional 2.6% emission reduction compared to the much simpler configuration that implies only the integration of the wind farm. Therefore, the integration of such system in this scenario might be questionable.

- The results achieved with the heat integration are more favourable, leading to a possible CO_2 reduction of 6.25% compared to the CAES system without air preheat, and of 8.67% compared to the scenario with only the integration of the wind farm. Therefore, air preheating seems to be of importance in order to reach the viability of the proposed CAES system.

- The available sea depth of 110 meters would require a total of 475 underwater storage vessels, each with a radius of 20 meters. This result make the CAES integration at this specific depth hardly applicable.

- Overall, with this limited sea depth, the simple integration of a wind farm seems to be the most effective concept to reduce the CO_2 emissions, even though this would not allow the removal of the second gas turbine on the platform.

6.3 CAES integration on higher sea depths

The case study investigated so far has the stringent limitation of a low storage pressure, resulting from the sea depth in that area (around 110 meters). On the other hand, the energy storage capacity of an underwater vessel, fixed its size, increases dramatically with installation depth. Moreover, the work carried out in (Jong, 2014) points out that UWCAES is particularly attractive between 400 and 700 meters. Therefore, it is imagined that a system similar to the case of study one, is collocated in those sea depths. The aim of this section then becomes to investigate the feasibility of the CAES system already described but with higher storage pressure, in order to provide useful information regarding the possible attractive sites for this technology.

Simulations are carried out for 2 significant storage pressures, 40 and 70 bar (corresponding to 400 and 700 meters), with the installation of a 45 MW wind farm. The possibility to integrate an air preheater is also investigated.

As discussed in section 3.7, the compression is two-staged with inter and after coolers, as shown in Figure (6-13) below.

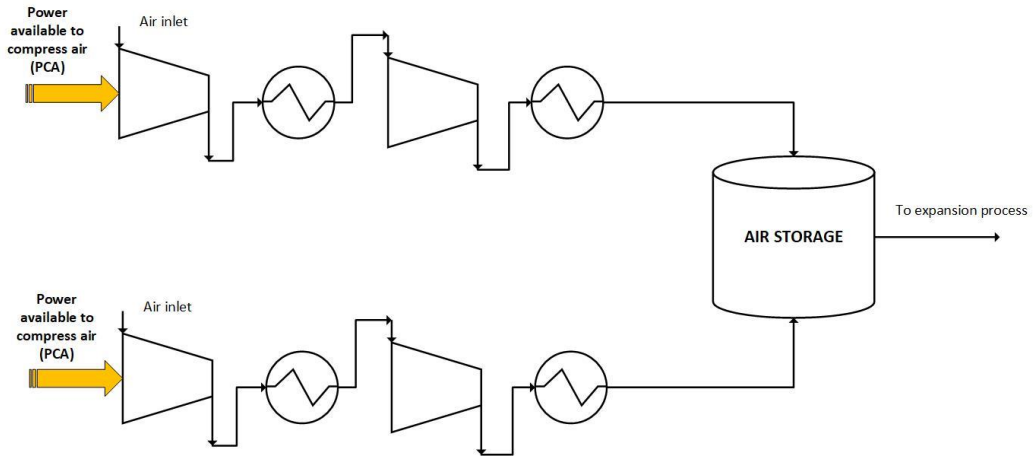

Figure 6-13: Layout of the air compressor for 40 and 70 bar storage pressure

Air compressor and air turbine design for 40 bar and 70 bar storage pressure

As seen in Figure (6-13), there are two trains of compressors. Each compressor elaborates a pressure ratio equal to the squared root of the total, meaning in this case, around 638 kPa. The intercooler is supposed with effectiveness of unity, meaning that it brings the air back

to ambient temperature before its entrance in the second compressor. The aftercooler brings the compressed air again back to ambient temperature before it enters the underwater vessels. Compared to the 11 bar scenario, given the higher pressure ratio needed, the compressors, given that the excess power from the wind is the same, elaborate a smaller mass flow, leading to a less steep charging curve for the storage. The new parameters are visible in Table 28.

Table 28: Air compressor design parameters for 40 bar storage pressure

T amb [K]	283.15
P amb [kPa]	101
h amb [kJ/kg]	283.5
T outlet adiab [K]	479.7574
P outlet [kPa]	638.32
h outlet adiab [kJ/kg]	482.8
Compressor min power [kW]	2714.296
Compressor max power [kW]	4582.77
Design efficiency	0.82

The air turbine elaborates the same mass flows at the same inlet temperature of 800 K. What changes compared to the 11 bar configuration is the pressure ratio, which is obviously higher in this case. This results in higher minimum and maximum power output compared to the previous scenario, using the same mass flow. The new parameters are summarized in Table 29.

Table 29: Air turbine design parameters for 40 bar storage pressure

Mass flow [kg/s]	50
T inlet [K]	800
P inlet [kPa]	4040
P outlet [kPa]	101
Efficiency	0.85
Min power output [kW]	9842.14
Max power output [kW]	22383.31

Analogous considerations can be done for the 70 bar scenario. The updated parameters of the air compressor and of the air turbine are respectively shown in Table 30 and Table 31. In this configuration, the pressure outlet of the compressor is around 845 kPa.

Table 30: Air compressor design parameters for 70 bar storage pressure

T amb [K]	283.15
P amb [kPa]	101
h amb [kJ/kg]	283.5
T outlet adiab [K]	519.8955
P outlet [kPa]	845.37
h outlet adiab [kJ/kg]	524.177
Compressor min power [kW]	3914.514
Compressor max power [kW]	5952.909
Design efficiency	0.82

Table 31: Air turbine design parameters for 70 bar storage pressure

Mass flow [kg/s]	50
T inlet [K]	800
P inlet [kPa]	7070
P outlet [kPa]	101
Efficiency	0.85
Min power output [kW]	10932.4
Max power output [kW]	24151.69

6.3.1 Lifetime simulations and results for the 40 bar scenario

Simulations are carried out for 45 MW installed wind power, with and without the addition of the air preheat section. The results are summarized in Table 32 and compared with the ones achieved for the base case with shared-load operation, with the system which integrates only the wind farm, and with the 11 bar storage pressure.

The main result is the reduced number of required vessels to store the air, from 475 in the 11 bar scenario to only 99 for the 40 bar one. While this number looks still hardly attractive, it represents a significant reduction, and is in perfect accordance to the fact that moving to higher depths drastically reduces the volume requirements of the underwater storage system. The system without air preheat is able to cut the CO_2 emissions from the base case by around 43.3%, resulting in a 4.6% reduction from the installation of only the wind farm.
These results are improved with the integration of the air preheater, which would allow to reach a 46.04% reduction on the base case and a 9.24% reduction on the wind only scenario.

Table 32: Results and comparison of the emissions for 40 bar storage pressure

	CO_2 [10^6 tonnes]	CO_2 savings [10^6 tonnes]	CO_2 Savings [%]	Reduction from wind only [%]	Number of vessels
Base case	3.65				
45 MW wind	2.17	1.48	40.55		
45 MW wind + CAES (11 bar)	2.11	1.54	42.19	2.60	475
45 MW wind + CAES (40 bar)	2.07	1.58	43.27	4.57	99
45 MW wind + CAES (11 bar) + preheat	1.98	1.67	45.75	8.76	475
45 MW wind + CAES (40 bar) + preheat	1.97	1.68	46.04	9.24	99

Summarizing:

- Increasing the storage pressure to 40 bar leads to a significant reduction of underwater vessels, down from 475 to 99. However this value looks still high, and might not represent a feasible option within the study parameters.

- The CO_2 reduction, compared to the base case, amounts to 43.27% or 46.04%, depending if the air preheat is included or not. Regarding the comparison to the wind integration only, cuts of 4.57% and 9.24% are possible.

- Air preheat gives the best results, but the system without it might still be attractive, CO_2-wise.

6.3.2 Lifetime simulations and results for the 70 bar scenario

Operating in the same way to what described for the 40 bar scenario, simulations for a higher sea depth are carried out (700 meters). The results are summarized in Table 33 below.

	CO_2 [10^6 tonnes]	CO_2 savings [10^6 tonnes]	CO_2 savings [%]	Reduction from wind only [%]	Number of vessels
Base case	3.65				
45 MW wind	2.17	1.48	40.55		
45 MW wind + CAES (11 bar)	2.11	1.54	42.19	2.6	475
45 MW wind + CAES (70 bar)	2.03	1.62	44.25	6.23	48
45 MW wind + CAES (11 bar) + preheat	1.98	1.67	45.75	8.76	475
45 MW wind + CAES (70 bar) + preheat	1.93	1.72	47.16	11.11	48

Table 33: Emission results and comparison for 70 bar storage pressure

The main result is the reduced number of required vessels to store the air, from 475 in the 11 bar scenario to only 48 for the 70 bar one. This number looks attractive, as it represents a significant reduction, and is in perfect accordance to the fact that moving to higher depths drastically reduces the volume requirements of the underwater storage system.

The system without air preheat is able to cut the CO_2 emissions from the base case by 44.25%, resulting in a 6.23% reduction from the installation of only the wind farm.
These results are improved with the integration of the air preheater, which would allow to reach a 47.16% reduction on the base case and a 11.11% reduction on the wind only scenario.

Summarizing:

- Increasing the storage pressure to 70 bar leads to a significant reduction of underwater vessels, down from 475 to 48.

- The CO_2 reduction, compared to the base case, amounts to 44.25% or 47.16%, depending if the air preheat is included or not. Regarding the comparison to the wind integration only, cuts of 6.23% and 11.11% are possible.

- Air preheat gives the best results, but the system without it might still be attractive, CO_2-wise.

7 ECONOMICS

The results obtained in the previous chapters and sections do not take into account the economic feasibility of the systems investigated. While this chapter does not pretend to be an exhaustive economic investigation, it shall be taken as an useful insight into some key parameters that should allow to understand if the configurations analysed are economical promising or not.

No discount of the cash flow was included in the analysis, nor the cost related to operation and maintenance (OPEX). The estimation of the CAPEX (capital investment cost) for the compressed air energy storage system requires extensive knowledge of the plant and its components; therefore a different approach for its evaluation is used instead, as will be discussed in the following.

In the base case, only the total outcome due to the cost of the CO_2 tax is considered. This cost is easily obtainable by multiplying the CO_2 tax [€/10^6 kg] for the amount of CO_2 [10^6 kg] released into the atmosphere during the lifetime of the platform, and results to be 200.75 M€. This value sets a higher limit for the investigated concepts in order to reach economic competitiveness.

The following criteria are considered:

- CO_2 Tax: 55€ per tonne emitted into the atmosphere

- Additional Fuel Sold (AFS): is the fraction of fuel gas that does not need to be burned on the platform and can therefore be sold on the market. The price is estimated yearly from the World Energy Outlook 2016, by IEA. Values vary between 14 and 33 $€_{2015}$/MWh

- The cost of offshore wind turbines, from [55], estimated to 2800 $€_{2013}$/kW. Given the adoption of the 5 MW wind turbine, the cost of the turbine is around 14 M€.

7.1 Wind farm results

The introduction of a wind farm into the system leads to reduced fuel consumption and less emissions of CO_2. These two effects result in lower CO_2 cost due to the tax and in a higher amount of gas fuel sold. A comparison between the avoided CO_2 costs resulting from the tax for the different wind farms investigated is presented in Table 34.

Table 34: CO_2 tax savings for different wind farms

	CO2 [10^6 tonnes]	CO2 cost [M€]	Tax savings [M€]	Tax savings [%]
Base case	3.65	200.75		
Wind farm				
5 MW	3.13	172.24	28.51	14.20
10 MW	2.92	160.47	40.28	20.06
15 MW	2.74	150.74	50.01	24.91
20 MW	2.60	143.23	57.52	28.65
25 MW	2.47	135.92	64.83	32.30
30 MW	2.39	131.36	69.39	34.57
35 MW	2.31	127.16	73.59	36.66
40 MW	2.24	123.06	77.69	38.70
45 MW	2.17	119.28	81.47	40.58

Introducing a wind farm reduces the emissions, and thus leads to economic savings due to the avoided tax. Depending on the size of the farm, savings are estimated to be between 28.51 and 81.47 M€. The percentage tax savings follows the same trend seen in the emission reduction, given the fact that the tax is supposed to be constant at 55€/tonne in every year. Table 35 includes the additional fuel sold and the cost of the wind turbines to estimate the Total Savings for each of the studied wind farm's sizes.

$$Total\ Savings\ [WIND] = CO_2\ savings + AFS - Wind\ farm\ cost$$

The Total Savings measures the beneficial effect of the introduction of a wind farm on the system: in the base case, the only considered cash flow is the outcome due to the cost of the CO_2 tax, which amounts to 200.75 M€. This cost diminishes thanks to the additional fuel sold and to the lower cost of the tax, since the emissions are lower, and amounts to

$$Outcome = 200.75\ M€ - Total\ Savings\ [WIND]$$

If the term Total Savings is positive, the introduction of a wind farm is beneficial. Moreover, the higher the Total Savings value is the smaller is the outcome would be, and the more economically attractive the investigated configuration would be.

Table 35: Evaluation of the Total Savings [WIND] for different wind farm sizes

	CO_2 savings [M€]	AFS [M€]	Wind turbine cost [M€]	Total Savings [WIND] [M€]
5 MW	28.51	69.42	14.00	83.93
10 MW	40.28	97.09	28.00	109.37
15 MW	50.01	119.63	42.00	127.64
20 MW	57.52	137.39	56.00	138.90
25 MW	64.83	154.56	70.00	149.40
30 MW	69.39	165.01	84.00	150.40
35 MW	73.59	174.46	98.00	150.05
40 MW	77.69	184.26	112.00	149.95
45 MW	81.47	193.49	126.00	148.96

The cost of the wind farm increases linearly with additional wind turbines, while the savings deriving from the avoided CO_2 tax and the extra income from the additional fuel sold follow the trend of the CO_2 reduction seen so far. This means that the most promising economic scenario differs, although slightly, from the one identified when taking into account only the energy system (Figure 7-1). Economically-wise, the best results are achieved with the integration of a 30 MW wind farm into the system, while CO_2-wise, the best result was obtained with a 45 MW wind farm.

The Total Savings term results to be positive in every studied scenario, ranging from 83.93 to 150.4 M€. This means that the installation of a wind farm in the surroundings of the case study offshore platforms looks economically promising compared to the base case configuration.

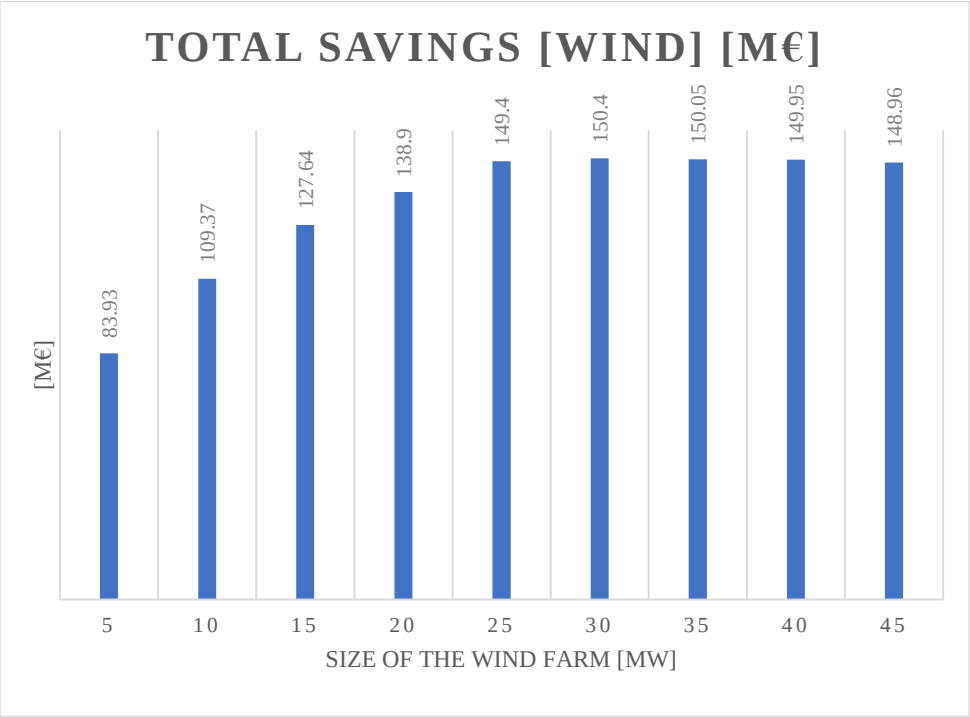

Figure 7-1: Economic output for different wind farm sizes

7.2 CAES results

The addition of the CAES system together with the offshore wind farm into the base case reduces the fuel consumption even further, leading to additional savings from the tax and more fuel gas available to be sold. The default wind farm's size is 45 MW. Table 36 below summarizes the CO_2 tax savings, compared to the base case, for the three pressure levels investigated (11, 40 and 70 bar), with and without the addition of the air preheat section.

The savings vary between 84.7 and 94.60 M€. Higher storage pressures give the best results, due to the more pronounced reduction of fuel consumption. Air preheat reduces the cost due to the tax even further. The best scenario is represented by a storage pressure of 70 bar including air preheat (94.6 M€ of savings), while the worst is the 11 bar without air preheat (84.70 M€ of savings).

The CAES system should aim to reach economic competitiveness with both the base case scenario and the configurations which imply only the integration of the wind farm. This means that the CAPEX max for the CAES is obtainable with the following definition:

$$CAPEX \max = Total\ Savings\ [CAES] - Total\ Savings\ [WIND] \quad (7.1)$$

Table 36: CO_2 tax savings for different CAES configurations

	CO_2 [10^6 tonnes]	CO_2 tax [M€]	Tax savings [M€]	Tax savings [%]
Base case	3.65	200.75		
45 MW wind farm + CAES				
CAES (11 bar)	2.11	116.05	84.70	42.19
CAES (11 bar) + preheat	1.98	108.90	91.85	45.75
CAES (40 bar)	2.07	113.85	86.90	43.29
CAES (40 bar) + preheat	1.97	108.35	92.40	46.03
CAES (70 bar)	2.03	111.65	89.10	44.38
CAES (70 bar) + preheat	1.93	106.15	94.60	47.12

The Total Savings [WIND] is the value of Table 35 for the selected wind farm's size of 45 MW, and amounts to 148.96 M€. The Total Savings [CAES] is evaluated in Table 37, and is defined by

$$Total\ Savings\ [CAES] = GT\ cost + CO_2\ savings + AFS - Wind\ farm\ cost$$

Where, GTcost is the avoided cost of the second gas turbine, which is not needed on the platform, and amounts to 10 M€.

Table 37: Evaluation of Total Savings [CAES] for different CAES configurations

	CO_2 savings [M€]	AFS [M€]	Wind turbine cost [M€]	GT avoided cost [M€]	Total Savings [CAES] [M€]
45 MW wind farm + CAES					
CAES (11 bar)	84.70	200.49	126	10	169.19
CAES (11 bar) + preheat	91.85	219.79	126	10	195.64
CAES (40 bar)	86.90	206.76	126	10	177.66
CAES (40 bar) + preheat	92.40	221.26	126	10	197.66
CAES (70 bar)	89.10	210.41	126	10	183.51
CAES (70 bar) + preheat	94.60	226.70	126	10	205.30

The trend is similar to the one discussed for Table 36. Higher sea depths and integration of the air preheating section give the best results, achieving a Total Savings value of 205.3 million €. The Total Savings results to be positive in every studied scenario, ranging from 169.19 to 205.30 million euros. This means that the installation of a wind farm and CAES system in the surroundings of the case study offshore platform looks economically promising. The simple integration of a 45 MW wind farm resulted in a Total Savings [WIND] of 148.96 M€. Therefore, the integration of the CAES leads to an additional 20.23-56.34 M€ benefit.

Table 38 summarizes the CAPEX max values for the investigated CAES configurations, in accordance to the definition given with Equation (7.1).

Table 38: Evaluation of CAPEX max for the different CAES configurations

	CAPEX max [M€]
45 MW wind farm + CAES	
CAES (11 bar)	20.23
CAES (11 bar) + preheat	46.68
CAES (40 bar)	28.7
CAES (40 bar) + preheat	48.7
CAES (70 bar)	34.55
CAES (70 bar) + preheat	56.34

The highest CAPEX max is achieved for the 70 bar storage pressure with the integration of the air preheater. While a higher CAPEX max means that there is a larger margin to reach economic competitiveness, it does not necessarily means that it will in practice result in the best configuration, economically-wise. In fact, higher sea depth would likely result in increased costs compared to lower depths, and the air preheat has of course its own cost.
In any case, the CAPEX max always results positive, meaning that every investigated scenario has the possibility to be effectively attractive.

Moreover, if the concept could be developed with a CAPEX lower than the CAPEX max, that configuration would be even more interesting, resulting in a batter performance. On the other hand, CAPEX values lower than the CAPEX max would result in a worse economical alternative compared to the base case.

Summarizing:

If $CAPEX < CAPEX\,max$

Then the CAES system might be economically attractive, compared to the base case configuration

If $CAPEX > CAPEX\,max$

Then the CAES system might not be economically attractive, compared to the base case configuration

8 CONCLUSIONS AND FURTHER WORK

The aim of this work was to investigate feasible CAES system configuration in order to reduce the environmental impact caused by the fuel consumption on oil and gas platform in the North Sea.

A specific case study, represented by Edvard Grieg and Ivar Aasen rigs, was used to model the components of the system. The model, while tailored for some specific parameters, can be easily adapted to a variety of different situations, and therefore aims to represent a starting point for further optimization work and for the analysis of different site conditions: different wind profiles, different power and heat demands, different sea depths, different design for the compressors and turbine in the CAES section.

In accordance to the objectives of this work, the studied solutions had the aim to remove one of the GTs on the platform, therefore leading to the utilization of only one gas turbine to provide the necessary power and heat to the offshore facility, while contemporary fully exploit the offshore wind resource.

For the available sea depth level, which is 110 meters, the integration of the CAES together with a 45 MW wind farm produces the best results. In particular, a total reduction of CO_2 emissions of 42.09% could be achieved, if integrating an air preheat system too. This value however represents only a 2.6% improvement compared to a much simpler solution, which would only imply the installation of a wind farm. On the other hand, the CAES system allows to remove the second gas turbine on the platform. Overall, it might not be attractive to develop such a complex system for the small benefits reached. Moreover, the sizing of the storage represents a significant downside, requiring up to 475 underwater storage vessels, each with a radius of 20 meters. When considering these downsides, it would probably more beneficial to avoid the integration of the CAES in this scenario, and only use the wind farm, which would still provide a significant reduction of the emissions (up to 40.6% for a 45 MW wind farm), even though it would require the use of both GTs on the offshore facility.

From an economical point of view, both the CAES and the wind farm look interesting. Focusing on the integration of a wind farm without CAES, while the most interesting configuration is represented by the 30 MW wind farm (Total Savings up to 150.4 M€), the 45 MW farm is not far behind (149 M€). Therefore, it is suggested that the 45 MW wind farm should be chosen, since it gives the best results CO_2-wise while still having a very high Total Savings value.

In any case, different approaches should be investigated. An example could be to keep the two existing GTs on the platform while still integrating wind farm and CAES system. This should lead to much smaller volume requirements for the storage, and the aim of the CAES section would shift from removing the additional GT to shaving the load peaks, reducing the shared-load operating hours and the overall GT loads.

For the studied power demands, a depth interval in which the CAES system is physically interesting was loosely identified to be above 400 meters, in accordance to the results available in [32]. More specifically, moving to higher depths reduces the emissions even further. In addition to this, the real advantage of considering higher sea depths is the smaller number of underwater vessels required to store the compressed air: from the 475 for the 11 bar, to the 99 for the 40 bar scenario to only 48 units required when studying the 70 bar case.

Air preheating should always be included in the CAES, as the air, which is stored at ambient temperature, would otherwise require a significant amount of fuel to reach the required temperatures for the expansion in the air turbine (set to 800 K). Further works should therefore focus on the optimization of the heat recovery unit, in order to reduce fuel consumption even further. Moreover, depending on the physical constrains of the platform, the possibility to adopt an adiabatic CAES should be evaluated.

From a CO_2 reduction point of view, interesting farm sizes are in the range of 50-110% of the maximum power demand of the platform. Values below 50% are still beneficial, but have a lower impact on the emissions. Values above 110% might lead to excessive storage requirements and additional dissipation of wind energy. Economically speaking, the combined advantages of avoided CO_2 tax and additional fuel sold make the integration of wind energy into the system attractive, with or without the addition of the CAES.

When investigating the effect of different installed wind powers, no attention was put into the electrical balance of the system, nor in the control system. These can prove to be challenging and important aspects that could limit the wind penetration, in order to maintain electrical stability.

The space required by the additional equipment (heat exchangers, compressors, turbine…) is not considered, but could be a limiting factor given the strict constrains on offshore oil and gas rigs.

The design and the anchorage of the vessels on the seabed are also very important parameters that should to be studied with more detail.

To conclude, the objectives of this thesis work were accomplished, and a variety of interesting configurations were studied, pinpointing the most promising ones in each of the studied conditions, and, at the same time, underlining their weaknesses.

REFERENCES

[1] Gavenas et al, "*CO_2 emissions from Norwegian oil and gas extraction*", April 2015

[2] Econ POYRY, "*CO_2 emissions effect on electrification*", commissioned by Statoil ASA, November 2011, Oslo

[3] Norwegian Petroleum, www.norskpetroleum.no

[4] Nord, Bolland "*Steam bottoming cycles offshore – challenges and possibilities*", January 2012

[5] Riboldi, Nord "*Lifetime assessment of combined cycles for cogeneration of power and heat in offshore oil and gas installations*", May 2017, Trondheim

[6] Pierobon et al, "*Multi-objective optimization of organic Rankine cycles for waste heat recovery: application in an offshore platform*", 2013

[7] He et al, "*Case study of integrating an offshore wind farm with offshore oil and gas platform and with an onshore electrical grid*", March 2013

[8] Korpas et al "*A case-study on offshore wind power supply to oil and gas rigs*", January 2012, Trondheim

[9] Riboldi, Nord, "*Concepts for lifetime efficient supply of power and heat to offshore installations in the North Sea*", February 2017

[10] Lazerte, "*Sizing of offshore wind energy storage*", October 2014, Trondheim

[11] www.oilfieldexpat.com

[12] Nguyen et al, "*Modelling and analysis of offshore energy systems on North Sea oil and gas platforms*", 2013

[13] Nguyen et al, "*Exergetic assessment of energy systems on North Sea oil and gas platforms*", 2013

[14] Nguyen et al, "*Energy efficiency measures for offshore oil and gas platforms*", 2016

[15] Voldsund et al, "*Exergy destruction and losses on four North Sea offshore platforms: a comparative study of the oil and gas processing plants*", 2014

[16] Badeer, "*GE's LM2500+G4 aeroderivative gas turbine for marine and industrial applications*", GE energy

[17] www.energy.siemens.com, "*SGT-500 industrial gas turbine*"

[18] Martorano, Antonelli, "*Elementi di Macchine a Fluido*", Edizioni ETS

[19] www.IEA.org, "*Technology roadmap, wind energy*", 2013

[20] Ibrahim et al, "*Energy storage systems – characteristics and comparison*", 2007

[21] www.windeurope.org, "*Wind Europe annual offshore statistics 2016*"

[22] Elmegaard, Brix "*Efficiency of compressed air energy storage*", 2015

[23] Luo et al, "*Overview of current development in compressed air energy storage technology*", 2014

[24] Yin et al, "*A hybrid energy storage system using pump compressed air and micro-hydro turbine*", 2013

[25] Barbour et al, "*Adiabatic compressed air energy storage with packed bed thermal energy storage*". 2015

[26] Kim et al, "*Potential and evolution of compressed air energy storage: energy and exergy analyses*", 2012

[27] Wang et al, "*Design and thermodynamic analysis of a multi-level underwater compressed air energy storage system*", 2016

[28] Katsaprakakis, "*Energy storage for offshore wind farms*", Greece

[29] Luo, Wang, "*Overview of current development on compressed air energy storage*", December 2013

[30] Samaniego, "*Modeling of an advanced adiabatic compressed air energy storage (AA-CAES) unit and an optimal model-based operation strategy for its integration into the power markets*", Zurich, October 2010

[31] Wang et al, "*Comparison of underwater and underground CAES systems for integrating floating offshore wind farms*", November 2017

[32] Jong, "*Commercial grid scaling of energy bags for underwater compressed air energy storage*", Thin red line aerospace, 2014

[33] VESTAS, "*Introducing the V164-7.0 MW*", 2011

[34] Jonkman et al, "*Definition of a 5-MW reference wind turbine for offshore system development*", NREL, February 2009

[35] World Energy Council, "*World Energy Resources, wind 2016*"

[36] Kurzke, "*Component map collection*", 2005

[37] Belaygue, Vigneau, "*Le compresseur centrifuge*", 1993

[38] Della volpe, "*Macchine*", Liguori Editore

[39] Lewins, "*Optimising an intercooled compression for an ideal gas model*", Cambridge

[40] Kotas, "*The exergy method of thermal plant analysis*", London, 2012

[41] Pierobon et al, "*Novel design methods and control strategies for oil and gas offshore power systems*", 2015

[42] Nguyen et al, "*Modelling, analysis and optimisation of energy systems on offshore platforms*", 2014

[43] Zhang, Cai, "*Analytical solutions and typical characteristics of part-load performances of single shaft gas turbine and its cogeneration*"

[44] *La regolazione della Potenza delle turbine a gas*

[45] Minghetti, "*La turbina a gas: tecnologie attuali e sviluppi futuri*", ENEA, December 1996

[46] Haglind, Elmegaard, "*Methodologies for predicting the part-load performance of aero-derivative gas turbines*", August 2009

[47] Cooke, "*On prediction of off-design multistage turbine pressures by stodola's ellipse*", July 1985

[48] Agromayor, "*Fluid selection and thermodynamic optimization of Rankine cycles for waste heat recovery applications*", January 2017

[49] Incropera et al, "*Fundamentals of heat and mass transfer*", 6th edition Wiley & sons

[50] Nord, "*Pre-combustion CO_2 capture: analysis of integrated reforming combined cycle*", Trondheim, June 2010

[51] Pierobon et al, "*Waste heat recovery technologies for offshore platforms*", October 2014

[52] Det Norske oljeselkskap ASA, "*Plan for utbygging og drift av Ivar Aasen*", September 2012

[53] Det Norske oljeselkskap ASA, "*Plan for utbygging, anlegg og drift av Luno*", September 2011

[54] www.IEA.org, "*World energy outlook 2016*"

[55] European Commission, "*ETRI: energy technology reference indicator projections for 2010-2050*", 2014

[56] Riboldi et al, "*Effective concepts for supplying energy to a large offshore oil and gas area under different future scenarios*", Trondheim, 2017

[57] Politecnico di Torino, "*Regolazione dei turbocompressori*", corso di macchine

[58] Cavallini, Mattarolo, "*Termodinamica applicata*"

[59] Cavallini, Mattarolo, "*Trasmissione del calore*"

[60] Croce et al, "*Energetica applicata*"

[61] Sathe, "*Atmospheric stability and wind profile climatology over the North Sea – case study at Egmond aan Zee*", 2010

[62] Buatois et al, "*Analysis of North Sea offshore wind power variability*", May 2014

[63] Orbelli, Riboldi, "*Life cycle energy optimization of upstream plants in the oil & gas field*", Politecnico di Milano, 2010

[64] Azerl et al, "*Offshore platform production*", Final report, October 2004

[65] Chen et al, "*Progress in electrical energy storage system: a critical review*", July 2008

[66] Nguyen et al, "*CO_2 – mitigation options for the offshore oil and gas sector*", October 2015

[67] Wang et al, "*Conventional and advanced exergy analyses of an underwater compressed air energy storage system*", August 2016

[68] Budt et al, "*A review on compressed air energy storage: basic principles, past milestones and recent developments*", March 2016

[69] Pimm, Garvey, "*Underwater compressed air energy storage*", Chapter 7

[70] McCalley, "*Compressed air energy storage*", Iowa 2012

[71] Salgi, "*CAES future scenarios: an investment analysis for Denmark*", January 2006

[72] Zhao et al, "*Review of energy storage system for wind power integration support*", May 2014

[73] Luo et al, "*Overview of current development in electrical energy storage technologies and the application potential in power system operation*", October 2014

[74] Diaz-Gonzalez et al, "*A review of energy storage technologies for wind power applications*", February 2012

APPENDIX A

Wind Turbine power curve

Table 39: NREL 5 MW power curve values

Wind speed [m/s]	Power output [kW]
0	0
1	0
2	0
3	170
4	391
5	731
6	1173
7	1752
8	2534
9	3452
10	4558
11	5000
12	5000
13	5000
14	5000
15	5000
16	5000
17	5000
18	5000
19	5000
20	5000
21	5000
22	5000
23	5000
24	5000
25	5000
30	0
100	0

Air compressor data fit coefficients

Table 40: MATLAB coefficients for Equation (3.2). 11 bar pressure

p1	-3.4E-07
p2	0.006287
p3	-9.386

Table 41: MATLAB coefficients for efficiency evaluation, 11 bar pressure

P1	-1.5E-08
P2	0.000141
P3	0.4868

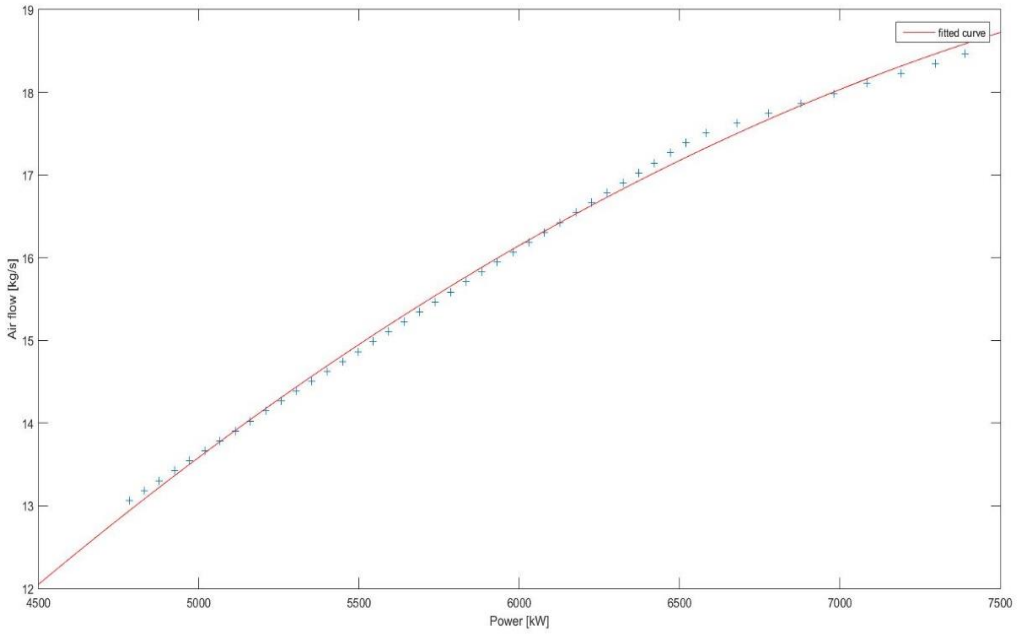

Figure A1: Example of accuracy between fitted data and map. 11 bar pressure

Table 42: MATLAB coefficients for Equation (3.2), 40 bar pressure

p1	-5.00E-08
p2	0.002173
p3	0.8479

Table 43: MATLAB coefficients for efficiency evaluation, 40 bar pressure

P1	9.18E-10
P2	-4.00E-05
P3	1.01

Table 44: MATLAB coefficients for Equation (3.2). 70 bar pressure

p1	-2.77E-08
p2	0.001812
p3	0.718

Table 45: MATLAB coefficients for efficiency evaluation, 70 bar pressure

P1	3.76E-10
P2	-2.46E-05
P3	0.9893

Air turbine data fit coefficients and design (B) parameters

Table 46: Air turbine MATLAB coefficients, 11 bar pressure

p1	-9.73E-09
p2	0.002413
p3	8.153

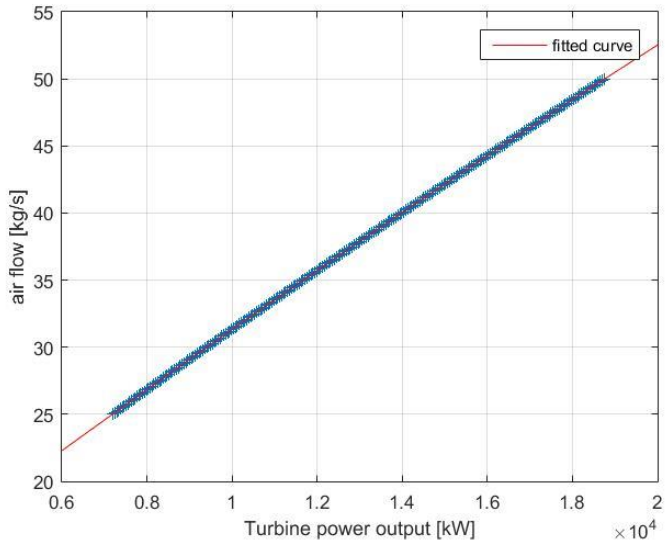

Figure A2: Exampla of accuracy between data and fitted curve, 11 bar pressure

Table 47: Air turbine MATLAB coefficients, 40 bar pressure

p1	-5.16E-09
p2	0.002157
p3	4.283

Table 48: Air turbine MATLAB coefficients, 70 bar pressure

p1	-3.84E-09
p2	0.002024
p3	3.343

Table 49: Design (B) parameters, 11 bar pressure

Mass flow [kg/s]	70
T inlet [K]	580
P inlet [kPa]	1111
P outlet [kPa]	101
Min outlet power [kW]	5241
Max outlet power [kW]	17287
Design efficiency	0.85

Table 50: Design (B) MATLAB coefficients, 11 bar pressure

p1	-1.78E-08
p2	0.003707
p3	11.14

Air turbine comparison of Stodola's ellipse approaches

The two approaches defined in Chapter 3 are recalled below.

In Equation 3.4, the Stodola's constant does not vary with operation. Outlet pressure is fixed to ambient conditions (101 kPa). This means that the air turbine can be operated in two different ways:

1) The first one is to keep the ΔP constant. This means that when the mass flow decreases, the inlet temperature increases following a quadratic law. The minimum inlet temperature is fixed at 800 K, in order to limit the air flow required to achieve

the desired power output. The maximum temperature is set to be 1100 K, as higher values would require complex and expensive cooling systems such as blade cooling. Therefore, with this approach, the temperature can vary between the above defined range. Once the maximum temperature is reached, it is kept constant and the ΔP is decreased instead. In particular the inlet pressure is lowered, with the use of a throttling valve.

2) The second one is to keep the inlet temperature constant at its minimum value of 800 K. In this configuration, the inlet pressure is continually adjusted with the throttling valve.

Firstly, the two cases were compared on the basis of fuel consumption, as shown in Figure A3.

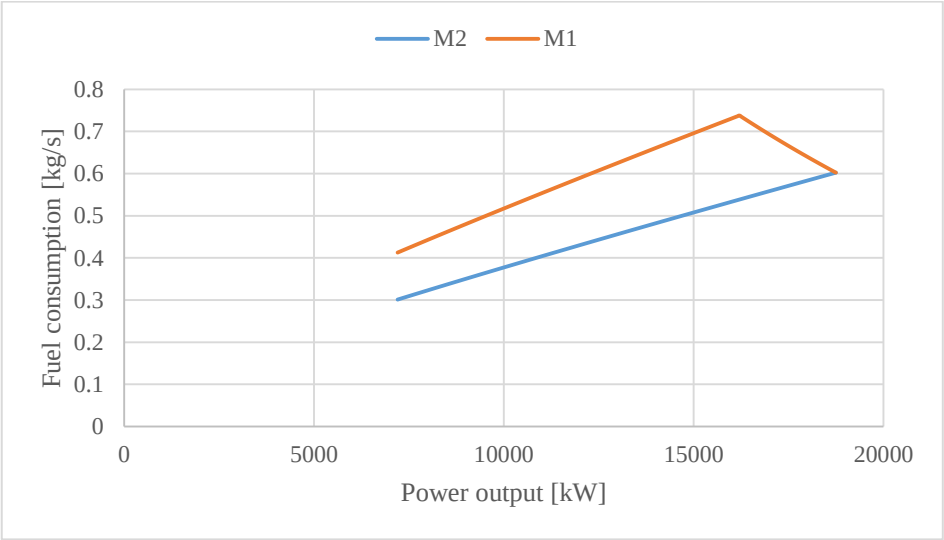

Figure A3: Fuel consumption for the two approaches

The second one always gives a lower fuel consumption and a linear profile, which better fits the system.

The temperatures, both inlet (i) and outlet (o) are lower using the second approach, as showed in Figure A4.

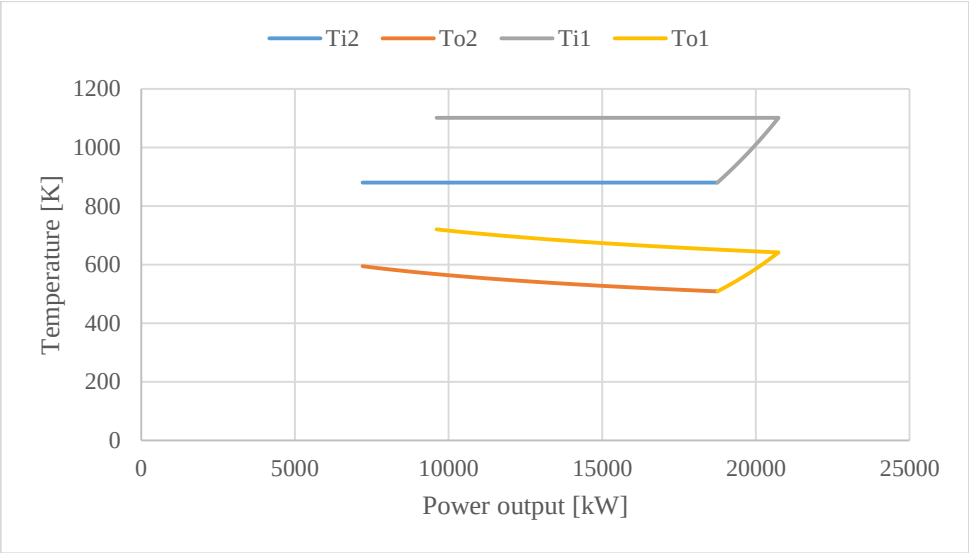

Figure A4: Inlet and outlet temperatures for the two approaches

For what concerns mass flows, the first approach gives the best results, since it always gives lower air flows values, which is beneficial since it empties the storage slower.

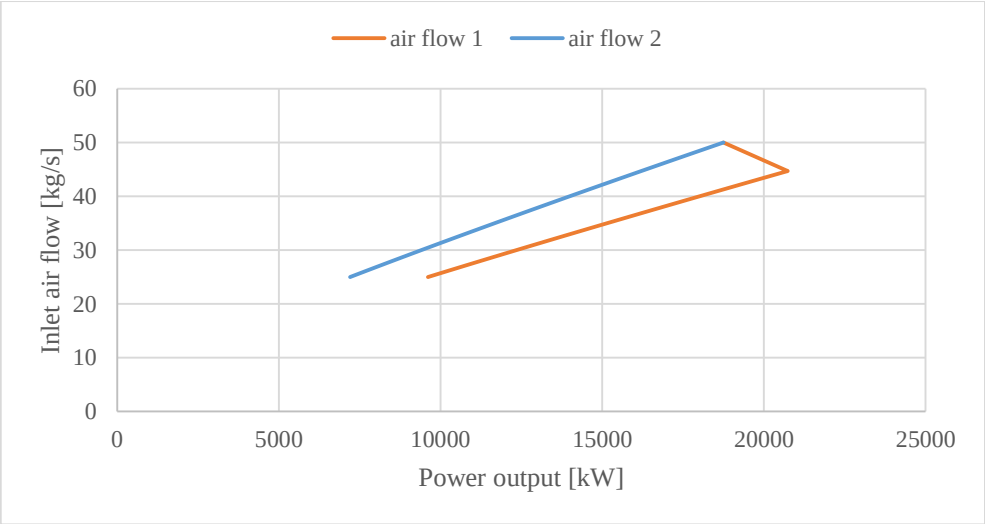

Figure A5: Inlet air flow comparison for the two approaches

The inlet pressure is showed in Figure A6 below.

Even though the second approach requires a larger mass flow and introduces a larger pressure loss, it was still favoured over the first, mostly due to the lower fuel consumption. Moreover, since most of the time the inlet pressure will be lower than the design one, it can be thought that the valve responsible for the pressure loss would also include the inevitable pressure losses along the whole process, which would otherwise be unaccounted for.

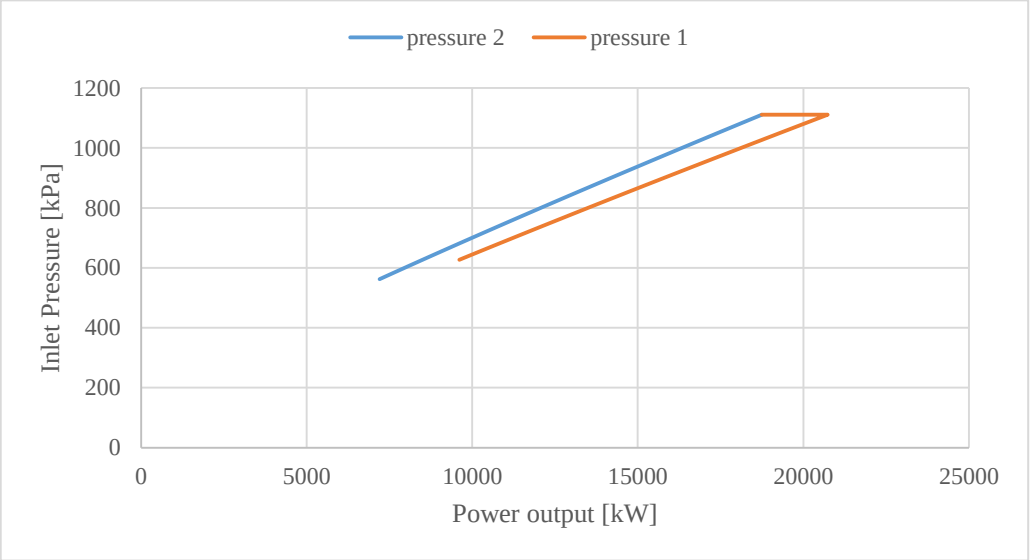

Figure A6: Inlet pressure comparison for the two approaches